Water, Sediment, Nutrient and Organic Carbon Fluxes in Small-Scale Agriculture Landscapes

Report to the
Water Research Commission

by

Vincent Chaplot, Phesheya Dlamini, Charmaine Mchunu, Ernest Oakes, Craig Orchard, Graham Jewitt & Simon Lorentz
School of Agricultural, Earth and Environmental Sciences
University of KwaZulu-Natal, Pietermaritzburg

WRC Report No. 1904/1/12
ISBN 978-1-4312-0304-8

August 2012

Obtainable from

Water Research Commission
Private Bag X03
Gezina, 0031

orders@wrc.org.za or download from www.wrc.org.za

DISCLAIMER

This report has been reviewed by the Water Research Commission (WRC) and approved for publication. Approval does not signify that the contents necessarily reflect the views and policies of the WRC, nor does mention of trade names or commercial products constitute endorsement or recommendation for use.

© WATER RESEARCH COMMISSION

EXECUTIVE SUMMARY

WHY THIS RESEARCH HAS BEEN UNDERTAKEN?

The fluxes of water, nutrients and carbon at landscape level, in response to natural processes such as soil infiltration by water, photosynthesis or organic matter decomposition, are key regulators of the main ecosystem functions. While most effort has aimed at describing and quantifying water fluxes at the hillslope or watershed level, little is known about interactions of nutrients and organic carbon in these land features.

This research study was undertaken in a 1000 hectare agricultural catchment of the Drakensberg foothills, in the Bergville District of KwaZulu-Natal. It shows a typical association between rangeland, small-scale farming and commercial farming. The watershed, part of the Drakensberg foothills which is a vital zone in KwaZulu-Natal since it contributes up to 80% of river systems' fresh water in the region. This, together with the large cultural, economic and cognitive discrepancies makes it an interesting case, a focal point, where many of the South African challenges for sustainable rural and cities development meet.

However, for several decades, the area, along with many marginal areas of the developing world, has shown increasing land degradation by water erosion, effected by the unstoppable development of Dongas (i.e. deep linear incisions) and bare soil areas, both thus far attributed to overgrazing.

MAIN OBJECTIVES

This study, concluded during 2009-2012, aimed at improving our understanding of the relationship between man and environment in a small-scale agricultural setting, a prerequisite for sustainable use of natural resources and development. Specifically, we aimed at understanding the mechanisms of land degradation by both sheet and linear erosion and their consequences on the fluxes of water, nutrients and organic carbon from the ecosystem. The main result of the study are summarised in the following section with reference to the various sub-studies and published literature.

MAIN RESULTS

Figure 1. ***Example of sheet erosion in the Drakensberg foothills. Note the link between abandoned contour banks and land degradation.***

Figure 2. ***Example of linear erosion in the Drakensberg foothills. Note the link between paths and gullies.***

Land degradation by sheet erosion and associated fluxes:

> Low vegetation cover induces increased soil nutrient losses (up to 2.6 times more soil C and N: *Mchunu and Chaplot, 2012*);
> Soil water content, crusting, clay content and crop and livestock management are other key factors controlling water, nutrient and carbon losses by sheet erosion (*Dlamini et al; 2010; Orchard et al., 2012)*;
> Rain-impacted flow is the main mechanism driving sheet erosion and associated fluxes (*Oakes et al; ESPL, 2012*).

Land degradation by linear erosion and associated fluxes:

> Piping, rather than overland flow is the main process of gully formation (*Chaplot and Beckedahl, submitted*);
> Paths created due to land mismanagement are key in the initiation of pipes and gullying (*Figure 2; Chaplot and Beckedahl, submitted; Chaplot et al., 2011*).
> Gully extension is due to bank collapse rather than by high velocity overland flow or overgrazing (*Chaplot et al., 2011*);

Tillage impact on water, nutrient and carbon fluxes:

No-tillage:
> Decreases soil, soil carbon and nitrogen by up to 3.8 times (*Mchunu et al., 2011)*;
> Decreases CO_2 emissions from soils up to 20% and from sediments by 45% (*Chaplot et al., submitted)*;
> Increases overall soil infiltration;
> Yields equal to higher crop production;
> Does not change soil carbon stocks.

Capacity building and outreach

> 16 research papers in international journals including 9 published, 2 in press and 5 submitted;

> Communications at workshops with publications (11); without publications (8); Posters (4); other papers (2),

> 13 post graduate degrees completed; 4 current PhD; 2 MSc;

> 2 workshops for scientists; 4 meeting in the field for results dissemination; 15 meetings with the community leaders; 2 in-field days for local schools; 2 winter schools for UKZN and SADEC MSc/PhD students (co-funding IRD, WATERNET, UKZN);

> No-tillage being adopted in the community (support of ARC, Farmer Support Group of UKZN).

Figure 3. ***Example of community-based capacity building. Case of land use change and its impact on soil erosion.***

RECOMMENDATIONS

Land degradation by sheet erosion and associated fluxes:

> increase soil surface cover:

- mulching;
- inter-cropping and intra-cropping;
- avoid undergrazing and formation of cattle and human pathways by promoting pasture rotation; increased cattle density for short periods of time.

Land degradation by linear erosion and associated fluxes:

> Set up land management practices that do not allow paths to form;

> Improve soil structure through a control of soil pH and clay saturation in certain cations; find preferential soil water paths;

> Reshape gully banks to the angle of repose and re-vegetate banks rather than use gabions.

Tillage impact on water, nutrient and carbon fluxes:

> No-tillage with low residue density practiced in small-scale farming, yields high economic and environmental benefits. Thus recommendations are as follows:

- Promote no-tillage;
- Allow cows to utilise crop residues;
- Promote intercropping and winter cover crops to promote soil C sequestration and soil protection while increasing ‘cattle-feed’;
- Communicate on the environmental benefits together with low equipment cost, labor inputs and technical aspects.
- Lobby for carbon credits, not due to increased soil C stocks, but decreased C erosion and CO_2 emissions.

Capacity building and outreach

> Constant communication with the community (during meetings at schools) from project onset to result restitution; participation of a *"farmer support Group"*;

> Build a team constituted by all partners with common and achievable objectives;

> Foster researchers-students interactions (both in the field and in the laboratory) as a way to master the different steps of the *Research Process* (from identification of a research question to scientific writing).

ACKNOWLEDGEMENTS

The study necessitated close cooperation between the researchers and the ARC. Particular thanks to Alan Manson for specialist advice and contribution to the project. We are also indebted to the farmers and community of the Potshini village for permissions to access the site, build structures and observe processes. We are grateful to the reference group for their advice and encouragement throughout the project.

Reference Group:

Mr W Nomquphu	(WRC)
Prof C Everson	(UKZN)
Dr A Samie	(UN)
Prof GPW Jewitt	(UKZN)
Prof GGS Pegram	(UKZN)
Prof CW van Huyssteen	(UFS)
Mr JN Rossouw	(Aurecon)
Dr A Manson	(ARC)

TABLE OF CONTENTS

LIST OF FIGURES

LIST OF TABLES

1. Characteristics of the study site

The Potshini Catchment is located in the KwaZulu-Natal province, South Africa (Figure 4). The area that this study focusses on, is a 1000 ha catchment (longitude: 29.36°; latitude: 28.82°) located in the upper Thukela Basin (30,000km²) near the town of Bergville.

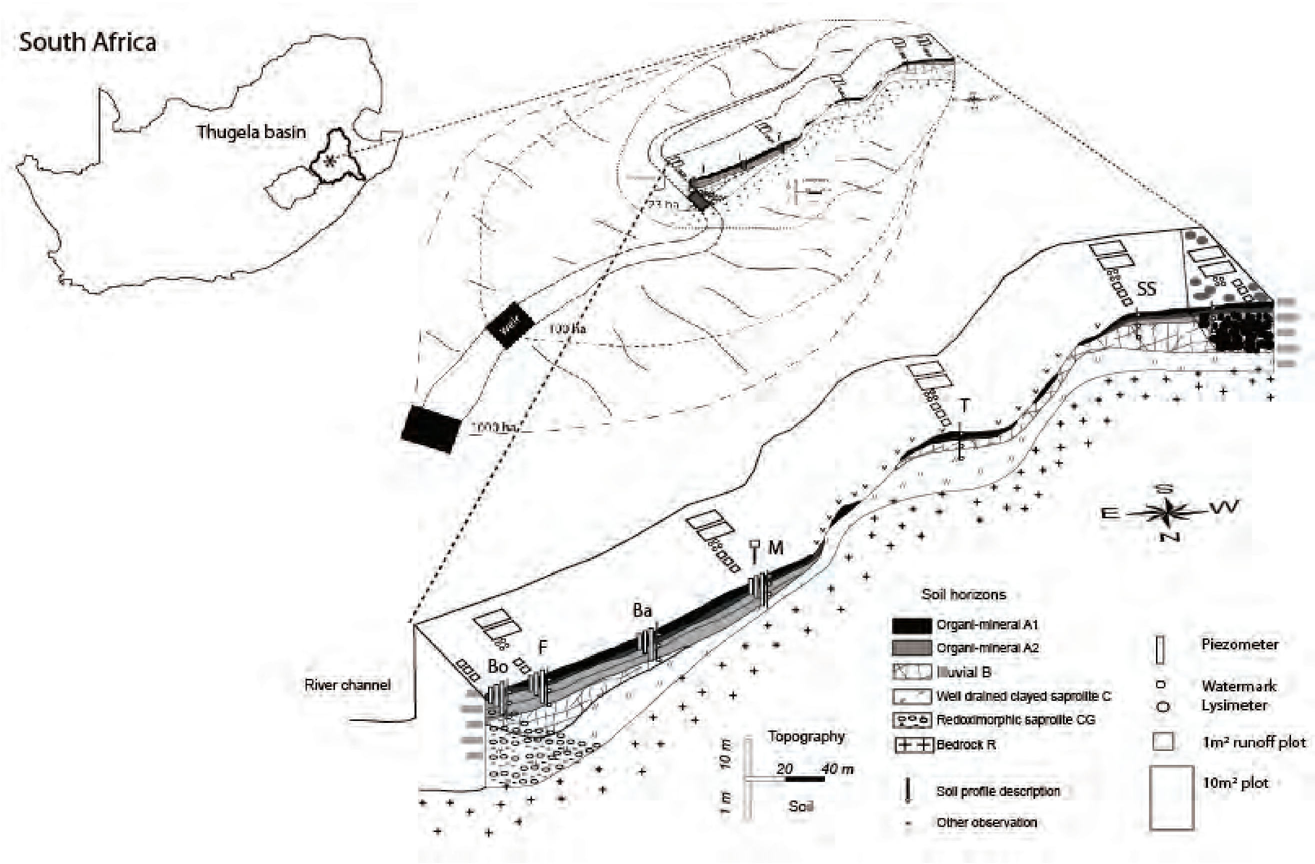

Figure 4. Location of the study site, the Potshini Catchment with the experimental setup

The climate in the area is sub-tropical, humid and with a strongly seasonal summer rainfall pattern (October-March) (Schulze, 1997). The nearest government-maintained weather station located 10 km to the east of the study site in the town of Bergville, had a mean annual precipitation of 684 mm per annum over the past 30 years, with a potential evaporation of 1600 mm per annum and a mean annual temperature of 13°C (Schulze, 1997), with frosts that are common in winter.

At the Potshini study site, altitude ranges from 1080 to 1455 masl. The relief is relatively gentle with a mean slope gradient of about 15.7%, but with steep slopes of 50-70% found in the lower part of the catchment, whereas in the vicinity of the catchment outlet and on the plateau, the topography is relatively flat all the way to the 1000 hectare catchment outlet. For research purposes the catchment has been divided into a headwater, catchment of 100 ha, within which is a headwater micro-catchment of 23 ha, primarily used for livestock grazing. The larger catchment includes the 100 ha Potshini village and small-scale agriculture area as well as commercial farms, and comprises 1000 ha

Soils are formed from the Karoo Supergroup and Beaufort Group parent materials (Figs 4-5; Table 1). The geology exhibits a horizontal, alternating succession of fine-grained sandstone, shale, siltstone and mudstone (King, 2002).

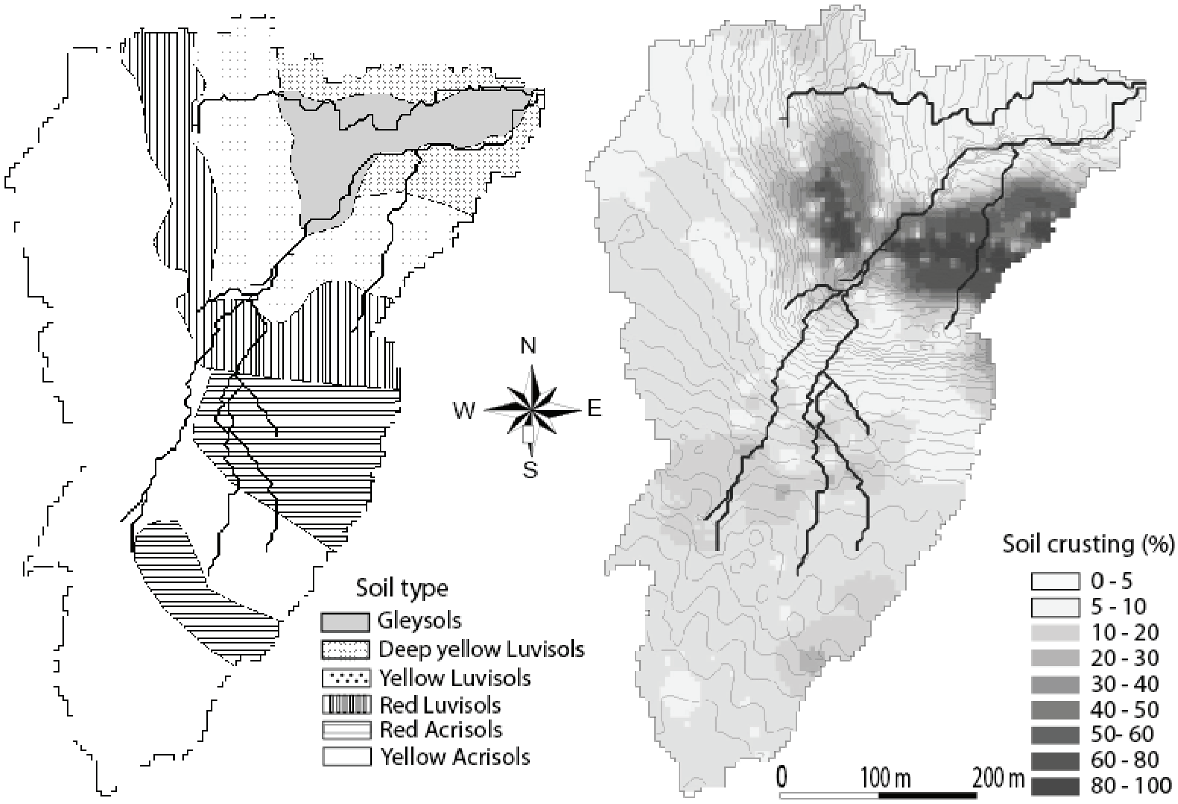

Figure 5. Spatial distribution of soil types and of soil surface crusting within the 23 hectare catchment. Kriged maps interpolated, using 200 georeferenced field observations

A main dyke of Karoo Dolerite is intruded in these horizontal layers in the upper portion of the micro-catchment, giving specific weathering features of rounded boulders. Soils developed from sandstones and dolerites are Acrisols (ISSS Working Group, 1998) and Inanda soil form (Soil Classification Working Group, 1991). Within hillslopes, deep Acrisols (~2 m) characterize the footslope and Gleysols the bottomland. Bottomlands (Bo) exhibit features of waterlogging, such as a surface dark grey A horizon, enriched in organic matter. At the footslope (F) position, the soils are well-drained. The midslope (M) position exhibits a similar soil profile, but much shallower. The soils at the terrace (T) and the shoulder (SD) have developed from dolerites. Finally, the soils found at the other shoulder location (SS) are derived from sandstones and are yellow in colour.

The land use of the catchment is predominantly grazed grassland. Cattle are seen as an important cultural asset and in good times, community members, both those living in the catchment and those who work and live in the major cities invest in cattle, leading to increasing herd sizes. This, combined with the highly acidic low productive soils, rapidly leads to overgrazing, with a decreasing proportion of soil surface coverage by the vegetation and an associated increase in bare soils. Microplots have been installed in areas of the micro-catchment that have different degrees of overgrazing intensities present, as well as other specific environmental factors.

There are three main embedded scales (as shown in Figure 4), which correspond to the three main land uses in the area. The land use of the 23 ha steep-sloped catchment (the smallest catchment surface area) is communal pasture for the local community. The land use within the 100 hectare catchment is predominantly small-scale agriculture where maize (*Zea mays*) and small cash crops are grown for domestic consumption. From the 100 hectare outlet to the 1000 hectare catchment outlet, the land use changes to commercial agriculture, where irrigation takes place. Two dams, which store water for irrigation, are located upstream of the monitoring site of the 1000 hectare catchment outlet.

Table 1. Location label, Slope position, Soil type, proportion of the soil surface covered by crusting (Crust), proportion of the soil surface covered by vegetation (Cov), mean slope gradient (Slope), soil clay content and soil bulk density (ρb) at the different plot locations. Three plot replicates are located at each site: bottomland (Bo); footslope (F); midslope (M); terrace (T); shoulder under dolerite (SD); and shoulder under sandstone (SS). (n = 18)

N	Label	Slope position	Soil type	Crust	Cov	Slope	Clay	ρ_b
				--------------------%----------------				g/cm^3
1	SS	Crest	Yellow Acrisols	15	85	19	30.5	1.12
2	SD	Crest	Red Acrisols	8	92	18	53.9	1.02
3	T	Terrace	Red Luvisols	5	95	23	39.8	1.13
4	M	Middleslope	Yellow Luvisols	50	50	26	27.4	1.32
5	F	Footslope	Deep Yellow Luvisols	2	98	25	27.8	1.24
6	Bo	Bottomland	Gleysol	1	99	6	27.8	0.96

2. The nested experimental design for water and nutrient fluxes evaluation

There are four main embedded/nested scales of research observation within the Potshini Catchment, (Figure 4).

a) Microplots and plots (7 monitoring nests installed along a hillslope, where overland flow plots, soil water tension monitoring equipment installed at different depths and piezometers are located at each site. An automatic rain gauge installed at the footslope location of the hillslope)
b) 23 hectare catchment (monitored hillslope is located within the 23 ha catchment. An H-Flume is installed, from which the flow height is recorded by a data logger. An automatic water sampler is also located at the outlet of this catchment)
c) 100 ha catchment (23 ha feeds into this catchment. An H-Flume is located at the outlet of this catchment to monitor flow, which is logged by a data logger. An automatic water sampler is coupled with the data logger to take water samples)
d) 1000 ha catchment (outlet of the greater Potshini Catchment. Flow heights are monitored and logged, using a pressure transducer and a data logger)

2.1. Microplots

Eighteen 1 m x 1 m overland flow microplots are installed within the micro-catchment. The microplots are installed at six different topographical positions or sites, with different soil types and intensities of overgrazing present (Figure 5).

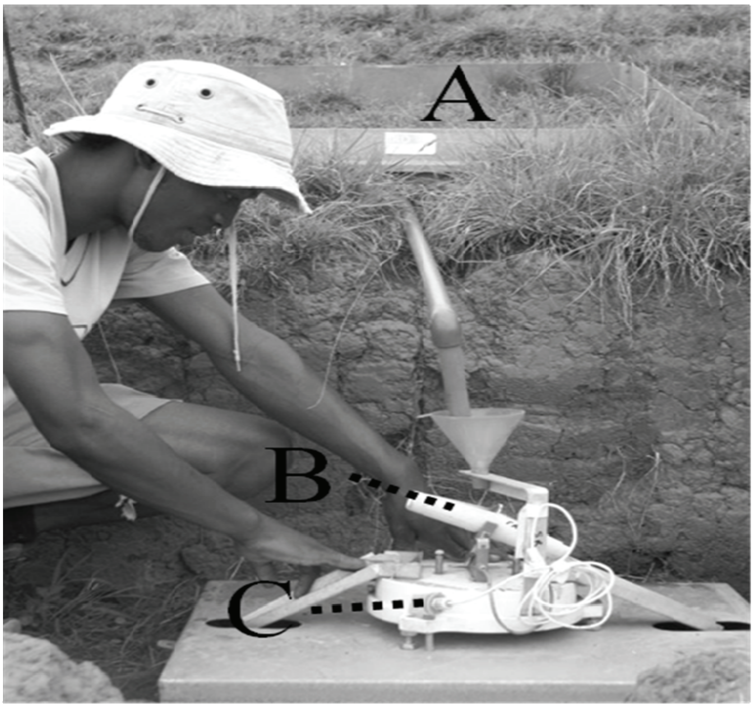

Figure 6. Example of a 1 m^2 microplot with its metallic frame inserted into the soil (A). View on the collection pipe which directs overland flow to a tipping bucket (B) aimed at recording the temporal variations of overland flow. The time of the tip is recorded by a HOBO® Event Logger©

The metal borders surrounding the micro-plots are inserted to a depth of 0.1 m in the soil. The microplots were installed parallel to the slope direction (as shown in Figure 6). This allows for any overland flow that was generated to be directed down the slope and into the gutter of the microplot. The gutter was designed to channel and concentrate water into the bottom of a gutter. The gutter feeds into the outlet of the microplot. This outlet is connected to a pipe, which feeds into a modified tipping bucket system. Finally, after the tipping bucket mechanism, the water generated by overland flow is collected in a bucket, installed in the subsurface. After each rainfall event, the total overland flow volume (R) from each microplot replicate (Figure 6) was measured with a measuring cylinder. The precision is ±10 ml for total runoff volumes between 10 and 2000 ml and ±10 ml at higher runoff volumes.

At each location, the tipping bucket mechanism was connected to a HOBO event-logger (pendant logger). The tipping bucket mechanism was designed to measure 40 ml for each tip. In addition, the specific time at which the tip occurred, was logged. This was to ensure that the exact temporal response of each individual microplot location (in terms of overland flow) was measured after the onset of a rainfall event. In addition, the intensity of the overland flow could be calculated.

2.2. Plots

Ten 5 m long × 2 m width =10 m^2 runoff plots were installed adjacent to the 1×1 m^2 microplots with only two replicates per position (Figure 5). The metal borders surrounding both the microplots and runoff plots were inserted in the soil to a depth of 0.1 m. All plots were installed parallel to the slope direction. This allowed for any overland flow that was generated to be directed down the slope and into the gutter of the plot. The gutter is designed to channel and concentrate water into the bottom of gutter. The gutter feeds into the outlet of the plot. This outlet was connected to a pipe, which feeds into a tipping bucket system. Finally, after the tipping bucket mechanism, the water generated by overland flow collected in a bucket. At each location, the tipping bucket mechanism was connected to a HOBO event-logger (pendant logger). The tipping bucket mechanism was designed to measure 2 litres for the 5 m x 2 m runoff plots. In addition, the specific time at which the tip occurred, was logged. This was to ensure that the exact temporal response of each individual microplot location (in terms of overland flow) was measured after the onset of a rainfall event. In addition, the intensity of the overland flow could be calculated.

2.3. Catchment monitoring

2.3.1. Rainfall measurements

Rainfall data were obtained from an automatic rain gauge located at the midslope position of a hillslope located within the micro-catchment. The rain gauge was calibrated to measure 0.2 mm per tip and was connected to a HOBO event logger that measured the exact time and date of each tip recorded by the tipping bucket. For the purpose of this study, it was assumed that the rainfall characteristics do not vary spatially within the catchment and that the rainfall is uniform and spatially distributed. Specific rainfall characteristics are to be used for this study and obtained from the data collected at the rain gauges within the catchment. These include the cumulative rainfall since the onset of the rainy season (RainC); 3-days prior rainfall amount (PreRain-3); event duration (Dur); event average rainfall intensity (I); and the maximum event 6-min rainfall intensity ($Max_{6min}I$). These rainfall characteristics will be used to determine their role in the spatial and temporal variations of OF generation. In addition, a manual rain gauge was present at the footslope position of the hillslope. This rain gauge was used to manually record the amount of rainfall for each rainfall event and was used to validate the rainfall amount recorded by the automatic rain gauge.

2.3.2. Measurements at weirs

Conventional H-flumes, coupled to ISCO 6712 and 3700 series, automatic samplers were installed at the outlets of the 23 and 100 ha catchments, respectively. The H-flume at the 100 ha catchment outlet was built in 2006, whilst the flume located at the 23 ha catchment was built in 2009. The height of flow at both catchment outlets were logged by a datalogger and were converted to runoff using site specific rating curves derived for each monitored site. The loggers were also programmed to trigger the automatic water samplers so that catchment runoff water quality (in terms of nutrients and soil losses) during base flow periods and on the rising and falling limb of a hydrograph during rainstorm events could be observed. At both the micro-catchment and catchment scales sediment and water samples were collected using automatic samplers during rainfall events and manual sampling in between events when visiting the field site.

At the 1000 hectare catchment outlet, a pressure transducer together with a HOBO data logger were installed, under a culvert bridge approximately 4km downstream from the monitored 100 hectare catchment outlet. Particulate nutrient and sediment loads were not monitored at this site due to the existence of small upstream reservoirs, which in turn, trap the sediment load in the stream. The pressure transducer was calibrated by subjecting it to pressure from a gradually increasing height of water from 0 to 1000 mm while recording the output voltage signal from the transducer. A similar exercise was done for a decreasing water column. The calibration equation for the pressure transducer is as indicated in Equation 1:

$$H = 13.5307564 + 0.45355129 \times V$$ **Equation 1**

where *H* is the stream flow depth (mm) and *V* is voltage output from the pressure transducer (mV). Velocity transect surveys, at different discharges, were carried out across the culvert bridge using a propeller current meter. The concrete culvert bridge had a regular rectangular shape and hence made it easier to apply the Manning's open channel flow equation and subsequent development of the rating curve. Equation 2 shows the established rating curve at the culvert bridge.

$$Q = 8.267 \times H^{1.6403}$$ **Equation 2**

where Q is the flow rate in m^3/s and H is the stream flow depth (m).

2.3.3. Spatial and temporal variations of overland flow

The installation of the microplots at different locations and in conjunction with a tipping bucket connected to a data-logger, was done to account for the spatial and temporal variations of overland flow in the micro-catchment. Eight representative runoff events were selected for detailed study of the temporal and spatial variations of overland flow. These events have been chosen, since all plot locations recorded overland flow and thus were assumed to be representative of events when overland flow was generated within the micro-catchment. Figure 7 shows the selected runoff events for the microplots.

The lag between the onset of rainfall and the start of the overland flow in each microplot can be derived from the curves and was used to estimate the Time to Runoff Initiation (TRI) in the microplot (calculated using Equation 3);

$$TRI = T_{rain} - T_{plot} \qquad \textbf{Equation 3}$$

The TRI can be defined as the difference in the time between the first tip of the microplot to the first measured tip of the rainfall that generated the overland flow. The time of the rainfall is labelled as time zero (T_{rain}).

TRI is a key index to describe the spatial variation of overland flow generated within a catchment. From the experimental setup of this study, TRI was estimated for different areas within the micro-catchment. This allowed for a better understanding of the spatial variations of overland flow. In addition, the TRI of each microplot location for a specific rainfall event was ranked to qualitatively assess the spatial variations of overland flow characteristics.

Three overland flow events were selected to investigate the spatial variations of overland flow, based upon the spatial extent of the soil surface crusting present within the micro-catchment. This was done by plotting each individual location's microplot TRI value versus the microplot soil surface crusting value. From this, a simple linear regression model can be used to predict the TRI in the catchment where there are no microplots.

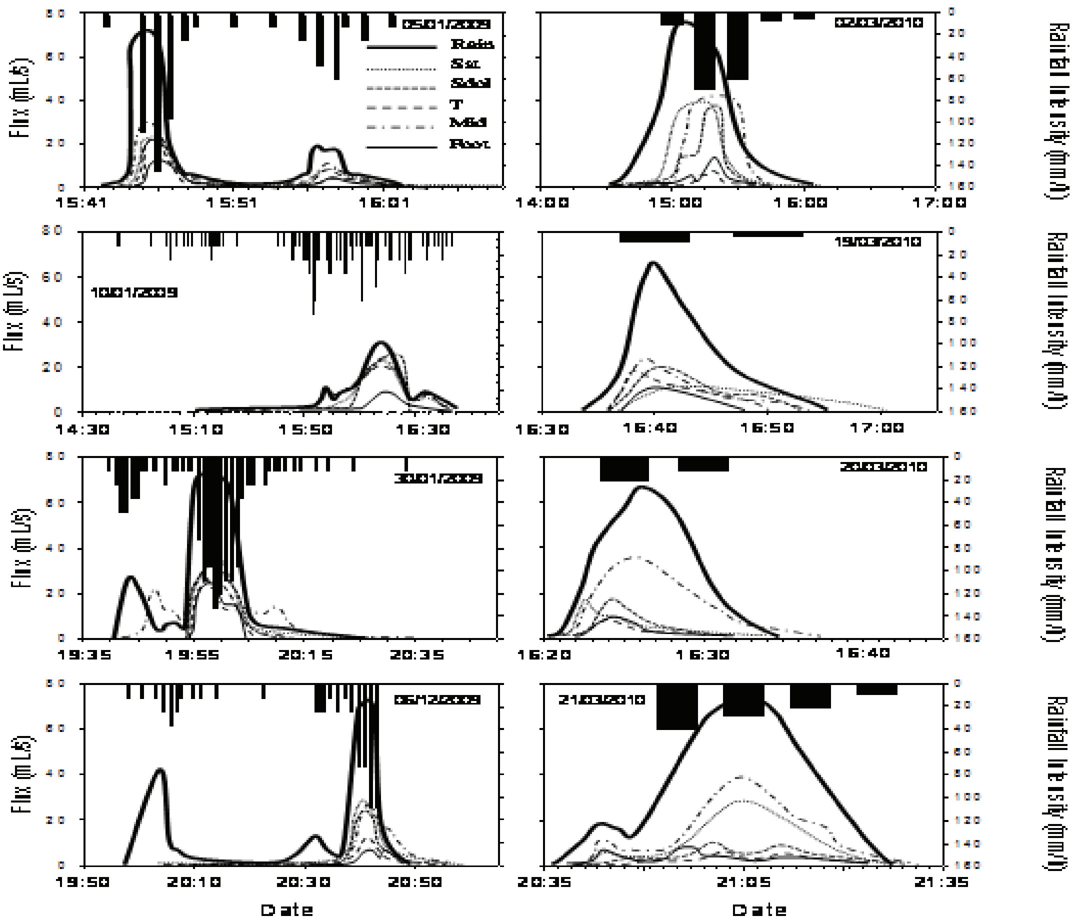

Figure 7. Overland flow response to rainfall at the 5 microplot locations and for 8 representative events selected from among the 90 events of the 2007-2010 period

The events chosen were chosen according the overriding antecedent moisture conditions of the micro-catchment prior to the overland flow events and the characteristics of the rainfall event that caused the overland flow event. The three selection criteria for the three different events were as follows:

a) Micro-catchment saturated, large and intensive rainfall
b) Micro-catchment dry, small rainfall event
c) Micro-catchment saturated after a prolonged period of rainfall in a season with lower than average rainfall

3. Rainfall conditions during the study period

The rainfall characteristics over the three-year study period are displayed in Table 2.

Table 2. General rainfall characteristics of the three rainfall years considered. Cumulative yearly rainfall amount (Cum); minimum, maximum, average event rainfall amount; standard deviation and coefficient of variation of average event rainfall amounts and maximum 6-minutes rainfall intensity of events ($Max_{6min}I$) (n = 52377)

	Cum	Min	Max	Av	StDev	CV	$Max_{6min}I$
	----------------------------mm-------------------------					%	$mm.h^{-1}$
2007/2008	761.9	4.2	30.8	14.7	7.8	53.3	38.4
2008/2009	852.0	0.6	79.6	11.7	15.1	128.2	42.3
2009/2010	627.8	1.0	53.8	7.3	8.1	111.5	36.4
2010/2011	1059	1.2	60.4	16.4	12.3	774.1	32.0
Average	747.2	1.9	54.7	11.2	10.3	97.7	39.0

The rainfall amounts for the three different rainfall seasons investigated are shown in Table 2. The total amounts of rainfall for each rainfall season was 761.9 mm in 2007/2008; 852 mm in 2008/2009; 627.8 mm in 2009/2010 and 1059 mm in 2010/2011. This indicates that each individual rainfall season was inherently different and as such had different characteristics of rainfall.

In support of this is the differing event minimum and maximum for each individual season. For 2007/2008 the maximum event depth was 30.8 mm whilst the event minimum was 4.2 mm; 2008/2009 the event maximum was 79.6 mm and the event minimum was 0.6 mm; the event maximum for 2009/2010 was 53.8 mm and the event minimum was 1 mm and in 2010/2011 the event maximum was 60.4 mm and the event minimum was 1.2 mm.

The maximum 6-min intensities for events in each specific season were 38.4 $mm.h^{-1}$ in 2007/2008, 90 $mm.h^{-1}$ in 2008/2009; 69.6 $mm.h^{-1}$ for 2009/2010 and 32.0 $mm.h^{-1}$ for 2010/2011. These specific event intensities corresponded to the maximum event amounts for each season.

The average rainfall amount per event was 14.7 mm in 2007/2008; 11.7 mm in 2008/2009; 7.3 mm in 2009/2010 and 16.4 mm in 2010/2011. The standard deviations and coefficients of variation reported in Table 2 indicated that the rainfall season of 2008/2009 showed highly variable rainfalls (Stdev 15.1 mm and CV 128.2 mm). High variations in event total rainfall also occurred in 2009/2010 (Stdev=8.1 mm; CV=111.5 mm). The 2007/2008 season showed smaller variations in event rainfall amounts, with for, example a CV of 53.3 mm, i.e. about half of this calculated from the 2008/2009 and 2009/2010 data. The rainfall for the 2010/2011 season showed the highest variations in event rainfall events with a CV of 774.1 mm which was considerably higher than that of the other seasons considered.

4. Spatial variations of overland flow

4.1. General statistics

General statistics of overland flow at the different plot locations and events and for the three rainy seasons under study are presented in Table 3.

Table 3. General statistics of overland flow (cumulative litre per square metre) and Time to Runoff Initiation at the different plot locations and events and for the three rainy seasons under study. A total of 15 plots and 90 events were considered

	SS	SD	T	M	F	Bo
2007/2008 (n=34)						
Mean	7.0	4.3	3.7	6.6	4.5	40.2
Rank	*2*	*5*	*6*	*3*	*4*	*1*
2008/2009 (n=37)						
Mean	10.6	10.1	10.6	10.7	8.1	58.2
Rank	*3*	*6*	*5*	*3*	*2*	*1*
2009/2010 (n=19)						
Mean	5.2	3.7	4.1	4.8	2.6	30.8
Rank	*3*	*4*	*5*	*2*	*6*	*1*
TRI (min)						
2007/2008	4.2	6.6	7.2	6.6	10.8	0.1
2008/2009	3.6	5.4	4.2	3	7.2	0.3
2009/2010	0.6	0.6	0.6	0.6	1.2	0.2
Average	2.8	4.2	4	3.4	6.4	0.2
TRI (rank)						
2007/2008	2	3	5	3	6	1
2008/2009	3	5	4	2	6	1
2009/2010	2	2	2	2	6	1
Mode	3	4	5	2	6	1

Overland flow varied considerably from plot location to plot location. The average 2007/2008 overland flow was the highest at Bo, then followed by SD; M; SS; T; and F. Bo was ranked one for all seasons. Bo remained ranked one for all seasons with SS, M and F were the next most productive situations. Reddish shallow and deep Acrisols at T and SD were the least productive microplot locations for all years.

In Table 3, it can be also seen that there was a greater within-site variability at the different locations of the OF generated. For example, F generated its largest event OF mean of 81 litres in 2008/2009; the next productive season was 2007/2008 with a mean of 4.5 litres; the least productive season was 2009/2010 with a mean of only 2.6 litres generated. This behaviour is consistent for all situations for the mean OF generated follows the seasonal patterns of the drivers.

4.2. Time to Runoff Initiation (TRI)

The overland flow response to rainfall for 8 representative events selected among the 90 events of the 2007-2010 period is presented in Figure 7. The events chosen exhibited a large range of rainfall characteristics. The highest maximum 6 minute rainfall intensity (42.3 mm h^{-1}) occurred on 30 January 2009 and the highest rainfall amount (37.6 mm) was recorded on 2 March 2010. Events were also selected to highlight antecedent rainfall and thus a priori soil moisture conditions. The rainfall characteristics of the 8 representative overland flow events selected to graphically investigate the spatial and temporal variations of TRI at the catchment level is shown in Table 3.

Table 4. Rainfall characteristics of the 8 representative overland flow events selected to graphically investigate the spatial and temporal variations of TRI at the catchment level

Date	Duration	Cum	I	$Max_{6min}I$	RainC	PreRain-3
	min	mm	-------mm h^{-1}------		--------mm-------	
05-Jan-09	19	10	31.6	39.3	504.6	15.2
10-Jan-09	121	21	10.4	38	517.6	6.0
30-Jan-09	54	23	25.6	42.3	650.6	82.2
06-Dec-09	44	11.4	15.5	36.3	182.4	4.2
02-Mar-10	60	37.6	37.6	20.3	434.0	1.8
19-Mar-10	30	2.8	5.6	19.8	528.4	10.6
20-Mar-10	30	8.4	16.8	22.6	531.4	4.8
21-Mar-10	45	24	32	36.4	544.4	13.2

The event on 06 December 2009 occurred relatively early into the rainy season, therefore having a low RainC (182.4 mm of cumulative rainfall since onset of season). In contrast, the event of 30 January 2009 occurred later on in its rainy season (RainC=650.6 mm). The cumulative rainfall of the 3 days prior to the event (PreRain-3) ranged between 1.8 mm on 2 March 2010 and 82.2 mm on 30 January 2009.

The hyetograph for the 8 events are displayed in Figure 7. The distribution of the rain was either mono-modal or bi-modal. Mono-modal events occurred on the following dates: 02 March 2010, 19 March 2010, 20 March 2010, and 22 March 2010. Bi-modal events occurred on 05 January 2009, 10 January 2009, 30 January 2009, and 06 December 2009. From the curves it is noticeable that the OF obviously commenced after the rainfall started, the time lag between the two corresponding to TRI. The evolution over time of OF, generated at the different locations, is mostly asymmetrical and OF peaks appeared to be considerably lower than that of the rainfall (if the curves were exactly the same then all the rainfall would have been converted into OF). Out of the 8 events, only 2 events showed a OF bi-modal behaviour, whilst OF for the remaining six events was mono-modal. M and SST locations had for all events the highest OF peaks, followed by SD, T and F. The evolution over time of OF for Bo was superimposed on the rainfall (100% OF) for all the events except on 6 December 2009 during which no OF occurred (100% infiltration). The frequency distribution of TRI, as shown in Figure 8, shows that the majority of TRI of the microplot locations for the selected overland flow events (44 data points out of 48) had a TRI of less than 60 minutes. The majority of microplot locations had a response of less than 20 minutes (32 data points out of 48 considered).

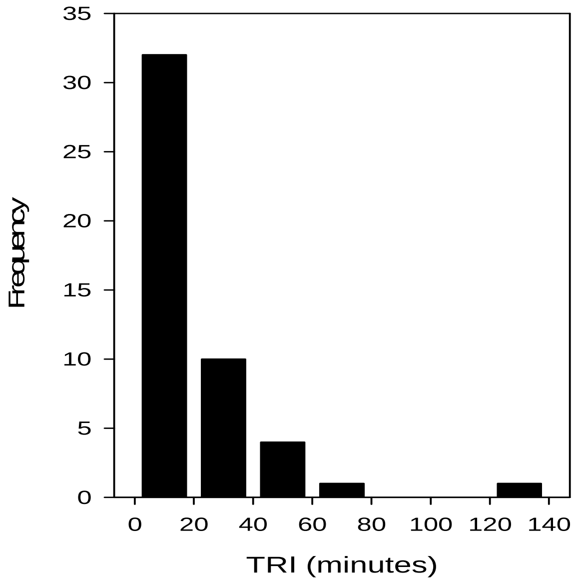

Figure 8. Frequency distribution of Time to Runoff Initiation (TRI) for all microplot locations

The average TRI at the different landscape locations and for each of the 3 rainy seasons are displayed in Table 3. Values varied between 0.6 minutes at Bo to 6.4 minutes at F. TRI was the lowest at Bo followed by M; SS, SD, T, and F. This ranking was consistent across the 3 rainy seasons. While at Bo, the average TRI only varied slightly from year to year, much higher variations have been observed at the other landscape positions. For example, at F, the average TRI ranged between 1.2 minutes in 2009/2010 and 10.8 minutes in 2007/2008. Overall, TRI values were the lowest in 2009/2010 and the highest in 2007/2008 (Table 3).

4.3. Controlling factors of TRI

One to one relationships between TRI and the selected environmental factors are displayed in Table 5. Due to a specific behaviour of OF in the bottomland (Bo) (i.e. 100% OF when the bottomland water table reaches the soil surface and 0% OF otherwise) two correlation matrices have been generated, one with and one without bottomland plots.

Table 5. Correlation matrix between TRI (with and without data from the bottomland) and the selected soil variables and environmental factors: Crust, Cov, Slope, Clay, ρ_b, ER (proportion of soil surface with exposed roots); SWT (soil water tension at depths of 20; 50 and 100 cm); Rain (total event rainfall amount); RainC (cumulative rainfall since the onset of the rainy season); PreRain-3 (3-days prior rainfall amount); Dur (event duration); I: event average rainfall intensity; $Max_{6min}I$ (maximum event 6-min rainfall intensity) (n = 144)

	TRI	
	Hillslope	Bottomland
Crust	-0.08	-0.16
Cov	0.08	0.16
Slope	-0.03	-0.27
Clay	0.06	-0.1
ρ_b	-0.05	-0.19
ER	-0.16	-0.13
SWT_{20}	0.08	-0.13
SWT_{50}	0.10	-0.11
SWT_{100}	0.20	-0.12
Rain	0.41*	-0.08
RainC	-0.47*	-0.35*
PreRain-3	-0.23	-0.08
Dur	0.80*	-0.03
I	-0.17	-0.09
$Max_{6min}I$	-0.15	-0.1

*Marked correlations are significant at $p < 0.05$

When including all locations, the TRI correlated significantly with only the cumulative amount of rainfall since the onset of the rainy season (*r*=-0.35). R coefficients were the lowest for Dur (r=-0.03), Rain and PreRain-3 (r=-0.08), and I (r=-0.09). The highest r was found in S (r=-0.27), Cov (r=0.16), Crust (r=-0.16), and ρ_b (r=-0.19). Overall, TRI decreased (i.e. increase of OF response) as mean slope gradient; proportion of the soil surface covered by crusting; exposed roots; percentage soil clay content; soil bulk density, the cumulative amount of rainfall since the onset of the rainy season, the cumulative rainfall 3 days prior to the event and the average rainfall intensity of the event and the maximum 6 minute rainfall intensity of the event, and soil water tensions increased.

Results from the multivariate analysis, a PCA whose two first axes explained 45 percent of the entire data variability (Figure 9a), revealed a strong correlation between TRI and the axis 1 of the PCA, an axis interpreted as a soil and soil surface degradation axis. TRI appeared to be the lowest at high crust, high ρ_b and steep slopes. The second axis, which explained 17% of data variance, correlated with the rainfall characteristics (positive coordinates on axis 2) and the soil water tensions (negative coordinates on axis 2). TRI did not correlate with this axis interpreted as an axis of wetness status of the micro-catchment.

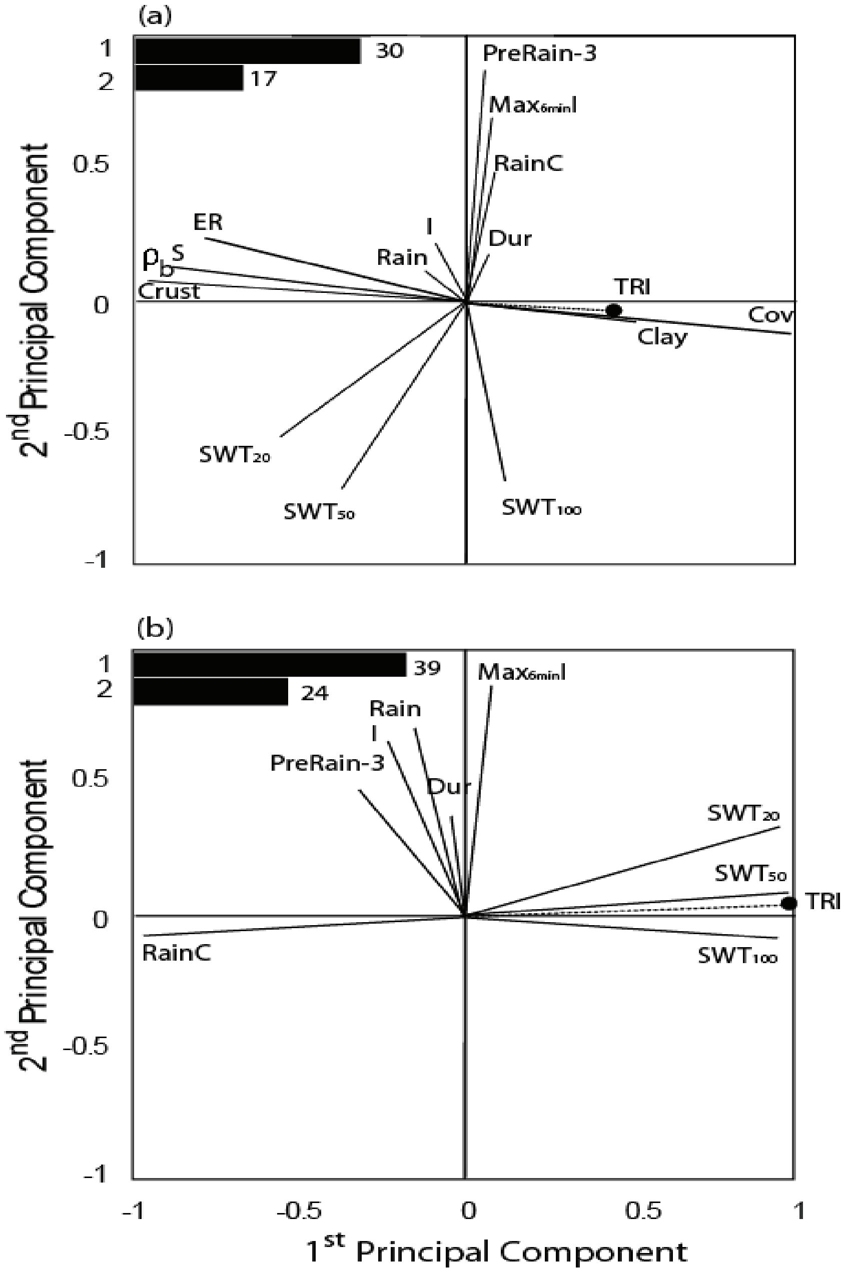

Figure 9. Principle Component Analysis of TRI and environmental variables for hillslope (a) and bottomland (b)

A second PCA has been generated using the data of only the bottomland location where the water table presence is expected to control OF generation (Figure 9b). This PCA explained 63 percent of the total data variability. The first PCA axis, which accounted for 39% of data variance, correlated the most with soil water content (from 20 to 100 cm depth) and RainC. It can be interpreted as an axis of bottomland soil wetness or water table establishment, soil wetness increasing as cumulative rainfall increased. The second PCA axis contrasts large and intense rainfall events with small and low intensity ones and can thus be interpreted as an axis of rainfall event characteristics. On the PCA, TRI correlated with axis 1 on which it showed a positive coordinate. These results revealed that the TRI, in the bottomlands, is primarily controlled by the soil wetness status in relation with water table establishment in rather than the characteristics of rainfall events. The TRI was shown to be high under dry soil conditions and close to zero when the water table reached the soil surface.

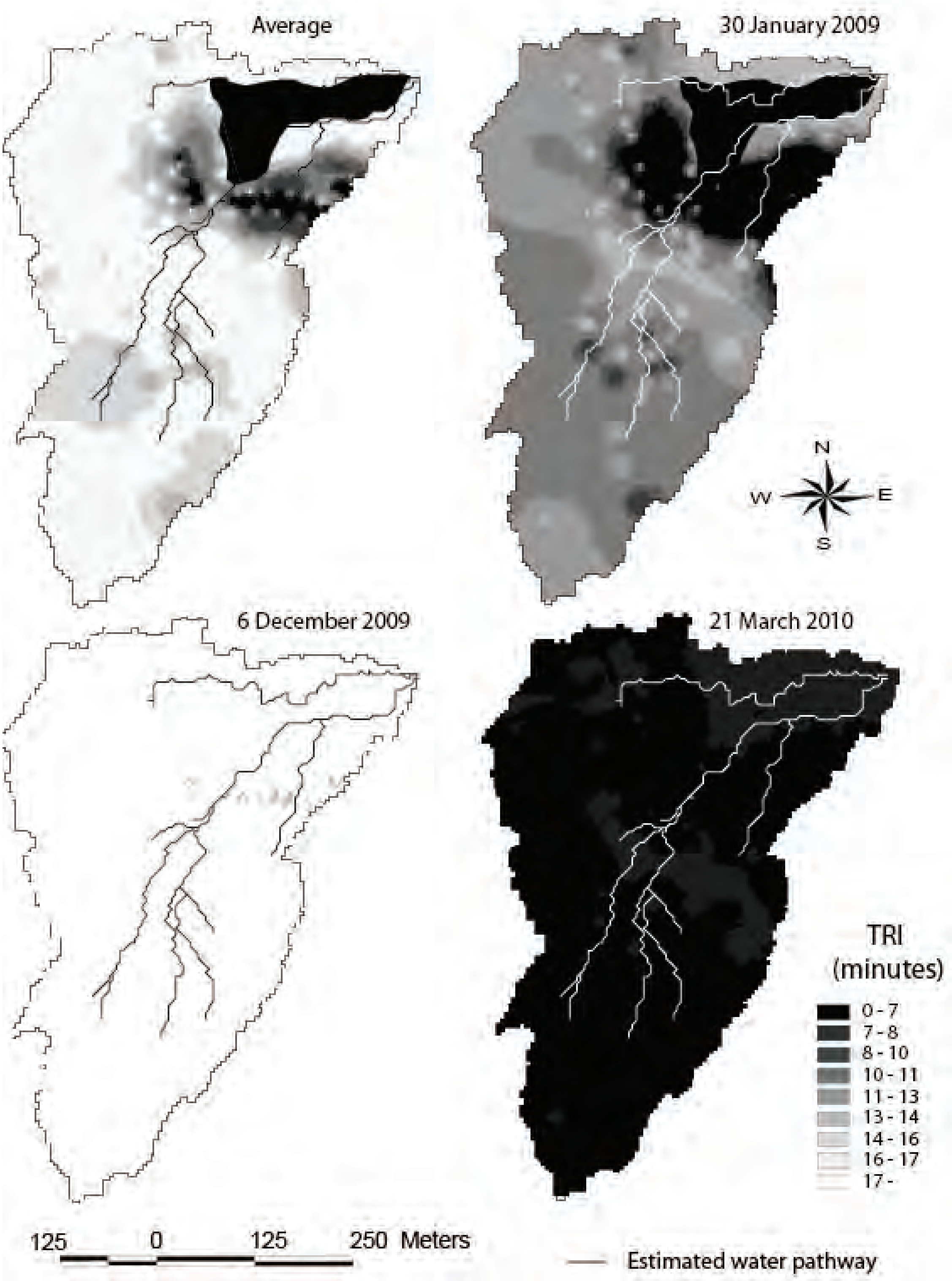

Figure 10. Spatial variations of TRI for three rainfall events of the 2007-2010 period. Data estimated at the micro-catchment level using Eq. 3.1 to 3.4

These results highlight a TRI control by the water table level in the bottomland and by soil surface features elsewhere in the micro-catchment. The strong relationship observed between TRI and soil crusting was used to evaluate the spatial and temporal variations of TRI within the micro-catchment, without bottomlands. In the bottomland, the TRI was zero when the soil surface horizon was saturated by water. Using this knowledge, simple regression models between TRI and soil crusting (Equations 4 to 7) were generated for three selected events and for the entire 2007-2010 period. The models, which explained between 59 and 95% of data variance, were applied to the whole micro-catchment (Figure 10) using a map of soil crusting spatial variations generated by Dlamini *et al*. (2011) and interpolated from 200 field observations and a map of bottomland extent generated for this study.

30-Jan-09:	$TRI = -0.259 \times Crust + 15.45$	$r^2=0.95$	**Equation 4**
06-Dec-09:	$TRI = -0.228 \times Crust + 38.26$	$r^2=0.72$	**Equation 5**
21-Mar-10:	$TRI = -0.128 \times Crust + 8.259$	$r^2=0.59$	**Equation 6**
Average:	$\boldsymbol{TRI = -0.139 \times Crust + 18.87}$	$\boldsymbol{r^2=0.65}$	**Equation 7**

The map of the average 2007-2010 TRI is displayed in Figure 10. From the model that explained 65% of data variability, the average TRI was 17.2 min with values between 4.9 and 18.9 min. The lowest TRI is expected to have occurred in the bottomland due to waterlogging conditions and at the middleslope position due to a high degree of crusting. In contrast, the TRI has been observed to have been the highest (>15 min.) on the steep convex crest and hillslope plateau, and at footslope under low crusting. The map for the 30th of January 2009 showed similar spatial trends, i.e. faster OF response to rainfall in the bottomland and middleslope than on the hillslope plateau. The model used to generate this map explained 95% of the TRI variance, which was the highest value among the selected events. On that date, TRI varied between 0 and 15.5 min. with an average of 12.3 min. The event of 6th December 2009 was characterized by an average TRI of 35 min. with values between 15 and 38 min. The faster OF response occurring at the middleslope position, where the soil surface crusting was the highest. The event of 21st of March 2010 showed the lowest data range (0<TRI<8.2 min.), indicating a more uniform OF response to rainfall. This model only explained 58% of TRI variance.

5. Water and its quality at different scales

5.1. Materials and Methods

5.1.1. Runoff flux monitoring

Runoff flux data from each of the catchment outlets, as well as the microplot and plot scale allowed for the calculation of the yields of water generated per unit area (in l/m^2). Overland flow generated within the plot and microplot area was manually measured after each rainfall event and was summed up at the end of each rainy season to determine the water generated per unit area (in l/m^2). The amount of water generated per unit area (in l/m^2) for the three catchment outlets was calculated directly from the automatically logged flow data where the time difference (s) between flows was multiplied by the average flux (l/s) to get a volume of water (l). Finally, this volume was then divided by the area of the catchment to obtain l/m^2. The spatial and temporal variations of the water fluxes for the different scales can, therefore, be easily quantified (both inter- and intra-season variability). Such data treatment results in a direct comparison of the different scales' productivity in terms of water movement.

5.1.2. Sediments fluxes

The total sediment fluxes corresponded to the mass of suspended sediments (about 200 samples per surface area per year, from 2009 to 2011) in the weir. Their dry weight (g) was evaluated after each rainfall event by drying the aliquot of water in an oven at 110°C. This was then multiplied by the volume of water (l) to get the sediment concentration (g/l). The sediment yields (g/m^2) for each nested scale was then calculated by multiplying the sediment concentration (g/l) by the runoff flux per unit area (l/m^2).

5.1.3. Nutrients fluxes

Water samples collected at the different spatial scales were used to assess the quality of the water. Water samples were collected both automatically (by the automatic samplers installed at the 23 ha and 100 ha catchment outlets) and manually (from runoff collecting buckets at the microplots and plots, and grab samples taken at all three catchment outlets during visits to the catchment). In addition, sampling was performed in the soil profile and in the groundwater following classical procedures (Allison and Walker, 2006; Gibson *et al*., 2006). The water quality constituents are the Nitrates-Nitrogen (NO_3-N), Total Phosphorus (P), Dissolved Organic Carbon (DOC), particulate carbon and nitrogen (POC, PON). Water samples were collected in the field by taking 100 mL aliquots and stored in a cooler box on site. Once back at the laboratory, samples were stored in a fridge, which was kept at a constant temperature of 4^oC until completion of analysis. The fluxes of nutrients were equal to the nutrient concentration multiplied by the flux of water.

5.1.4. Nitrates and total phosphorus measurement

NO_3^- and P concentration in water samples was obtained, using a HACH DR/2000 spectrophotometer (Hach Company 1989). The absorbances of the water samples were read, using a Hach DR2000 spectrophotometer and converted to concentrations (given as mg/l but converted to g/l), using frequently calibrated standard curves. The accuracy of all nutrient analyses were within 10% of the actual concentrations. Concentrations were converted to yields (in g/m^2) by multiplying the concentrations by the runoff flux per unit area (l/m^2).

5.1.5. Dissolved organic carbon

Dissolved organic Carbon (DOC) was determined after sampling, using a Shimadzu TOC-5000 analyzer with an ASI-5000 autosampler and Balston 78-30 high purity total organic carbon (TOC) gas generator. In this technique, the organic solutes were converted to CO2 and the CO2 produced is measured as DOC (in g/l). Concentrations were converted to yields (in g/m^2) by multiplying the concentrations by the runoff flux per unit area (l/m^2).

5.1.6. Particulate carbon and nitrogen

Sediments were dried at 105°C for 24 hours. The sediments were weighed to determine sediment concentration in runoff and ultimately to compute sediment losses. Sediment samples from these aliquots were dried and stored to be further analysed for total soil organic carbon and nitrogen. C and N were estimated, using a LECO CNS-2000 Dumas dry matter combustion analyzer. The output from this analysis Particulate organic carbon (POC) and particulate organic nitrogen (PON) is given as a percentage of total soil analysed. This percentage can be used to calculate the yields of POC and PON in (g/m^2) by multiplying the sediment yield (in g/m^2) by the percentage of POC and PON.

5.2. Results

5.2.1. Runoff fluxes at different scales

Data of cumulative water fluxes for the 2 seasons and for the different scales (1 m² for microplots; 5 m² for plots; 23 ha micro-catchment; 100 ha catchment; and 1000 ha catchment) are presented in Figure 11.

For the first rainy season (2009/2010) the greatest cumulative volume of water generated was observed for microplots (average of 58.6 L m^{-2} y^{-1}, n=15 *vs.* 41.3 L m^{-2} y^{-1} for plots, n=10). The first overland flow event on 1x1 m² occurred on 06 October 2009, after there had been 11.2 mm of rainfall since the start of the rainy season. The first overland flow on 5x2 m² plots occurred at the end of November 2009, which corresponded to a cumulative rain since the rainy season onset of 173 mm. Such a result indicated that runoff generation at this scale was more dependent on the antecedent soil moisture status of the soil than on microplots. The average runoff coefficient estimated using an annual rainfall amount of 628 mm was 9.3% on microplots and 6.6% on plots.

The 2010/2011 rainy season exhibited much higher cumulative overland flows at both spatial scales (1×1 m and 5 m×2 m). The increase was from 58.6 to 208.0 L m^{-2} y^{-1} for microplots and from 41.3 to 350.0 L m^{-2} y^{-1} for plots. The resulting runoff coefficients for this wetter year (1059.2 mm of cumulative rain) were 19.6% for microplots and 33.0% on plots.

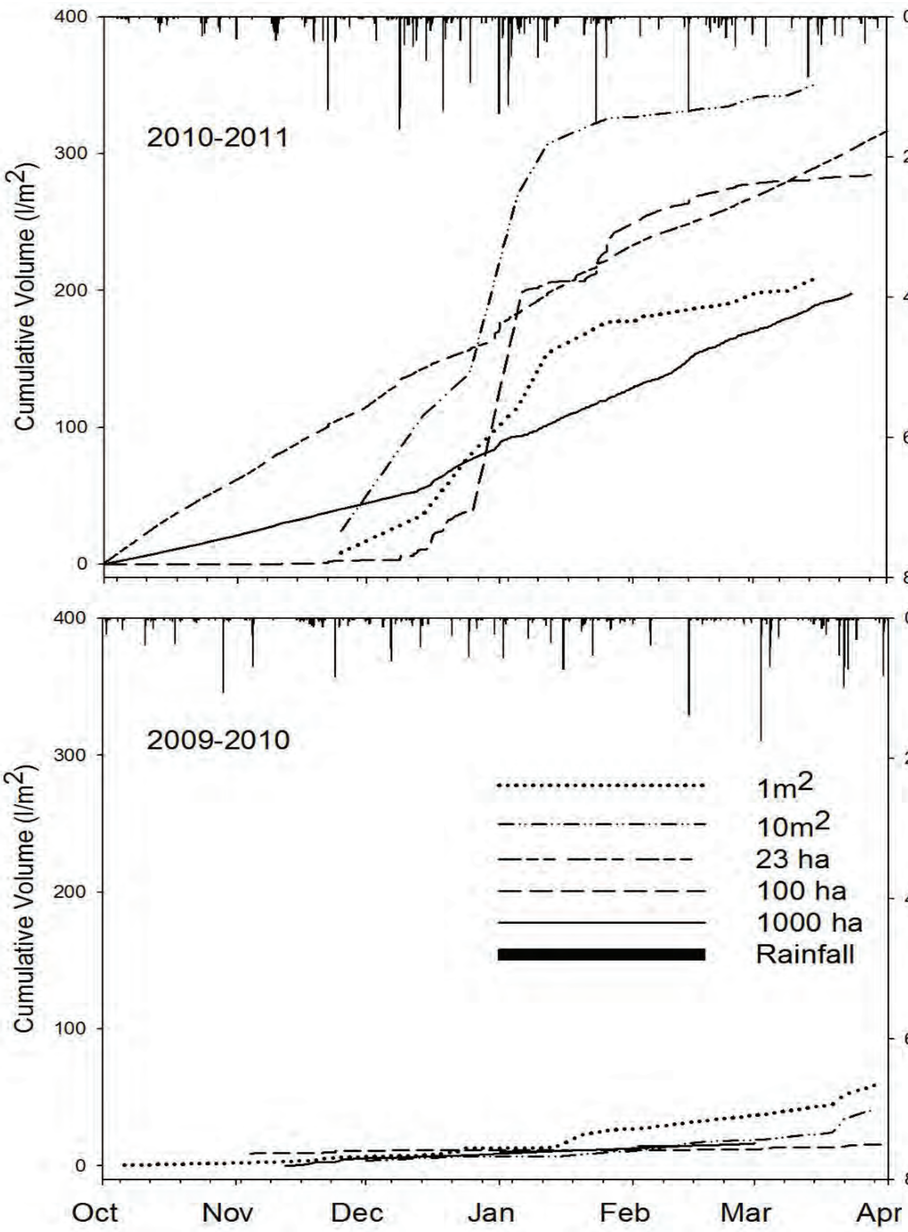

Figure 11. Cumulative runoff volume per unit area for the 2 seasons of the different scales monitored in the research catchment (in l/m^2)

The first overland flow event in 2010/2011 occurred on 25 November 2010 which corresponded to an antecedent rainfall of 201.6 mm. The general trend for this season was for the 10 m² plots to produce more overland flow than the microplots. The plots were the most productive out of all the monitored scales within the catchment. The 1 m^2 microplots were the fourth most productive scale. The 10 m² plots appear to be more sensitive to rainfall as a result of the steepness of the cumulative curve while microplots show a more gradual increase of cumulative flux over time.

The 23 hectare catchment shows a relatively constant flow over time as exhibited by a linear shape for the line of cumulative fluxes. The yearly cumulative flux was 316 L m^2 y^{-1} in

2010/2011 (rainy season at which the catchment was instrumented) which made it the second most productive scale (with a runoff coefficient of 29.8% in relation to annual rainfall). The existence of constant flows (presence of low flows during dry periods together with slight flow increases during rainfall events) points to the existence of a source of water in the subsurface which acts as a buffer between overland flow generated on slopes and the catchment runoff of the river network.

At 100 ha, the cumulative flux was 16.66 L m^2 y^{-1} (this corresponded to a runoff coefficient of 2.6%). The first recorded change in water flux at the 100 hectare catchment occurred after there had been 74 mm of rainfall recorded in total since the onset of the rainy season. There was minimal flow throughout the rainy season indicative of the impact that the quantity of rainfall has on the hydrological response of the 100 hectare catchment. There was a greater amount of rainfall in the month of March 2010 and the flux of water at the 100 hectare catchment does increase.

The 100 hectare catchment initially displayed a slow response to rainfall. It appeared that the hydrological response of this catchment outlet was dependent on the antecedent moisture status of the catchment. The first monitored flow at the 100 hectare catchment occurred on the 10 November 2010. The amount of rainfall that had occurred since the start of the rainy season (01 October 2010) totalled 133.4 mm. Once this rainfall amount had fallen, there was consistent low flow occurring at the 100 hectare scale through to the middle of December 2010. From the middle of December 2010, there was a sudden increase in the amount of cumulative flow. This coincided with a period of high rainfall amounts. From this period the 100 hectare catchment produced large quantities of flow until the start of January 2011. In a period from the middle of February to the middle of March 2011, the 100 hectare catchment produced more flux than the 23 hectare catchment. This period, again coincided with a period high rainfall and pointed to the flux at this scale being antecedent soil moisture content driven whereby large amounts of flux occurred when the catchment was wet. The 100 hectare catchment was the third most responsive monitored scale for this study period (284 l/m^2). This cumulative flux value corresponded to a runoff coefficient of 26.8%.

At the 1000 ha catchment outlet, the cumulative runoff flux was 16.25 L m^2 y^{-1} in 2009/2010 and 197.6 L m^2 y^{-1} in 2010/2011. These cumulative flux values corresponded to runoff generation ratios (calculated in terms of the total seasonal rainfall amounts) of 2.6 (2009/2010) and 18.7% (2010/2011) respectively. The yearly fluxes were ranked last among the study scales but fluxes appeared second in 2010/2011 at the early stages of the rainy season. It was interesting to note that during this period, the cumulative flux showed a lower slope than that of the end of the rainy season.

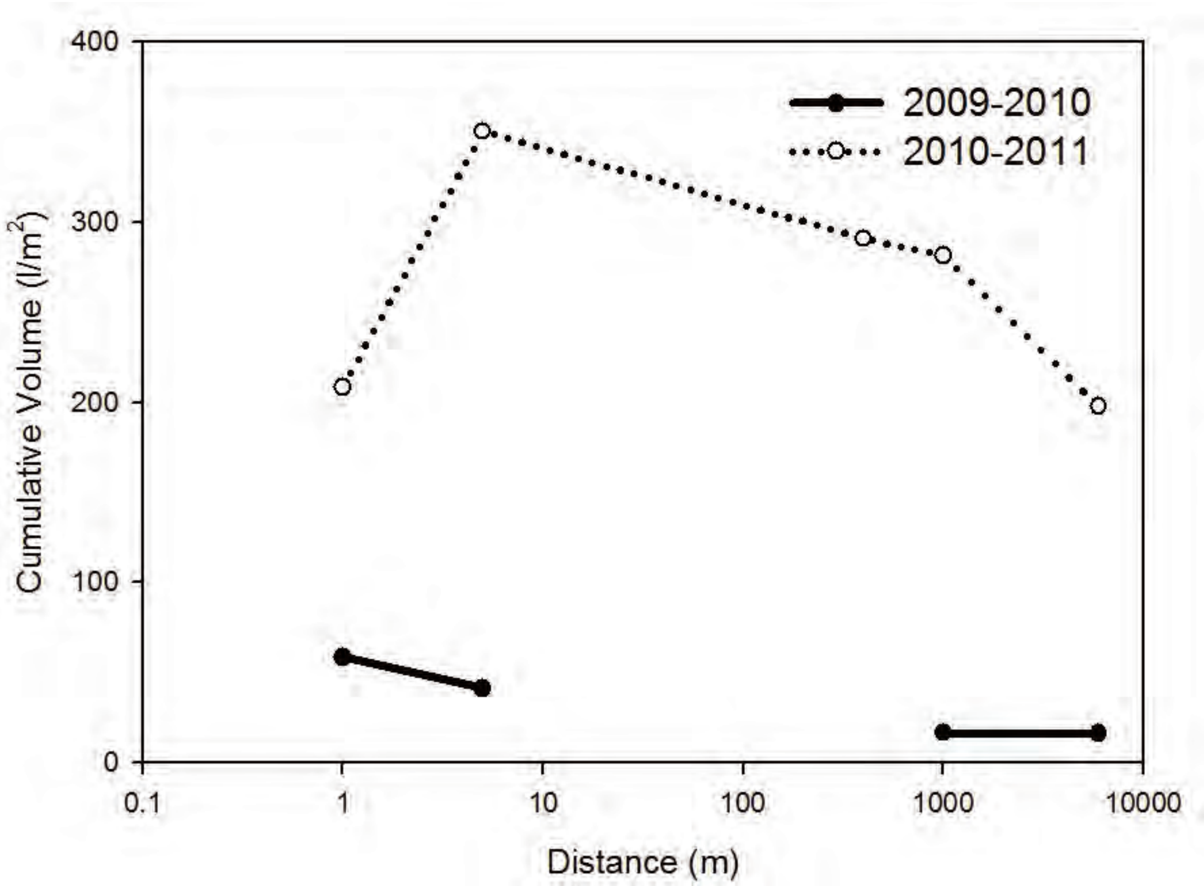

Figure 12. Cumulative yearly flux of the water as a function of distance from catchment upper limit for the 2 rainy seasons. One metre corresponds to microplots data; 5 m to plots; 500 to 23 ha; 1000 m to 100 ha and 5000 m to 1000 ha

A summary of cumulative yearly fluxes at the different spatial scales (plotted as a function of longest flow path for each nested scale; determined from the catchment Digital Elevation Model) is presented in Figure 12. In order to understand (and explain) the variations in the flux of water at the different scales, the use of the longest flowpath distance of each individual nested scale from the catchment upper limit can be helpful in highlighting the spatial variations in the generation of water flux. As was shown in Figure 12, the 2009/2010 rainy season had fluxes that were significantly lower than the fluxes that were generated in the 2010/2011 rainy season.

In 2009/2010, the 1 m^2 microplots generated the most water per unit area out of the scales. With an increase in the distance from the catchment limit, there was a decrease in the amount of water per unit area generated at the nested scales with the 10 m^2 runoff plots (5 m distance) generating the second highest amount of water, followed by the 100 hectare catchment outlet (1000 m distance) and finally the 1000 hectare catchment outlet (6000 m distance). Since there was no data available for the 23 hectare catchment outlet (400 m distance), one can assume that the amount of water generated at the this catchment outlet would be between the amount of water generated at 10 m^2 runoff plots and the 100 hectare catchment outlet.

The rainy season of 2010/2011 shows a significantly higher amount of runoff generated at the nested scales. In contrast to the 2009/2010 rainy season, the 1 m^2 microplots did not generate the highest flux of the nested scales. A greater quantity of flux was generated at the 10 m^2 runoff plots (5 m distance; the greatest amount of flux generated), 23 hectare catchment outlet (400 m distance; second highest amount of flux generated) and the 100 hectare catchment outlet (1000 m distance; third highest amount of flux generated) than at the 1 m^2 (1 m distance; fourth highest amount of flux generated). This change in behaviour could be a result of there being a methodological error associated with the 1 m^2 microplots whereby there was preferential infiltration at the metal borders of the microplot perimeter. The decrease from 5 m to 1000 m is linear indicating that there was possibly a constant decrease in the amount of water being delivered to each site (*i.e.* infiltration and/or evaporation). The least productive scale was that of the 1000 hectare catchment outlet (6000 m distance). The cumulative flux at both the 1 m^2 microplot scale and the 1000 hectare catchment outlet was similar. The decrease in flux between the distances of 1000 m and 6000 m (100 hectare catchment and 1000 hectare catchment outlets respectively) could be pointing to higher infiltration (along the stream channel) and evaporation (as a result of the storage dams located between the two catchment outlets). The use of environmental tracers such as the stable isotopes of water could be a useful tool to support such an issue.

5.2.2. Sediment fluxes at the different spatial scales

The cumulative sediment yields for 2 different rainy seasons (2009/2010 and 2010/2011) are presented in Figure 13. At first glance it is noticeable that the 2 seasons were inherently different, with the 2010/2011 rainy season having considerably higher sediment yields (at all observation scales) than the 2009/2010 rainy season.

With regards to the 2009/2010 season, all scales showed a slow accumulation of sediment yields. The first scale that showed any response was that of the 1 m^2 microplots. The next scale that responded was that of the 100 hectare catchment outlet followed by the 1000 hectare catchment outlet and finally the 10 m^2 runoff plots. The 10 m^2 runoff plots showed the highest sediment loads for any specific event (*i.e.* the 10 m^2 runoff plot curve had the steepest gradient of any of the observation scales' curves) with the 1×1 m^2 microplots having the next highest event sediment yield.

The 2009/2010 rainy season accumulated sediment yields for the different scales indicated that the 10 m^2 runoff plots had the highest sediment yield (122.74 g/m^2) followed by the 1 m^2 microplots (72.11 g/m^2), 100 hectare catchment outlet (0.83 g/m^2) and finally the 1000 hectare catchment outlet (0.16 g/m^2).

At first all the observation scales showed little to no accumulated sediment yields. The first scale that showed an increase in accumulated sediment yields was that of the 23 hectare catchment outlet. Subsequently, the 5×2 m^2 runoff plots and 1 m^2 microplots responded at the same time. Both of the hillslope scales showed a gradual increase in sediment yields as a response to erosive rainfall events. At the end of the rainy season, both hillslope scales' curves did taper off. The 100 hectare and 1000 hectare catchment outlets both exhibited a slow accumulation of sediment yields, with the 100 hectare catchment outlet responding before the least responsive observation scale, the 1000 hectare catchment outlet. In terms of the greatest event specific sediment yields, the 23 hectare catchment exhibited the greatest instantaneous change in sediment yields.

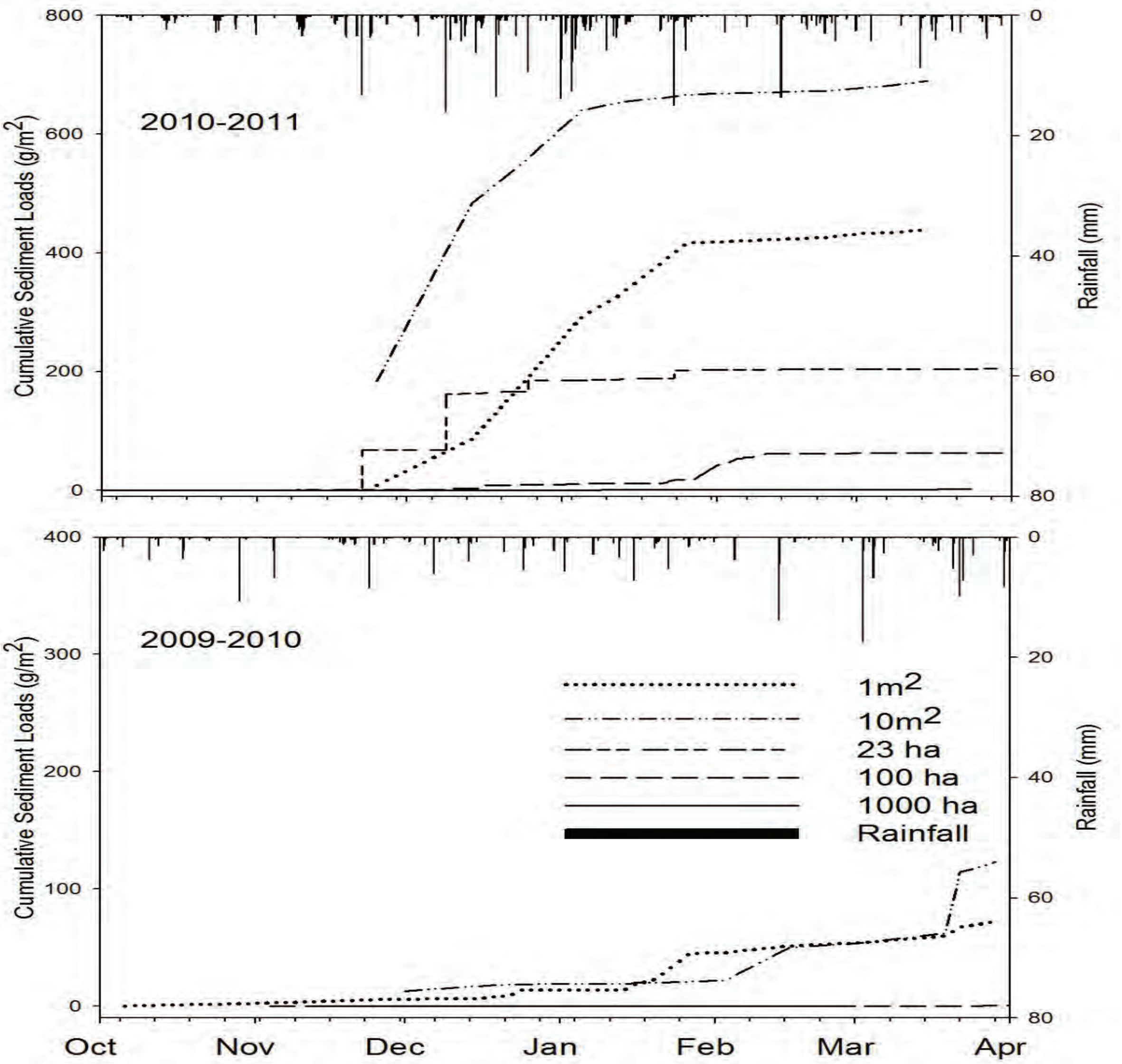

Figure 13. Cumulative sediment loads for the 2 seasons of the different scales monitored in the research catchment (in g/m^2)

From Figure 13, the final accumulated sediment yields for the different scales are shown. The scale with the highest sediment yield was that of the 10 m^2 runoff plots (689.92 g/m^2). The scale with the next highest sediment yield was that of the 1 m^2 microplots (439.86 g/m^2), then the 23 hectare catchment outlet (204.97 g/m^2), 100 hectare catchment outlet (62.93 g/m^2) and finally the 1000 hectare catchment outlet (1.98 g/m^2).

In terms of water fluxes (as presented in Figure 11), it appeared that on the hillslope, sediment yields increased with greater surface water flux along the hillslope. The sediment yield transport between the hillslope and the 23 hectare catchment appeared to be low as there was difference in sediment yields between the two. The sediment yield data for the 23 hectare and 100 hectare catchment outlets indicated that there was low continuity possibly due to an increase in sedimentation between the two catchment outlets. The 1000 hectare catchment outlet sediment yield data highlights the influence that the storage dams immediately upstream from the sampling site had on the transport of sediments. All soil particles (sand, silt and clay) would have been deposited within the dams. This would have resulted in the decrease in the sediment yield observed at the 1000 ha catchment outlet.

5.2.3. Nitrate fluxes

Table 6 displays the basic statistics of the concentration of dissolved nitrates (NO_3^--N) of the nested scales.

Table 6. Basic statistics of the concentrations of the dissolved elements and particulate elements of the nested scales (n = 160)

		1 m^2	10 m^2	23 ha	100 ha	1000 ha	Hillslope Piezometers	Boreholes
Dissolved (mg/L)								
NO_3^-	Mean	27.10	29.65	14.46	30.58	9.65	40.74	5.18
	Stdev	26.72	25.59	5.71	30.74	1.13	48.98	5.39
P	Mean	0.56	0.50	0.11	0.19	0.06	1.01	0.07
	Stdev	0.58	0.60	0.04	0.11	0.05	1.18	0.05
DOC	Mean	40.52	42.61	15.90	33.65	32.50	105.31	45.39
	Stdev	52.25	43.30	20.29	31.73	36.79	72.56	49.99
Particulate (g/100 g of sediment)								
C	Mean	5.82	3.94	4.30	0.10			
	Stdev	1.48	0.99	0.98	1.35			
|	Mean	0.59	0.35	0.24	0.10			
	Stdev	0.23	0.07	1.23	0.64			

The average nitrate concentration for the different scales had a range between 9.65 mg/l (1000 hectare catchment) and 30.58 mg/l (100 hectare catchment). Similar nitrate concentrations were found at the 1 m^2 microplot scale (27.10 mg/l) and the 10 m^2 runoff plot scale (29.65 mg/l). The nitrate concentration of the 23 hectare catchment scale (14.46 mg/l) was found to be lower than what was found from both sets of runoff plot scales. Therefore, it was apparent that the nitrate concentration decreased from the runoff plot scale to the 23 hectare catchment outlet from where the concentration increases to the 100 hectare catchment and finally a decrease to the 1000 hectare catchment. There was a great deal of variability of the nitrate concentration with the 100 hectare catchment having the highest standard deviation (30.74 mg/l). The monitored scale with the smallest deviation was the 1000 hectare catchment (Stdev = 1.13 mg/l).

In terms of the nitrate concentrations for the monitored groundwater sampling points, it was found that there was a higher mean concentration in the hillslope piezometers (40.74 mg/l) than the groundwater monitoring boreholes (5.18 mg/l). The hillslope piezometers showed a variable total phosphorus concentration (Stdev = 48.98 mg/l) with the boreholes being considerably less variable (Stdev = 0.07 mg/l).

From the mean nitrate concentrations of the different sampling points and scales, it is evident that there possibly 3 different behaviours occurring within the catchment. Firstly there appears to be some sort of nitrate depletion from the hillslope (the 1×1 m^2 microplot scale, the 5×2 m^2 runoff plot scale and the hillslope piezometers) to the 23 hectare catchment. Secondly, it seems as if there additional contributions to the 100 hectare catchment. Thirdly the 1000 hectare catchment has a similar nitrate concentration as the deep groundwater/boreholes.

The cumulative nitrate loads for the different scales for the period of October 2010 to April 2011 is shown in Figure 14. From Figure 14, it is noticeable that the nitrate loads at the different monitored scales are inherently different. The curves show that for all scales, there was a consistent and steady yield of nitrates coming from these scales. However, the 100 hectare catchment outlet showing the greatest change in nitrate loads, *i.e.* the greatest instantaneous change in cumulative nitrate loads.

The range of the cumulative nitrate loads for the different monitored scales was between 0.04 g/m^2 (1000 ha catchment outlet) and 10.38 g/m^2 (5×2 m^2 runoff plots). The scale with the second highest Nitrate yield was the 100 hectare catchment outlet (8.7 g/m^2) followed by the 1×1 m^2 microplots (5.65 g/m^2) and the scale with the fourth highest nitrate yield was the 23 hectare catchment (4.57 g/m^2).

From the curves plotted, it was noticeable that the monitored scales located on the hillslope had different yields. It would appear that there could be a link between the nitrate loads occurring as overland flow over long distances. However, the nitrate loads for the 23 hectare catchment outlet are lower than that of both the microplot and plot scales. From the 23 hectare catchment outlet to the 100 hectare catchment outlet, the nitrate loads increased indicating that have been some additions of nitrate from the landscape between the two monitored scales to the streamflow. Further along the stream, the nitrate load decreases to the 1000 hectare catchment outlet. The influence of the 2 small storage dams located upstream from the sampling point may have had an influence on the nitrate loads calculated by storing and impeding the transport of the Nitrates from upstream.

Table 6 lists the different scales' mean particulate organic Nitrogen (PON) values per 100 grams of sediment. The scale with the highest composition of PON was the 1 m^2 microplots (0.59 g N/100 g sediment). The scale with the next highest PON composition was that of the 10 m^2 runoff plots (0.35 g N/100 g sediment), then the 23 hectare catchment outlet (0.24 g N/100 g sediment) and then finally the 100 hectare catchment outlet (0.10 g N/100 g sediment). The scales were found to have variable PON compositions with the 23 hectare catchment outlet being the most variable (Stdev = 1.23 g N/100 g sediment) and the 5×2 m^2 runoff plots being the least variable (Stdev = 0.07 g N/100 g sediment).

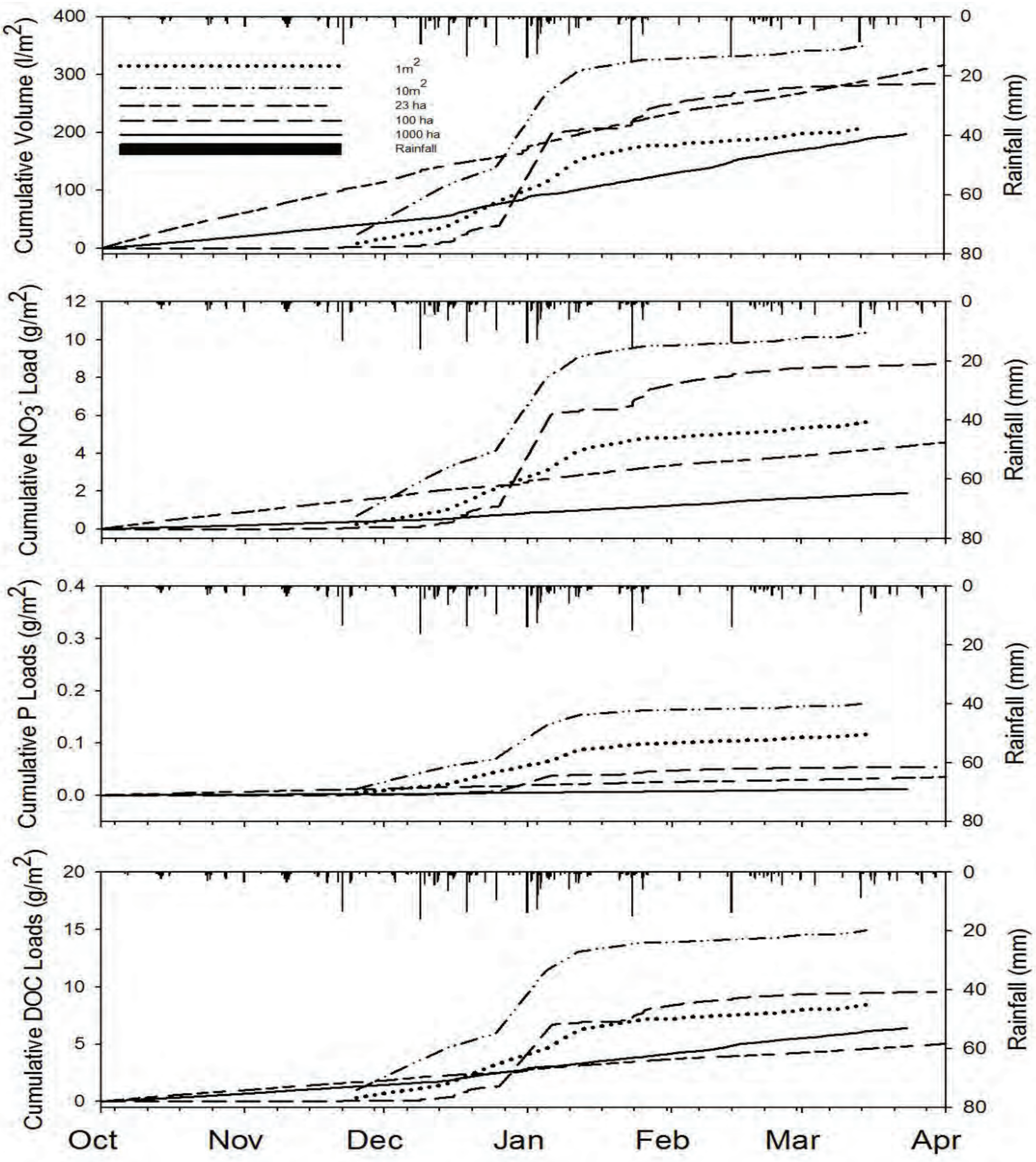

Figure 14. Cumulative Dissolved Nutrient Loads (in g/m^2) of the different nested scales for the 2010/2011 rainfall season

Figure 14 shows the PON yields for the 5 different nested scales. There was a distinct spatial variability in the loads of PON. The nested scale with the highest particulate N yield was that of the 10 m^2 runoff plots (2.76 g/m^2). The nested scale with the second highest PON yield was that of the 1 m^2 microplots (2.64 g/m^2). Following the 1 m^2 microplots, the 23 hectare catchment outlet was the third highest PON yield (0.41 g/m^2). Finally, the nested scale with the fourth and lowest PON yield was that of the 100 hectare catchment outlet (0.06 g/m^2).

5.2.4. Total phosphorus fluxes

Table 6 shows the basic statistics of the concentration of dissolved Total Phosphorus of the nested scales. The mean concentration of the total phosphorus for the monitored surface scales has a range between 0.06 mg/l (1000 hectare catchment) to 0.56 mg/l (1 m^2 microplots). Similarly to the behaviour of the nitrate concentration whereby there are similar total phosphorus concentrations for both the 1×1 m^2 microplot scale and the 10 m^2 runoff plot scale (0.5 mg/l). The mean total phosphorus concentration decreased at the 23 hectare catchment outlet (0.11 mg/l) and then increased at the 100 hectare outlet (0.19 mg/l). Finally, the total phosphorus decreased to the 1000 hectare catchment outlet (0.06 mg/l). The total phosphorus concentration was the most variable at 10 m^2 runoff plot scale (Stdev = 0.60 mg/l) with the 23 hectare catchment outlet being the least variable (Stdev = 0.04 mg/l).

In terms of the concentration of total phosphorus for the monitored groundwater zones there was a higher concentration for the shallow groundwater (1.01 mg/l for the hillslope piezometers) than the deep groundwater (0.07 mg/l for the boreholes). There were fluctuations in the measured total phosphorus concentration for the Hillslope piezometers (Stdev = 1.18 mg/l) with the borehole total phosphorus being less variable (Stdev = 0.05 mg/l). Figure 14 shows the cumulative total Phosphorus yields of the different nested scales for the 2010/2011 rainy season. The cumulative Total Phosphorus loads (g/m^2) curves for all 5 monitored scales within the Potshini Catchment indicates that the Total Phosphorus yields, initially, did not vary. However, the first observation scale to have a response (an increase in curve gradient), in terms of Total Phosphorus yield, was that if the 10 m^2 runoff plots. The next scale to exhibit a change in the yield Total Phosphorus was that of the 1 m^2 microplots, followed by the 100 hectare catchment outlet, 23 hectare catchment outlet and finally the 1000 hectare catchment outlet.

The final cumulative Total Phosphorus yields show that the order of the highest yields was as follows: 10 m^2 runoff plots (0.18 g/m^2), 1 m^2 microplots (0.12 g/m^2), 100 hectare catchment outlet (0.05 g/m^2), 23 hectare catchment outlet, and finally the 1000 hectare catchment outlet (0.01 g/m^2). There are similar loads for the monitored scales at the hillslope level with the 10 m^2 runoff plots (larger scale) having a slightly greater Total Phosphorus yield of 0.06 g/m^2 than the 1 m^2 microplot scale. When comparing the hillslope scale to the 23 hectare catchment outlet, the catchment loads decreased from the hillslope. However, the loads increased from the 23 hectare catchment outlet to the 100 hectare catchment outlet. This indicated that there were additions to the system between the two observation scales. The 1000 hectare indicated that there was a net loss in the total Phosphorus load which could be caused by retardation and storage within the storage dams located immediately upstream of the observation scale.

5.2.5. Dissolved organic carbon fluxes

Table 6 displays the basic statistics of the concentration of DOC at the different nested scales The mean DOC concentration ranged from 15.90 mg/l (23 hectare catchment outlet) to 42.61 mg/l (5×2 m^2 runoff plots) for the surface hydrological process zones monitored. The 1 m^2 microplots had a mean DOC concentration that was slightly lower than that of the 10 m^2 runoff plots (40.52 mg/l). From the 23 hectare catchment outlet, the mean DOC concentration was found to have increased at the 100 hectare catchment outlet (33.65 mg/l) possibly as a result of additions coming from elsewhere in the landscape. The mean concentration of DOC at the 1000 hectare catchment outlet was 32.50 mg/l which was only slightly lower than that of the mean DOC concentration at the 100 hectare catchment outlet. The standard deviations of the different sampling sites indicate highly variable DOC concentrations with the Stdev varying between 31. 73 mg/l (100 hectare catchment outlet) and 52.25 mg/l (1×1 m^2 microplots).

The mean DOC concentration for the two different subsurface monitoring zones show that the hillslope piezometers had a higher mean DOC concentration (105.31 mg/l) than the boreholes (45.39 mg/l). It was found that the mean DOC concentration was more variable in the hillslope piezometers (Stdev = 72.56 mg/l) than in the monitored boreholes (49.99 mg/l).

The cumulative DOC yields (g/m^2) of all monitored scales for the 2010/2011 rainy season is shown in Figure 3.7. The yields of the three catchments, initially, did not vary. However, due to the consistent flow occurring at the 23 and 1000 hectare catchment outlets, there was a consistent load of DOC at these two catchment outlets. The 100 hectare catchment outlet only started transporting DOC loads when some flow occurs but the 100 hectare catchment outlet was the monitored scale that exhibited the steepest cumulative curve. The hillslope scales (1×1 m^2 microplots and the 5×2 m^2 runoff plots) were the last scale to respond, with the 5 mx2 m runoff plots being more responsive than the 1 mx1 m microplots.

In terms of the final cumulative DOC yield values for the different scales, the 5×2 m^2 runoff plots had the highest DOC yield (14.92 g/m^2). This was then followed by the 100 hectare catchment outlet (9.58 g/m^2), 1×1 m^2 microplots (8.44 g/m^2), 1000 hectare catchment outlet (6.42 g/m^2) and finally the 23 hectare catchment outlet (5.03 g/m^2).

The different accumulated yields for the monitored scales located on the hillslope could be attributed to the greater overland flow response of the 5×2 m^2 runoff plots. There was a decrease in the DOC from the hillslope to the 23 hectare catchment outlet. In contrast there was an increase in the DOC yield from the 23 hectare catchment outlet to the 100 hectare catchment outlet. There was increase in the DOC yield from the 1000 hectare catchment outlet to the 1000 hectare catchment outlet

5.2.6. Particulate organic carbon fluxes

In Table 6, the mean particulate organic Carbon (POC) fluxes for the different scales is shown. The scale with the highest mean particulate C was that of the 1 m^2 microplots (5.8 g C/100 g sediment). The scales with the next highest amount of mean particulate C was that of the 23 hectare catchment outlet (4.30 g C/100 g sediment) followed by the 10 m^2 runoff plots (3.94 g C/100 g sediment) and finally the 100 hectare catchment outlet (0.10 g C/100 g sediment). The nested scale with the most variable particulate C was that of the 1 m^2 microplots (Stdev = 1.48 g C/100 g sediment) and the least variable nested scale was the 23 hectare catchment outlet (Stdev = 0.98 g C/100 g sediment).

Figure 3.8 displays the yields of particulate nutrients for all the nested scales monitored In terms of the particulate C yields there was a high spatial variability. At the hillslope scale, the 5×2 m^2 runoff plots had a higher particulate C yield (26.91 g/m^2) than the 1 m^2 microplots (25.51 g/m^2). The particulate C yield decreased from the hillslope to the 23 hectare catchment outlet (8.18 g/m^2) and decreased even further to the 100 hectare catchment outlet (0.06 g/m^2).

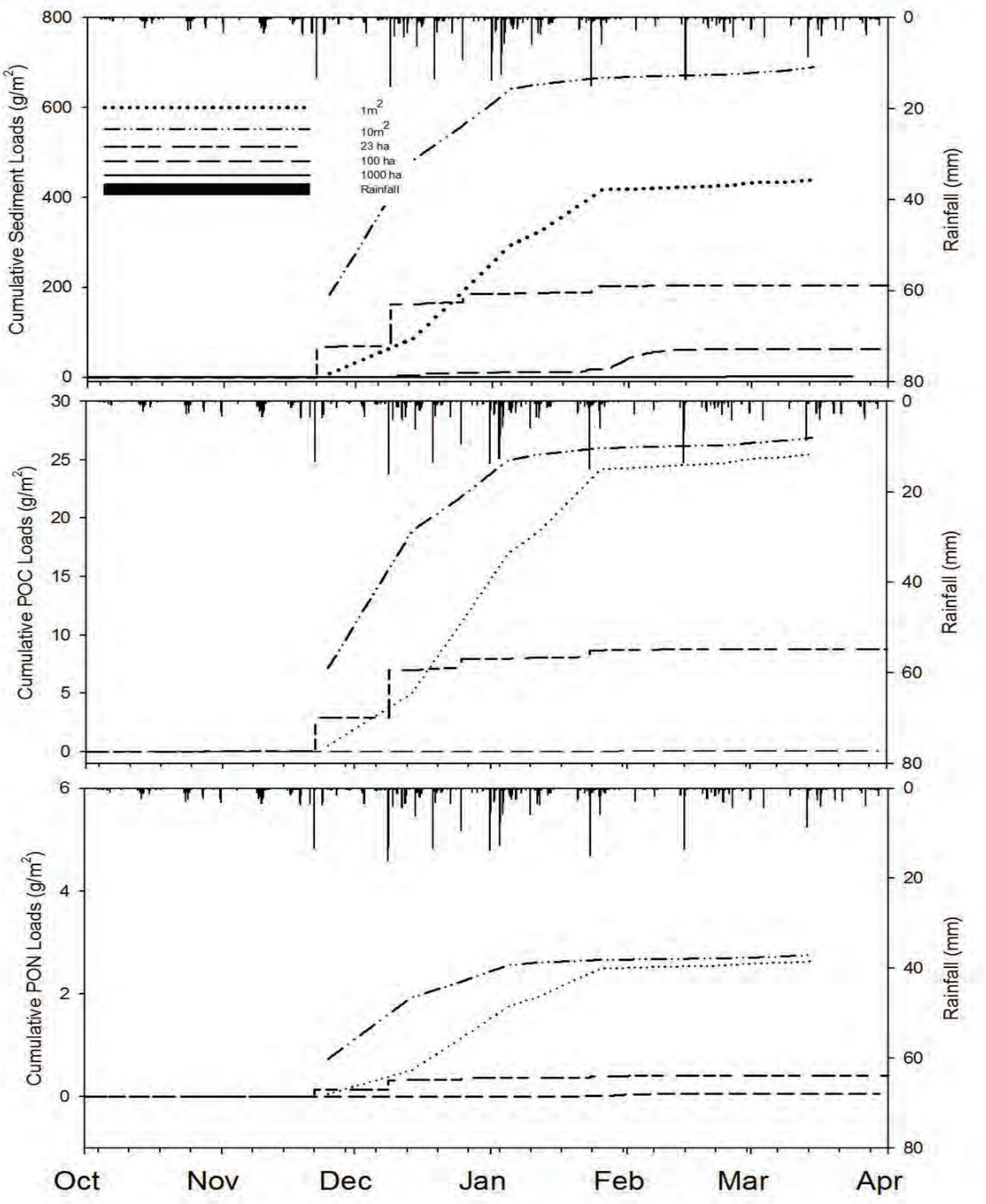

Figure 15. Sediment Loads and selected particulate nutrient loads of the different scales monitored for the 2010/2011 season.

6. Origin of water at catchment outlets

6.1. Tracers and end member mixing analysis

One commonly-used application of stable water isotopes, is aimed at the identification of river flow sources, *e.g.* rainwater, overland flow or groundwater flow, with the composite signature in the river being an indicator of the portion of the different sources contribution. The water samples were analyzed for the isotopes of water, δ^2H and $\delta^{18}O$, using the Liquid-Water Isotope Laser Analyzer at the School of Bioresources Engineering and Environmental Hydrology, University of KwaZulu-Natal (Los Gatos Research, 2007). The OA-ICOS technique uses the absorption of a laser beam passing through an evaporated water sample to calculate the isotopic composition of the sample (Los Gatos Research, 2007). The laser scans the isotopes' spectral absorption, so the technique can detect several isotope species simultaneously. Sample measurements were calibrated with five standards, which were iteratively measured after each set of five sample measurements. Each measurement was conducted 6 times to provide a high value precision. Results are presented in δ notation, *i.e.* parts-per-million deviations from Vienna Standard Mean Ocean Water (V-SMOW) as δ^2H and $\delta^{18}O$.

The oxygen and deuterium isotope ratios of the water collected at the different water source zones, as well as in shallow to deep aquifers (through the use of existing boreholes), will allow for the understanding of the movement of water through the different pathways in the catchment. Analysis was done on water samples that were automatically collected by the automatic samplers and grab samples at all the nested scales.

The use of isotopes of the different monitored hydrological zones in conjunction with other naturally-occurring tracers, such as Silica, allows for the determination of end member mixing at a catchment's outlet and its different sources as used by Uhlenbrook and Hoeg (2003). Hydrograph separations, the stable isotopes of water determine the new event water and old water (*i.e.* pre-event water). In addition, the use of silica (determined using a Technicon TRAACS 2000 continuous flow auto-analyzer) in conjunction with the stable isotopes of water, can be used to differentiate between the reactive water (that flowed through the soil compartment) and the unreactive water (that had minimum soil contact, *i.e.* overland flow) (Huth *et al.*, 2004). The end member mixing analysis of the 23 hectare micro-catchment and 100 hectare catchment outlets, are determined using Equations 8 and 9, respectively. These were utilised by Huth *et al*. (2007) in a study conducted in a catchment located in the Sierra Nevada, California.

$$Q_n = \frac{Q_s \times (C_s - C_o)}{(C_n - C_o)}$$ **Equation 8**

$$Q_r = \frac{Q_s \times (C_s - C_{unr})}{(C_r - C_{unr})}$$ **Equation 9**

$$Q_{unr} = \frac{Q_s \times (C_s - C_r)}{(C_{unr} - C_r)}$$ **Equation 10**

Where Q_n is the event water flux, Q_s is the discharge when the sample was taken, C_s the concentration of the water at the catchment outlet, C_o the pre-event water (groundwater), C_n the new water, *i.e.* rainfall, Q_r the soil water contribution, Q_{unr} the contribution from the unreactive water, *i.e.* overland flow, C_{unr} concentration of overland flow from runoff plots, and C_r concentration of soil water which was collected from piezometers. For reactive and unreactive water fractions, the water samples of both the runoff plots and piezometers were analysed for their silica (Si) content as Si has been found to differentiate between reactive water and unreactive water. From Equations 9 and 10, the amount of water stored within the soil profile can be calculated using Equation 11.

$$Q_{nsw} = Q_n - Q_{unr}$$ **Equation 11**

Where Q_{nsw} is the event water generated from the soil profile and interpreted as the contribution of soil water to catchment runoff.

Hydrograph separations and end member mixing analysis are used to better understand the spatial and temporal variations in runoff and nutrient fluxes. Such an approach gives insight into the sources as well as the response of the catchment runoff. An in-depth analysis will not be attempted, as whole research projects are dedicated to hydrograph separations and end member mixing analysis. The end member mixing analysis performed in this study is an initial attempt.

6.2. Isotopic and tracer data

Concentrations of selected dissolved elements as a function of distance from catchment upper limit are displayed in Figure 16.

Water collected from microplots (Distance of 1 m), plots and the 23 ha catchment (distance=600 m) were enriched in N-NH_3, N-NO_3^-, Al, and depleted in Na, Si, Mg, Ca. The 23 ha outlet water showed a higher concentration in Si, Fe, Ca, Mg, Na than the hillslope runoff but showed similar concentrations as water sampled from the piezometers. The deep groundwater (25 meters depth) was depleted in most of the measured elements such as both N species, Fe, Mg, Al but enriched in Na (24 mg/L). Water from the 100 ha catchment outlet exhibited depletion in these elements except Na, which was found in much higher concentration than at the other spatial scales. The 1000 ha outlet showed enrichment in all elements especially Ca, Mg, Fe and Si while N and Na concentrations remained in the same order as found at 100 ha. Figure 16 displayed the evolution of isotopes from the hillslope to the 1000 hectare catchment outlet. The general pattern within the landscape was for both isotopes to be depleted from 1 m^2 to 23 ha and to afterwards increase to 1000 ha.

Both stable isotopes (δ^{18}O and deuterium) showed similar patterns of fluctuation among the seasons, implying that the travel-time distributions of both tracers have similar shapes (Figure 16). Small plots runoff and shallow groundwater of the hillslope tracked the rainfall signature closely. Important variations were observed from one event to another with values ranging from δ_{18}O 0.71 to -3.90‰, δ_2H 26.85 to -14.95‰ for rain and -2.63 to -6.44‰, δ_2H

38.92 to -30.86‰ for plots; while 23 ha, 100 ha and 1000 ha outlets and groundwater remained constant with $\delta_{18}O$ mean values of -3.26, -2.60, -1.62, -3.73‰ and δ_2H of -8.79, -5.38, -2.63, -14.37‰ respectively.

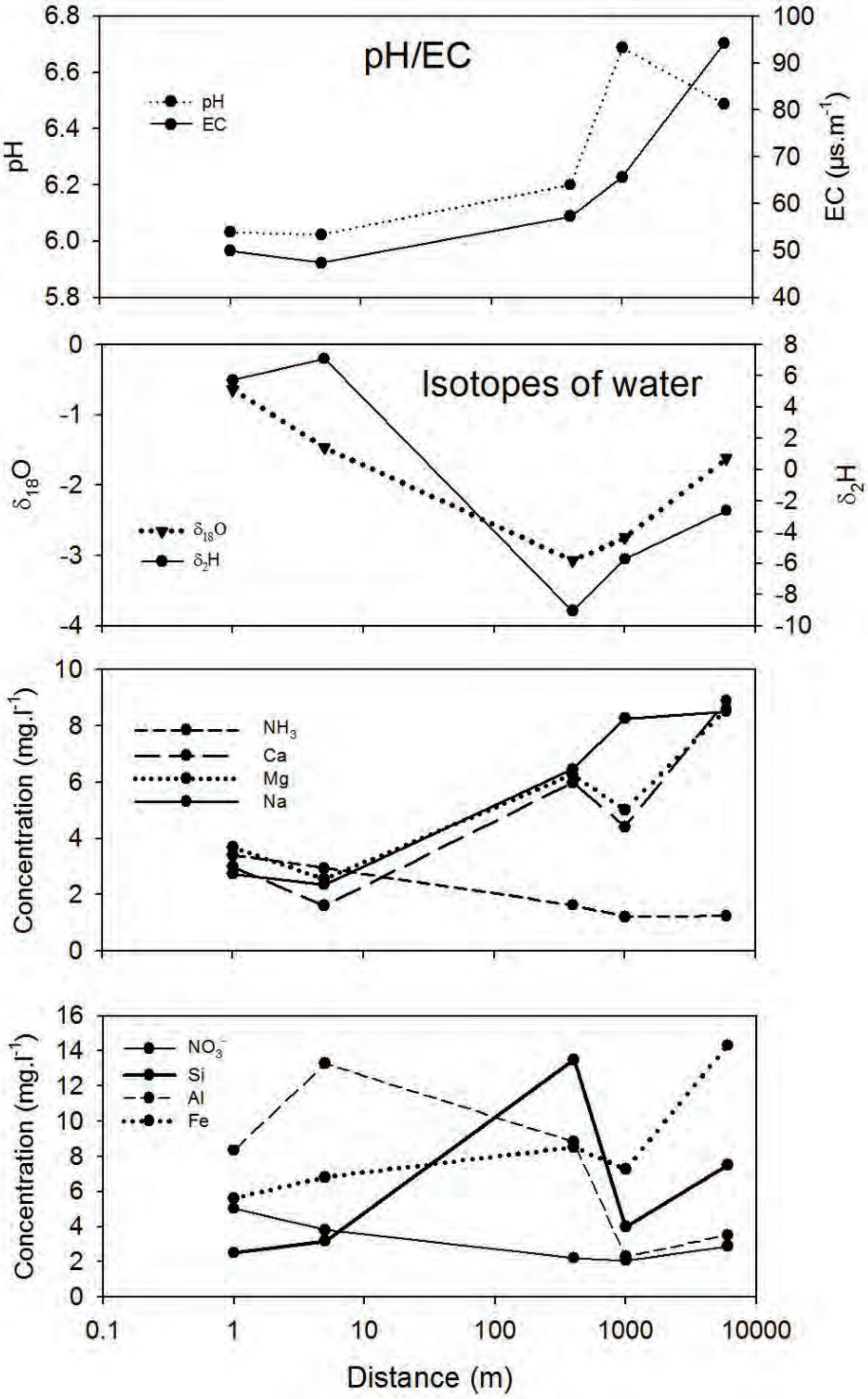

Figure 16. Concentration of selected dissolved elements as a function of distance from catchment upper limit

Such an evolution of the concentration of elements in the downstream transport tends to point to an interaction between different compartments of water and/or the change in status of some specific elements. For example, nitrate can be consumed by the vegetation during its downstream transport or released to the atmosphere as NO_2 through denitrification. DOC can be decomposed and leave the system as CO_2. In the following, a focus is made on the mixing of the different water compartments.

The use of single elements, individually, does not allow adequate insights into the mixing occurring within a catchment. The use of water isotopes in conjunction with chemical elements in equations 8 to 11 allowed end for member mixing analysis for the period from 22 February to 1 April 2011 and for all 3 monitored catchments to be performed.

The mean contribution of the three selected water sources (Overland Flow, Soil Water, Groundwater) is presented in Table 7. This gives an indication and insight of the spatial variations of the runoff generated at the different scales.

Table 7. The mean contribution of the 3 main water sources for the 3 catchment scales observed

	23 ha	100 ha	1000 ha
	--------------%-------------		
Overland Flow	22	22	8
Soil Water	15	28	37
Groundwater	63	50	55

The results presented are an initial attempt at performing initial general estimates of the sources contributing to runoff at the three monitored catchment outlets. Groundwater contributed the most to runoff fluxes at all the three nested catchments. The mean groundwater contribution was 63% at 23 ha, 50% at 100 ha and 55% at 1000 ha. The mean soil water contribution to catchment runoff increased from 15% at 23 ha to 28% at 100 ha and to 37% at 1000 ha. Overland flow contribution was almost stable at 22% at 23 ha and 22% at 100 ha but highly decreased to 8% at the 1000 ha catchment outlet. From these results there was a general trend for soil water contributions to increase with the increase in catchment size. The relative overland flow contribution was similar at the 23 ha and 100 ha catchments but was much lower at 1000 ha. Groundwater was the major contributor at all scales.

The evolution over time of the contribution of the three water compartments at the 23 ha micro-catchment and 100 ha catchment outlet is displayed in Figures 17 and 18 respectively. On 22 February 2011 the antecedent cumulative precipitation was 22.8 mm and 31.2 mm for the previous 3 and 7 days, respectively, which can be considered as a rainy period. A dry spell occurred between the 3^{rd} to the 15^{th} of March, followed by a wet period. As discussed earlier, the calculation of the mixing of sources at the 1000 ha catchment outlet showed that the largest contributions to catchment runoff were that of groundwater, during both events and periods of low flow. This approach allows for an insight into the temporal variations of the sources of runoff at the catchment outlets in conjunction with the spatial variations of catchment runoff at different scales.

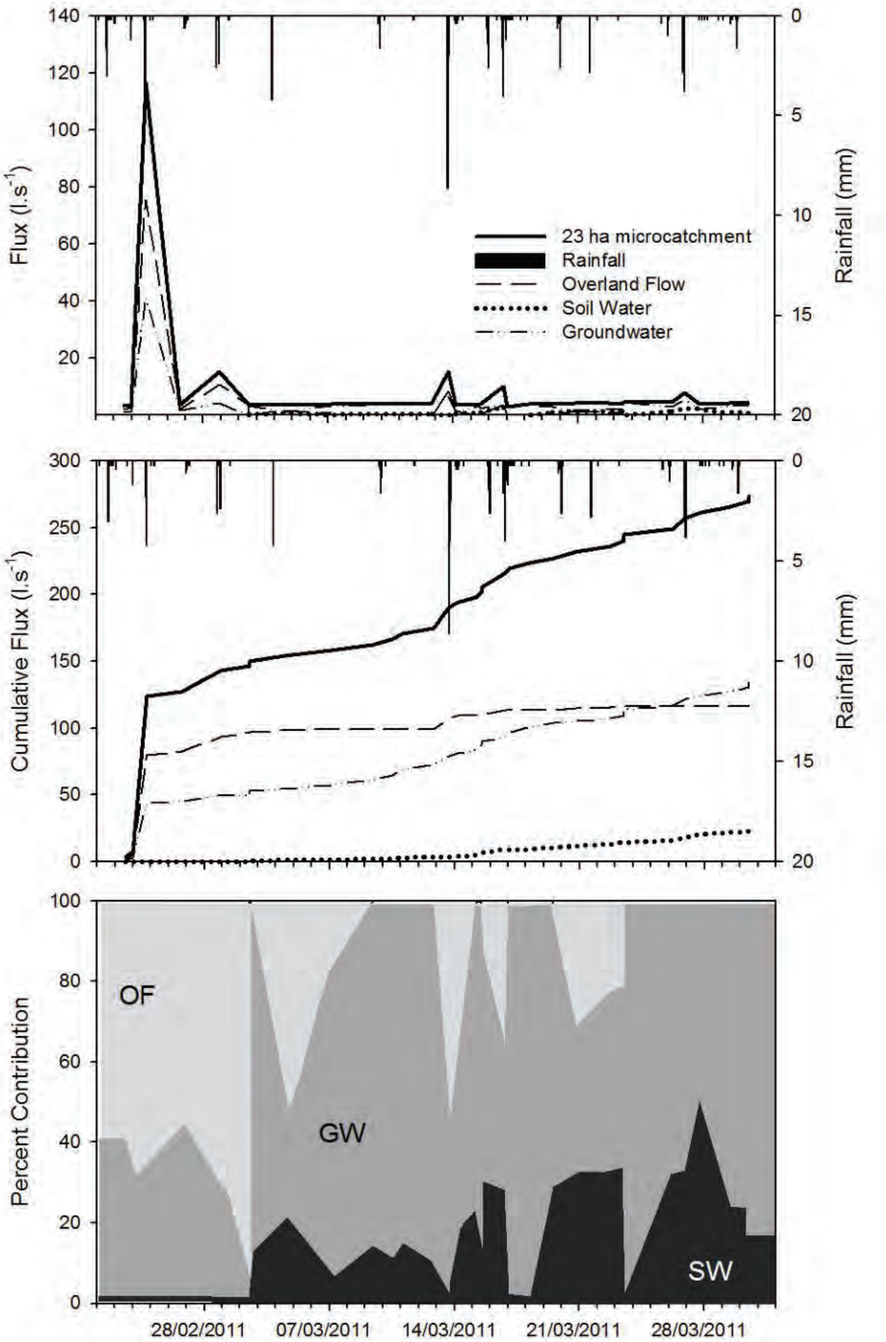

Figure 17. Mixing and contributions of the sources contributing to catchment runoff at the 23 ha micro-catchment

Overland flow was, at 60%, the highest contributor to runoff at the 23 ha micro-catchment during the initial rainfall event. It increased to 97% on 2 March 2011. Over time the OF contributions decreased, which coincided with increased contributions from soil water. OF contribution was 0% during the dry spell of the first half of March and towards the end of the period. Soil water, that initially contributed nothing to the micro-catchment runoff, increased over time with a peak at 51% on 27 March 2011. A reason for the low initial contribution of soil water is that the water from the first rains is stored in the soil profile rather than moving through it. Once the soil moisture deficit is satisfied, soil water contributions increased. However, soil water started contributing on 2 March 2011, after which soil moisture consistently contributed water to micro-catchment runoff. Groundwater contributions at the micro-catchment outlet were, at 100%, the highest during periods of low flow when there was no rainfall. Groundwater still contributed to micro-catchment flow during events but the contribution was low (lowest event contribution being 2.5%).

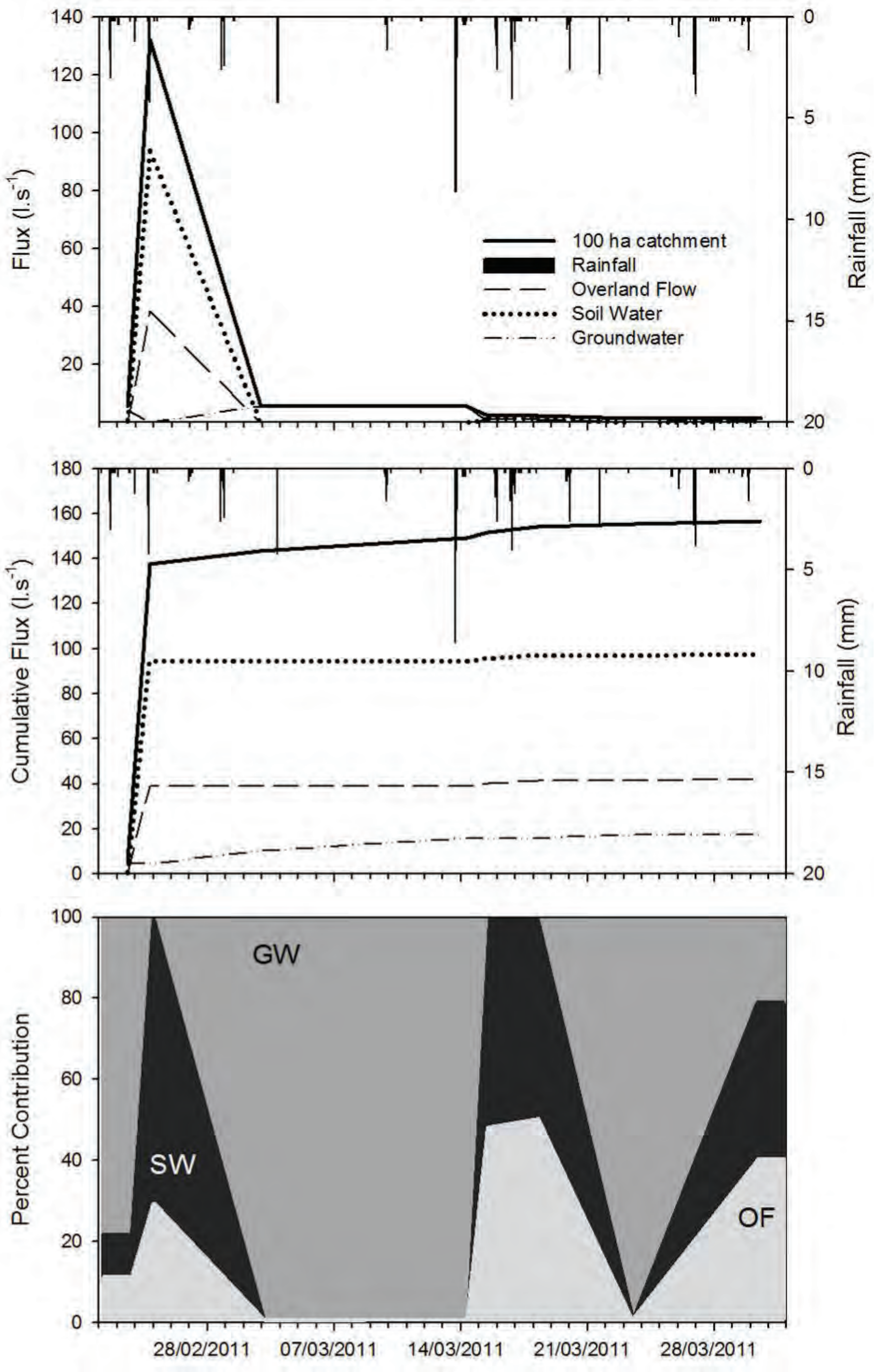

Figure 18. Mixing and contributions of the sources contributing to catchment runoff at the 100 ha catchment

The mixing and contributions of the sources contributing to catchment runoff at the 100 ha catchment is shown in Figure 18. Soil water had the greatest contribution (40%) to catchment runoff at the initial storm, followed by OF (30%) and groundwater (30%). The groundwater contribution was 100% during periods of low flow. For 2 out of the 3 distinct events of the period for the 100 ha catchment outlet, soil water and overland flow contributed similar amounts of water to the catchment runoff (50% contributions from each of soil water and overland flow). The event which occurred on 24 February 2011 had a 71% contribution from soil water and 21% from overland flow. It was found that soil water and overland flow only contributed to catchment runoff during events.

7. Controlling factors of runoff generation

7.1. Soil surface conditions

The topographic information at the study microplots and plots was derived from a Digital Elevation Model (DEM) with a 5-m resolution and a vertical precision of 0.05 m. It was generated for the purpose of this study from 36,000 data points of altitude. This DEM has been generated with a differential GPS and interpolated by using the inverse distance weighting function of ArcView3.2 (ESRI, 2004). From this, the altitude above sea level of each microplot was extracted, using the DEMAT function of ArcView3.2. The mean slope gradient of the eight cells surrounding each plot was estimated using the same ArcView function.

The proportion of the soil surface crusting and soil surface coverage at the microplots and plots was evaluated by Podwojewski *et al*. (2011). A grid of 100 nodes was placed on each of the 18 microplots, to evaluate the soil surface coverage (Cov).

The proportion of the soil surface covered by the vegetation at each microplot has been characterized visually in the field by qualitative assessment, using a 1 m^2 grid with 100 cm^2 cells, which is a well-documented methods (e.g. Auzet *et al*., 2004). The proportion of the soil surface with crusts has also been considered because of its recognised impact on overland flow generation (e.g. Casenave and Valentin, 1992). Following the field methodology of Casenave and Valentin (1992), the type of crust was recognised in the field using a knife and a magnifying glass and its proportion on the soil surface was evaluated using the 1 m^2 grid. The proportion of each crust type was summed to obtain the proportion of the soil surface with crusts. Additional information of exposed roots was gathered. Over 200 field observations were performed throughout the catchment. Information was obtained at the 15 microplots and at 185 randomly-selected points (at the boundaries between the different crusting percentages), the location of which was captured in the field using the differential GPS with a 0.2 m lateral accuracy. The resultant information is shown in Figure 2.2. GIS layers for the proportion of soil surface coverage and crusting were afterwards interpolated, using ArcMap and ordinary kriging, which is well-adapted for lower sampling densities (McBratney and Webster, 1983).

Core rings were used to sample the plot surface 0-0.05 m soil layer for soil bulk density (ρ_b) estimation at the microplot and plot positions. Three core samples were dried at 105°C for 24 hours to determine ρ_b, expressed as g cm^{-3}. Finally, classical soil analysis was used to estimate soil clay content.

7.2. Soil water

At each location where the microplots have been installed, nests of Watermark sensors were also installed. The nests consist of three sensors installed at different depths within the soil profile. The depths to which the Watermark sensors were installed were 20, 50 and 100 cm.

The Watermark (Irrometer Company, Riverside, CA) is a granular matrix sensor, used to monitor soil water tension/soil water potential. It consists of two concentric electrodes placed within a reference matrix material, which is bounded by an artificial covering for protection against deterioration. Movement of water between the soil and the sensor results in changes of electrical resistance between the electrodes within the sensor. The electrical resistance is then converted to soil water tension (in mm), using calibration equations specific to the site. The range of the soil water tension that a Watermark sensor can monitor is between 0 to -2 bars or 0 to -200 kPa.

To ensure proper functioning, the Watermark sensors were soaked overnight and installed to the desired depth, as above, using an access hole, dug with an auger. The hole was subsequently filled with the excavated soil material to reconstruct the original soil profile and its horizon order. The soil material was firmly stamped during the process, but excessive compaction was avoided. An extensive watering was finally performed to improve the filling of voids and the contact between the Watermark sensors and the soil matrix. The sensors were finally connected to a four-channel HOBO logger, which was programmed to log the electrical resistance in the sensors every hour. A temperature sensor was placed at a 20 cm depth to record soil temperature. The electrical resistance at the three depths was converted to soil suction using Equation 12, a non-linear equation developed by Shock *et al*. (1998) and currently recommended by the manufacturer.

$$SMP = \frac{4.093 + (3.213 \times mV)}{(1 - (0.009733 \times mV)) - (0.01205 \times Ts)}$$ **Equation 12**

Where *SMP* is the soil matrix potential in kPa, *mV* is the sensor output and *Ts* is the measured soil temperature.

No specific calibration was performed on the sensors, but because it has been reported that the sensors' response may vary across soils and can be poor under wet soil conditions, the Watermarks' readings were compared to additional observations made at piezometers installed nearby the sensors at depths of 20, 50 and 100 cm. The soil water tension for all three depths, at each location prior to the overland flow events (*i.e.* the hour before), has been extracted and used to investigate the impact that antecedent moisture conditions have on the generation of overland flow. Soil water tensions of the entire study period have been monitored to link water and nutrient fluxes at different scales with the catchments' state of wetness.

8. Mechanisms of soil and sediments losses by water erosion

8.1. Sheet erosion

8.1.1. Main acting processes

Table 8 shows that the average vegetation coverage (cov %) at the plot positions was 78% and varied between 64% at the midslope and 93% at the footslope. The soil clay content (clay %) was 36% with a variation between 28% at the footslope and 54% at shoulder dolerite. The average slope gradient (slope %) of the plots was 22% and varied between 18% at the shoulder dolerite and shoulder sandstone positions and 29% at the midslope positions. Of the plot soils derived from dolerite (footslope, midslope, terrace and shoulder dolerite), the surface at the midslope was the most degraded. The soil surface at the shoulder sandstone was comparable to the shoulder dolerite in terms of vegetation cover and slope gradient. However, the sandstone material gave rise to a considerably lower clay content at the shoulder sandstone position (31%), compared to the shoulder dolerite position (54%).

Table 8. Characteristics of the study hillslope positions F (footslope), M (midslope), T (terrace), SDOL (shoulder dolerite) and SST (shoulder sandstone): Crust: percentage of soil surface with crusts; Cov: percentage of soil surface coverage by vegetation; Clay: soil clay content; ρ_b: soil bulk density; S: mean slope gradient; ρ_b: bulk density

Plot	Crust (%)	Cov (%)	Clay (%)	S (%)	ρ_b (g cm^{-3})
F	7	93	28	25	1.23
M	36	64	27	29	1.19
T	19	81	40	22	0.96
SDOL	22	78	54	18	0.96
SST	25	75	31	18	1.15
Average	*22*	*78*	*36*	*22*	*1.10*

The series of measured soil erosion events are summarised in Table 9. The maximum values of SC and SL (40.6 g L^{-1} and 149.5 g m^{-2} respectively) were higher for the 10 m^2 plots than the 1 m^2 plots (27.4 g L^{-1} and 30.9 g m^{-2}, respectively). A similar trend was followed for the averages of R, SC and SL at the two spatial scales. The median values of R indicate that the 1 m^2 plots were generally more responsive to rainfall than the 10 m^2 plots. The mode, first and third quartile values for R, SC and SL indicate that there were few erosive rainfall events, which is concordant with the rainfall characteristics.

The mean and maximum values of R, SC and SL at the footslope, midslope, terrace, shoulder dolerite and shoulder sandstone positions are given in Table 4. The average R at each of the plot locations was similar, although the maximum R values varied considerably. Average and maximum sediment concentration and soil loss values were the highest at the midslope and shoulder dolerite positions, which may be explained by the steep slope and low vegetation coverage at the midslope and the sandstone derived soil material at the shoulder dolerite, which is prone to crusting (Table 8). SC and SL at the footslope, terrace and shoulder dolerite positions were notably lower, in comparison.

Table 9. General statistics (SD: standard deviation; SE: standard error; CV: coefficient of variance) for selected rainfall characteristics of the 17 rainfall events of the 2009/2010 rainy season. (I: average rainfall event intensity; Imax: maximum rainfall event intensity; I_{30}: average thirty minute rainfall event intensity; I_{30}max: maximum thirty minute rainfall event intensity; RA: rainfall amount; RDur: rainfall hours; ARD: cumulative antecedent rain days; AR: antecedent rainfall from onset of rainy season to end of erosion event; AR_3: three day antecedent rainfall; AR_{10}: ten day antecedent rainfall).

	I	Imax	I_{30}	I_{30}max	RA	RDur	ARD	AR	AR_3	AR_{10}
Mean	3.1	23.3	2.7	18.0	25.6	2.1	62.0	201.1	16.9	38.3
SD	1.7	18.2	1.6	16.1	19.8	1.6	39.7	138.8	14.2	18.7
SE	0.4	4.4	0.4	3.9	4.8	0.4	9.6	33.7	3.8	4.3
CV	54.7	78.0	59.0	89.2	77.3	75.1	64.0	69.0	84.2	49.0
Variance	3.1	350.6	2.7	274.7	417.4	2.7	1671.1	20468.7	215.2	373.0
Min	0.8	0.8	0.4	0.4	0.2	0.3	6.0	21.0	0.6	13.4
Max	6.6	69.6	6.1	64.8	64.8	6.4	142.0	435.6	54.6	68.8
Mode	0.8	0.8	0.4	10	n/a	1	n/a	n/a	10.8	25.4
Quartile 1	2.2	9.6	1.7	7.2	8.2	1.0	36.0	101.4	5.6	20.6
Median	2.6	20.8	2.3	17.2	21.0	1.8	49.0	181.4	14.4	35.8
Quartile 3	3.8	28.8	3.8	21.6	42.8	3.3	100.0	328.6	20.6	59.2
Skewness	0.6	1.1	0.4	1.5	0.6	1.2	0.5	0.4	1.4	0.2
Kurtosis	-0.3	1.2	-0.4	2.8	-0.7	1.3	-0.9	-1.3	1.9	-1.7

Table 10. General statistics (SD: standard deviation; SE: standard error; CV: coefficient of variance) for runoff (R), sediment concentration (SC), soil loss (SL) and soil loss by unit width (SLw) at the 1 m^2 (n = 255) and 10 m^2 (n=170) plot scales.

	R $L\ m^{-2}$		SC $g\ L^{-1}$		SL $g\ m^{-2}$		SLw $g\ m^{-1}$	
	1 m^2	10 m^2	1 m^2	10 m^2	1 m^2	10 m^2	1 m^2	10 m^2
Mean	4.9	5.4	1.5	2.2	3.2	9.8	3.2	4.9
SD	5.6	7.2	3.7	4.8	5.0	23.4	5.0	11.7
SE	0.4	0.6	0.2	0.4	0.3	1.8	0.3	0.6
CV	114.1	133.4	250.9	220.7	152.7	240.0	152.7	120
Variance	31.8	52.5	13.6	23.1	24.9	554.6	24.9	277.3
Min	0.0	0.0	0.0	0.0	0.0	0.0	0.0	0.0
Max	33.0	38.1	27.4	40.6	30.9	149.5	30.9	74.75
Mode	3.5	1.7	0.2	n/a	n/a	0.8	n/a	0.4
Quartile 1	1.0	1.1	0.2	0.3	0.3	0.6	0.3	0.3
Median	2.8	2.6	0.5	0.8	1.3	1.9	1.3	0.95
Quartile 3	8.0	8.0	0.9	2.5	3.9	5.7	3.9	2.85
Skewness	2.4	2.5	5.3	6.5	3.2	4.1	3.2	2.05
Kurtosis	8.0	6.7	31.9	49.9	12.6	18.3	12.6	9.15

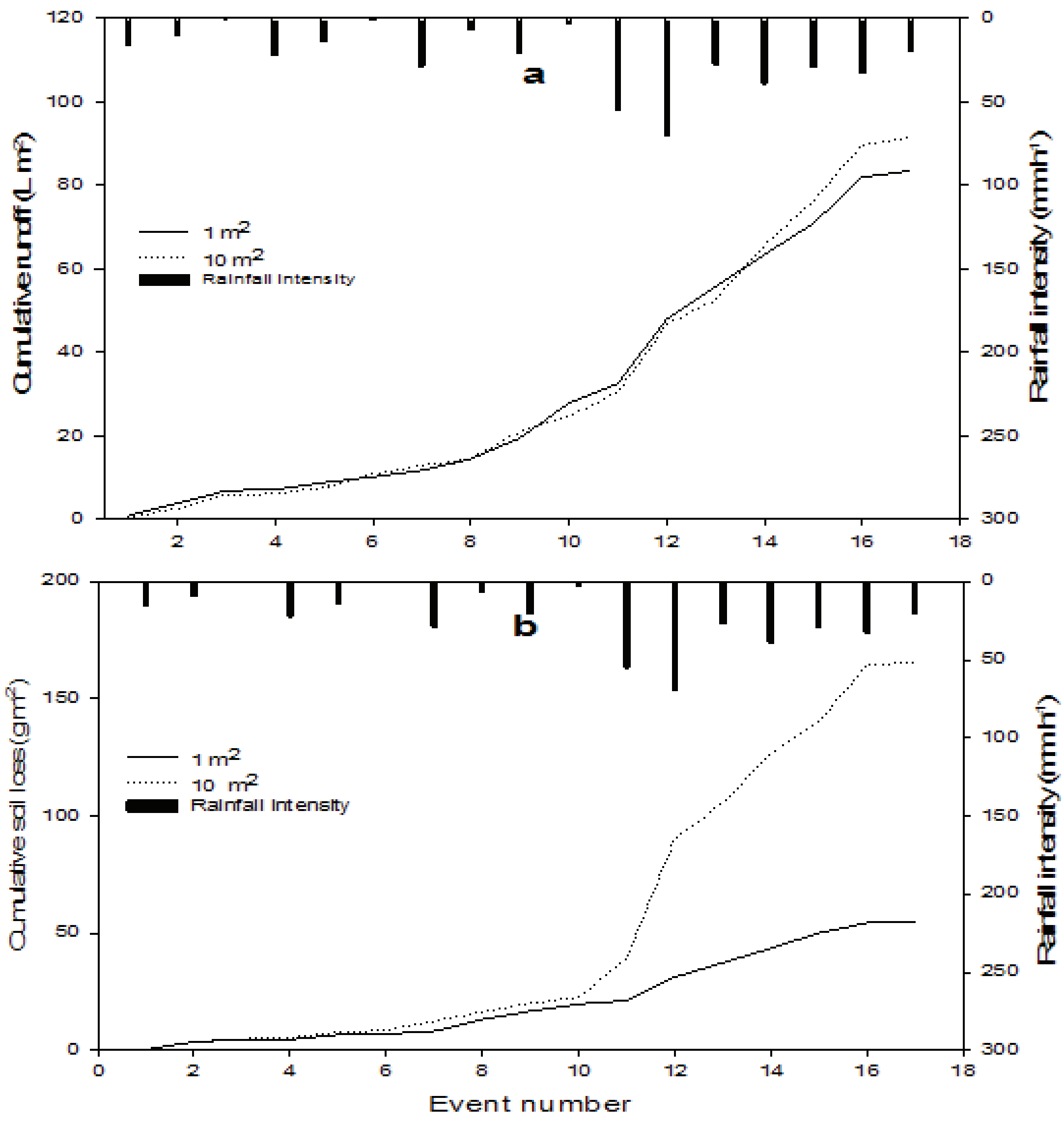

Figure 19. Average cumulative runoff (a) and cumulative soil loss (b) at the 1 m^2 and 10 m^2 plot scales.

Table 11. Mean and maximum runoff (R), sediment concentration (SC) and soil loss (SL) from the 1 m^2 (n = 255) and 10 m^2 (n = 170) plot scales for the five hillslope positions; F (footslope), M (midslope), T (terrace), SDOL (shoulder dolerite) and SST (shoulder sandstone).

	R L m^{-2}				SC g l^{-1}				SL g m^{-2}			
	Mean		Max		Mean		Max		Mean		Max	
Plot	1 m^2	10 m^2	1 m^2	10 m^2	1 m^2	10 m^2	1 m^2	10 m^2	1 m^2	10 m^2	1 m^2	10 m^2
F	2.5	2.7	9.3	5.9	1.4	1.7	16.0	15	0.9	1.9	3.9	8.1
M	7.6	10.2	33	38.1	1.1	5.4	3.7	52.6	7.7	26.2	30.9	149.5
T	3.7	4.3	10.5	30.5	3.4	3.8	27.4	4.6	2.7	3.7	13.4	12.9
SDOL	3.9	3.3	11.8	11.1	1.9	0.9	8.0	3.4	1.8	1.7	5.4	3.9
SST	7.0	7.0	25.7	23.7	0.5	2.6	2.5	20.1	3.1	15.2	10.6	92.2

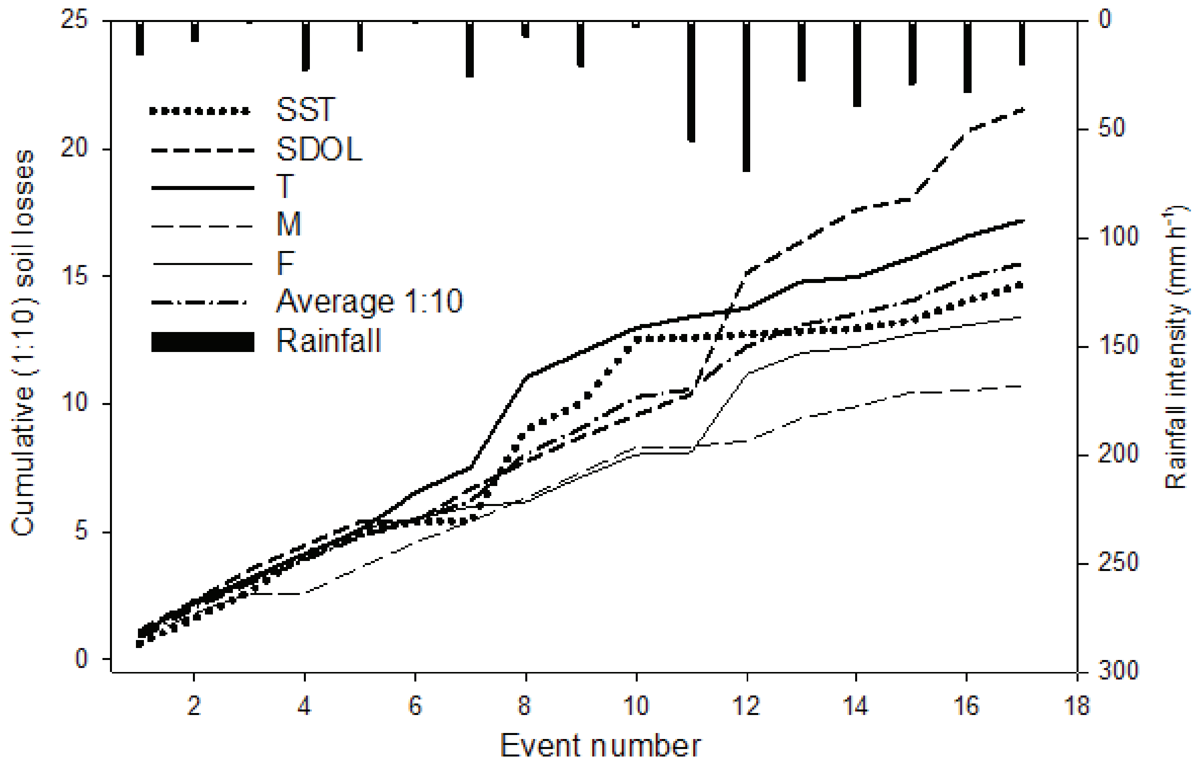

Figure 20. Cumulative 1/10 soil loss ratios at each hillslope position SST (shoulder sandstone), SDOL (shoulder dolerite), T (terrace), (M) midslope, F (footslope) computed from the 17 erosive rainfall events for the 2009/2010 rainfall season and the maximum rainfall intensity of the events.

Table 12. ANOVA between the 1/10 m^2 soil loss ratio and some selected environmental factors: (I: average rainfall intensity; Imax: maximum rainfall intensity; I30: average thirty minute rainfall intensity; I30max: maximum thirty minute rainfall intensity; RA: event rainfall amount; RDur: rainfall event duration; ARD: cumulative antecedent rain days; AR: cumulative yearly antecedent rainfall amount; AR3: antecedent three day rainfall; AR10: antecedent ten day rainfall; Crust: percentage of soil surface with crusts; Cov: percentage of soil surface coverage by vegetation; Clay: soil clay content; ρb: soil bulk density; S: mean slope gradient.

Variable	r	Degree freedom	F	p
I	-0.44	4	3.11	0.1
Imax	-0.12	4	4.11	0.06
I_{30}	-0.40	4	3.18	0.09
I_{30}max	0.03	4	3.68	0.07
RA	0.13	4	0.98	0.34
RDur	0.25	4	0.17	0.67
ARD	-0.31	4	5.46	0.03
AR	-0.29	4	5.45	0.03
AR_3	0.10	4	0.9	0.34
AR_{10}	0.13	4	1.4	0.23
Crust	-0.07	4	0.4	0.52
Cov	0.07	4	0.4	0.52
Clay	0.26	4	6.14	0.01
ρ_b	0.22	4	4.6	0.03
S	-0.2	4	3.38	0.07

The cumulative ratio of the soil loss rates from the 17 events is shown in Figure 19. A lower total cumulative soil loss value is indicative of the fact that RIF erosion is more operative at a given location, in comparison to the other hillslope positions. It can be seen that the midslope had the lowest cumulative soil loss ratio, followed by the footslope and shoulder dolerite positions.

An evaluation of the impact of the selected rainfall characteristics and soil factors listed in Table 10 on the 1/10 m^2 soil loss ratios for each of the 17 erosive rainfall events (Figure 20), was performed using an ANOVA analysis (Table 12). Cumulative antecedent rain days (ARD), cumulative antecedent rainfall amount (AR), clay and soil bulk density (ρ_b) were the only significant variables ($p<0.05$).

Figure 19 indicates that the R values (L m^{-2}) at both plot scales were approximately equal for the majority of the rainfall season. However, slightly more runoff was generated from the 10 m^2 plots (91.6 L m^{-2}), compared to the 1 m^2 plots (83.5 L m^{-2}).

Cumulative SL values indicate that soil losses increased steadily and approximately equally at the two plot scales until the 10th event (Figure 19). Subsequently, soil losses from the 10 m^2 plots increased more rapidly than those from the 1 m^2 plots in response to an increase in the number of rain days, cumulative rainfall amount and an increase in frequency of intense rainfall events. Total cumulative SL values were 55.2 g m^{-2} and 165.8 g m^{-2} at the 1 and 10 m^2 plots, respectively.

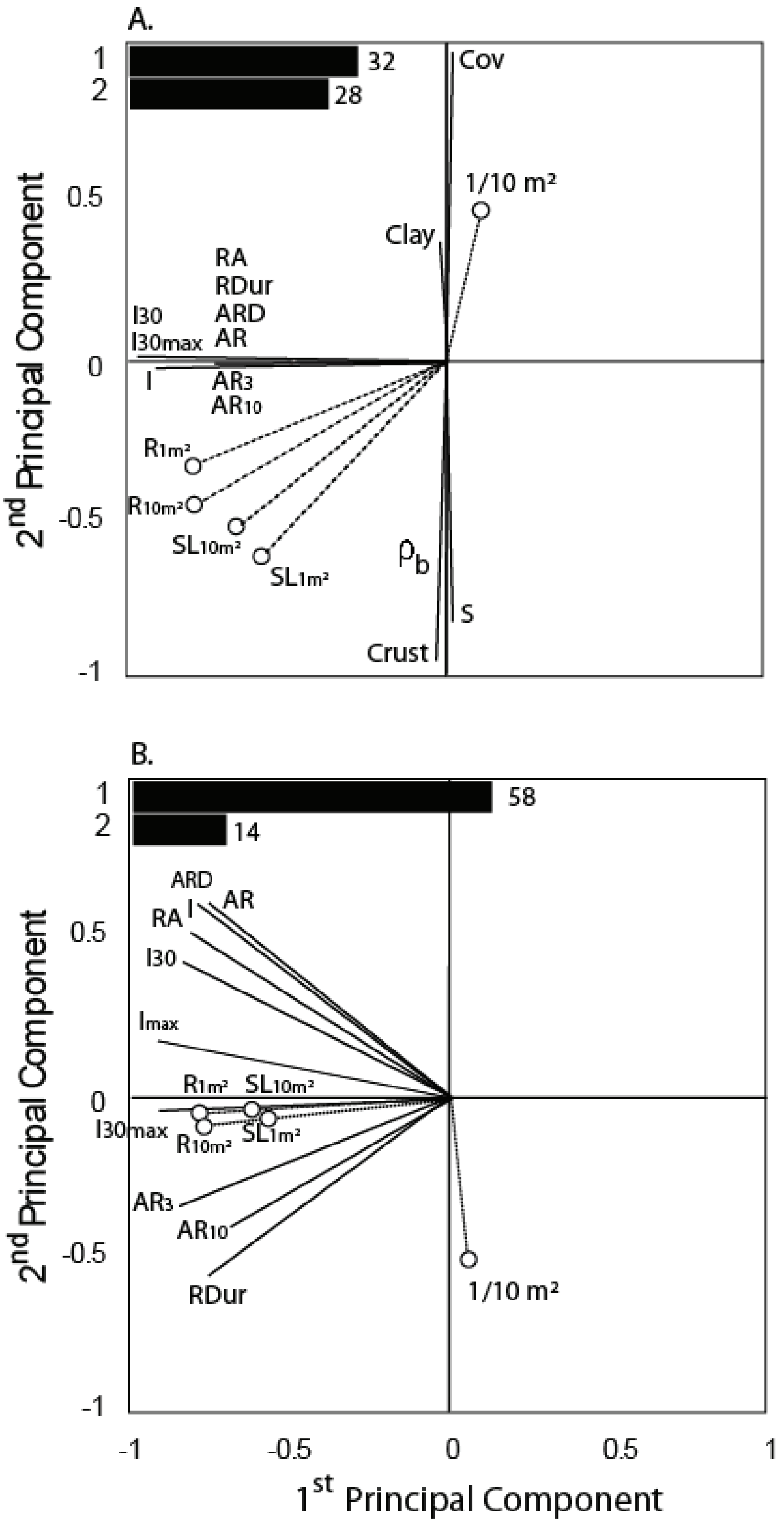

Figure 21. Principal components analysis (PCA) of 'factor scores' for (A) soil and rainfall factors; and (B) rainfall factors only. Position of the centroids for runoff (R) and soil losses (SL) at the two plot scales, and the 1/10 m^2 scale ratio for soil loss are shown.

8.1.2. Controlling factors

The average slope gradient of micro-plots was 22% with values between 18 and 26% (Table 8). M plots were on the steepest slope and plots on the shoulder were on more gentle slopes. The average proportion of the soil surface under crusting (*Crust)* was 9.6%. *Crust* varied between 1% at T to 15% at SS. Lower *Crust* values occurred on dolerite, both at the shoulder and terrace positions whereas a much higher occurrence of soil surface crusting characterized soils developed from sandstones at F, M, and SS positions (Table 8).

The average soil surface coverage by the vegetation (*Cov*) was 84%. Greater *Cov* occurred at F (88%) and SD (87%). With 85 and 83%, T and SS were of intermediary *Cov* values. Finally, M was the situation with the lowest *Cov* (74%).

SD plots showed the highest clay content (*Clay*) but the lower soil bulk density (ρ_b) whereas M and F plots were significantly more compacted (ρ_b of respectively 1.32 and 1.24 Mg m^{-3}) and exhibited the lowest clay content among microplots.

Table 13 revealed that R significantly correlated with *Cov* and ρ_b. With a pearson r coefficient of -0.68 with *Cov* and -0.71 with ρ_b, R increased as *Cov* decreased and ρ_b increased. In contrast, the correlation between R and *S*, *Crust* and *Clay* was not significant. Consideration of the relationship between SL and the environmental factors under study indicated that *Cov* and ρ_b were significantly correlated with SL. But *S*, *Clay*, and *Crust* had no significant impact on SL. *Cov* appeared to be more highly correlated to SL (r=-0.87) than it was to R (r=-0.68). Such a strong relationship between SL and *Cov* modeled by equation 1 is displayed in Figure 22.

$$SL = -45,84 \times Cov + 4613 \qquad r^2=0.76 \qquad \text{Equation 13}$$

Table 13. Correlation matrix between erosion variable and environmental factors with R: runoff coefficient; SL: soil losses; *S*: slope gradient; *Crust*: proportion of crusting on the soil surface; *Cov*: proportion of soil surface coverage by the vegetation; *Clay*: soil clay content; and ρ_b: soil bulk density (n = 37). Significant correlations at p < 0.05

	R	**SL**	*S*	*Crust*	*Cov*	*Clay*	ρ_b
R	1.00						
SL	0.81	1.00					
S	0.49	0.45	1.00				
Crust	0.44	0.43	0.24	1.00			
Cov	-0.68	-0.87	-0.34	-0.87	1.00		
Clay	-0.50	-0.52	-0.88	-0.36	0.40	1.00	
ρ_b	0.71	0.70	0.89	0.45	-0.62	0.16	1.00

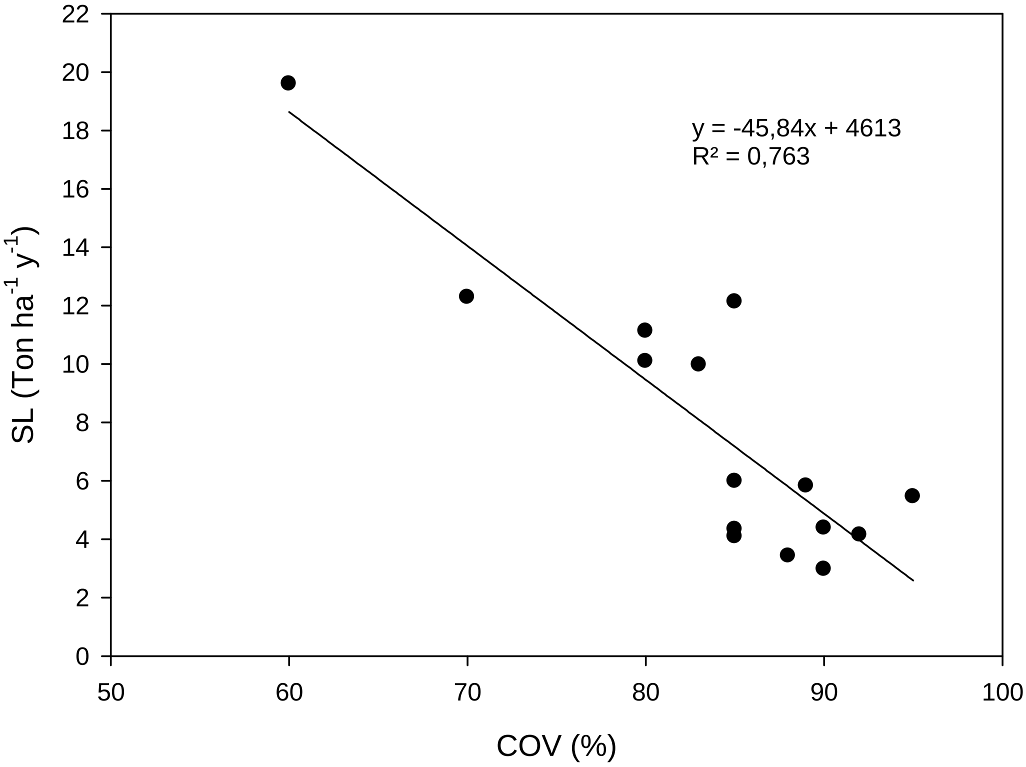

Figure 22. Relationship between annual soil losses due to sheet erosion (SL) and the proportion of soil surface coverage (*Cov*) from the 15 micro-plots.

The observed data revealed that SL significantly decreased from about 10 ton ha^{-1} y^{-1} for *Cov*=60% soil coverage to less than 6 ton ha^{-1} y^{-1} at *Cov*=93%.

The two first axes of the principal components analysis (PCA) between *S, Crust, Cov, Clay*, and ρ_b as variables for the analysis, explained 98% of the variability in data (respectively 75% for axe 1 and 23% for axe 1). From this PCA displayed in Figure 21 it is noted that the two variables most highly correlated to axe 1 are *Cov* (contribution to this axis of 0.91) ρ_b (r=-0.83) and *Crust* (r=-0.64). From this axis with a trend associated with soil surface degradation and soil compaction it is concluded that as *Cov* decreases and *Crust* increases, SC and SL increase. R is correlated with axe 1 (r=0.68) but also with the second PCA axis (r=0.73) with a trend associated with *Clay*. Finally as shown by the PCA, S had only a small contribution to the two first axes.

8.2. Linear erosion

8.2.1. The methods used to evaluate the mechanisms of gully bank retreat

Rainfall was simulated on 20 November 2008 to evaluate the potential gully bank retreat resulting from rainfall erosion. This date followed a dry period of about six months and the soil horizons were all dry. The gully bank was covered with plastic sheeting, except for a 1 m wide portion which remained exposed. Rainfall intensity was applied to the exposed portion at a rate of 60 mm h^{-1} for 45 minutes, simulating a typical rainfall event of the region (Schulze, 1997). The rainfall was produced using an ORSTOM simulator (Valentin, 1978). The simulator comprised an oscillating nozzle (Teejet SS 6560) which was aligned with the center of the exposed portion of the vertical bank, approximately 4 m above the soil surface. A valve and a pressure gauge were located at the same altitude as the nozzle, allowing for precise control of water pressure and consequently the maintenance of a consistent rain kinetic energy. At a water pressure of 40 kPa the estimated kinetic energy was 25 J m^{-2} mm^{-1}.

The rainfall intensity was set and controlled electronically prior to the experiment. Error for rainfall intensity was assumed to be less than 5%.

The vertical runoff, along with its sediments was evaluated using a 1 m² microplot inserted within the base of the bank during the rainfall period. The sampling protocol involved sampling the initial runoff in three consecutive 500 ml bottles. The proceeding 500 ml aliquots were collected every 5 minutes to the 20th minute and every 5 minutes to the end of the experiment. These bottles were then labelled and the time taken to fill them recorded. The splash material was collected using twelve rectangular 0.27×0.17 m (0.045 m²) buckets, positioned at the node of a regular grid of 0.5 m increments. The minimum distance from the source (i.e. the gully bank) was 0.5 m and the maximum was 1.5 m. Finally, fallen soil aggregates were gathered from the 1 m² microplot after the simulation had stopped.

The 500 ml aliquots of runoff water were dried at 105°C to evaluate the sediment concentration in the runoff. The runoff fluxes were estimated over time by using the filling duration of bottles. Total sediment lost during a bottle filling period corresponded to the product of the sediment concentration in that bottle and its runoff volume. Data were then integrated over the duration of the rainfall to calculate the total soil loss as a result of runoff. Sediments resulting from the splash and fallen aggregates were dried at 105°C and the dry weight was recorded. The overall splash erosion corresponded to the average erosion in each bucket (in kg m²) multiplied by the surface of the sampling grid, i.e. 4 m² (2×2 m).
Finally, the erosion from the three mechanisms was added to evaluate the total erosion induced by the rainfall.

8.2.2. The methods used to evaluate the controlling factors of linear erosion at landscape level

The survey of gully bank retreat has been performed during an entire hydrological year, from September 2007 to September 2008. The location of existing gully banks in the area was evaluated in-situ and prior to the rainy season using a GPS with a 0.5 m horizontal accuracy. A total of 20,120 geo referenced data points have been collected. Erosion pins consisting of metallic nails set entirely into the gully banks, a method adapted from Haigh (1977), were used to evaluate the retreat of gully banks. The top of the pin gives a datum from which changes in the length that protrudes above the soil surface can be recorded (Figure 23). Pins were pushed into the soil to give a firm and stable medium that was easily found at 0.15 m considering the high bulk density of the soils under study. Here we used principally 0.15 m nails with a small diameter of about 5 mm in order to limit interferences with soil erosion processes. A metal washer was placed between the top of the nail and the gully bank to give a better base from which to measure. Additional 0.5 m long and 10 mm thick metallic bars were utilized to record larger erosion rates such as those induced by the collapse of gully banks.

Pins were inserted within the surface A horizon (at 0.15 m deep) of 102 randomly selected gully bank profiles of the 8 gullies found in the area plus their head cut, resulting in 110 profiles. Three pin replicates were installed per bank profile plus an additional 0.5 m long metallic bar resulting in 440 data points. The pins have been installed in early September 2007 and the length that protrudes above the gully bank surface was evaluated in late September 2008. This period was characterised by a total rainfall amount of 850 mm and 37 rainfall events (with a cumulative amount of 766 mm) caused sheet erosion (Dlamini et al., 2010).

The bulk density of soil horizons at 55 of the 110 profiles was estimated using 141 cm^3 cylindrical cores. Both the 0-0.2 m and 0.8-1.0 m layers were considered. The soil samples were oven dried at 105°C for 24hrs to determine soil the soil bulk density (ρ_b, g cm^{-3}) (equation 14)

$$\rho_b = \frac{M_s}{V_t} \qquad \textbf{Equation 14}$$

where M_s (g) the mass of the dry sample; and V_s (cm^{-3}) the volume of the soil sample, i.e. the cylinder.

Data of yearly bank retreat (GBR) were transformed in yearly soil losses (SL) in ton per hectare per year (ton ha^{-1} yr^{-1}) by multiplying GBR by the gully depth and the average bulk density bulk density of the soil.

$$SL = \frac{1}{A}[\frac{1}{n}\sum_{i=n}^{i=1}(\rho_b \times h \times l)] \qquad \textbf{Equation 15}$$

where A the surface area of the study site (ha), h is the gully bank height (m), and l the total length of gullies (m).

A correlation matrix was generated to quantify the univariate links between GBR and the selected environmental factors (Figure 25). Because the information on the type of soil and of bedrock is qualitative, t-tests for independent samples were used. In addition, a principal components analysis (PCA) was used to evaluate the multiple relationships between the study variables and to display the main trends in the data set. PCAs convert the variables into principal components (PCs) which are linear combinations of the actual variables (Jambu, 1991). The first and second PCs explain most of the data variance. The environmental variables were used as primary variables in the construction of PCs and GBR was displayed as secondary variable. The ADE4 software (Chessel et al., 2004) was used for this study.

The probability distributions of GBR was positively skewed as displayed by a skewness of 14 (e.g. skewness of 1.6 for SOC stocks at 0.3 m) and had a sharp peak (kurtosis = 208) whereas for a population following a normal frequency distribution, these coefficients should have values of 0 and 3, respectively. The log-transformed GBR data had rather small skewness (1.0) and kurtosis (4.0), and thus passed the Kolmogorov-Smirnov normal distribution test at $P<0.001$.

Figure 23. Gullying at the study areas. Gully feature in the area and pins with a 0.15 and 0.5 m length for assessing gully bank retreat (A); Gully sections parallel to contour lines and incising red Luvisols (upper bank) and gleyic Luvisols (lower bank) (B) and shallow yellow Acrisols (upper bank) and deep yellow Luvisols (lower bank) developed from sandstones (C); narrow gullies along the steepest slope and their relationship with cattle and human paths on dolerite derived deep red Acrisols (D).

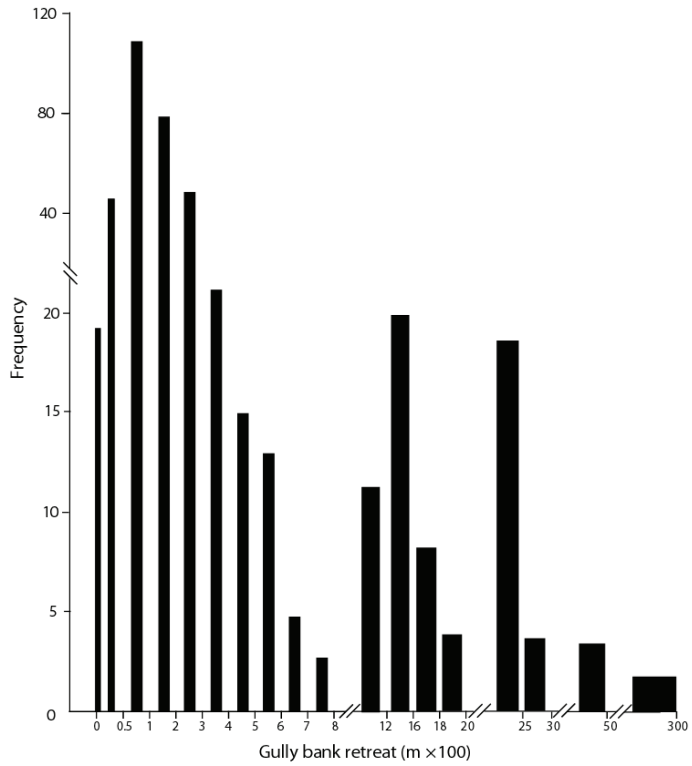

Figure 24. Frequency distribution of the gully bank retreat (n=440). Data collected during the 2008/2009 rainy season.

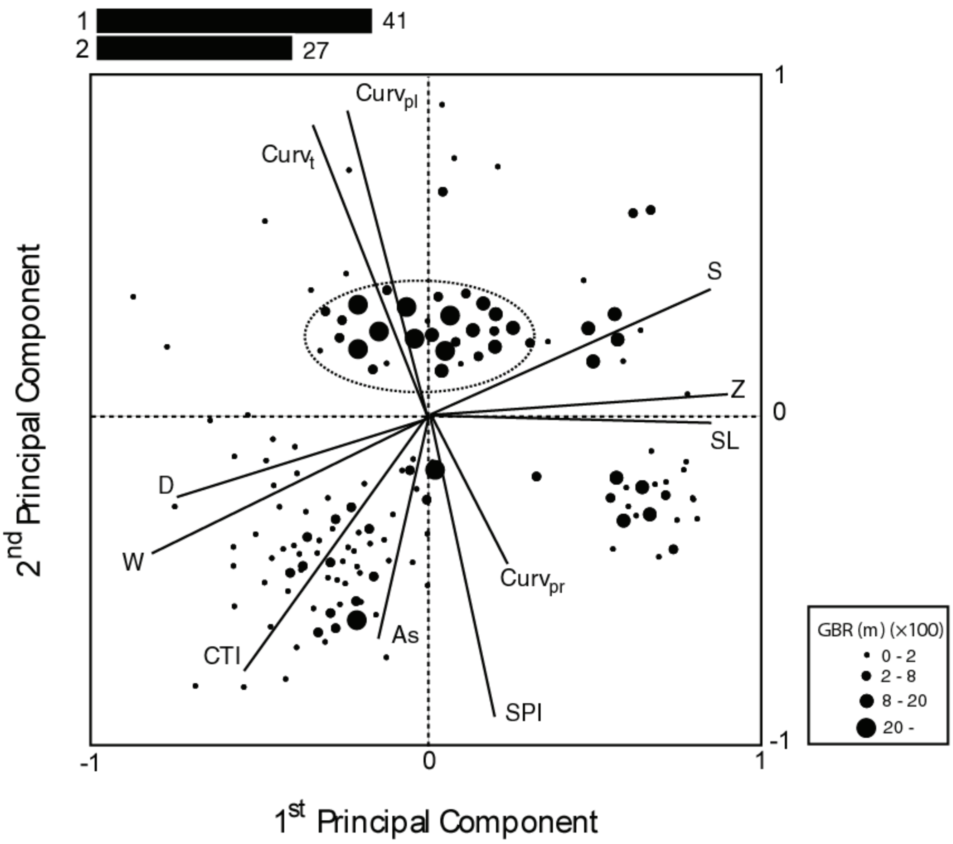

Figure 25. Principal Component analysis between the selected terrain attributes as primary variables and average gully bank retreat at the 110 pits.

General statistics for the selected terrain attributes indicate that over the set of 110 data points, the altitude above sea level ranged between 1251 in the north of the area and 1421 m at the head cut of gully number one, in the South-East of the area. The gully width was between 12 and 50 m and the average distance to gully head cut was 201 m with values between 0 and 876 m. Large and short gullies were found in the northern gully system compared to the southern one. As was between 1 and 39 m^2m^{-1}. The lowest values were observed at upslope facing banks of gully sections stretching along contour lines as observed midslope (Fig 23A) or at the headcut (Fig 23C). The highest As were found at the downslope positions of gullies, mostly in the northern and eastern parts of the area. The mean slope gradient of data points was 0.17 m m^{-1} with values from 0.02 in the bottomlands of the North and East to 0.32 m m^{-1} at the head cut of (Fig 23A). SPI ranged between 0 and 4.3 and CTI between 5.8 and 9.1 with in both cases lower values in the vicinity of the gully head cut and higher values downstream (Fig 23).

While the correlation coefficient between the terrain attributes were in most cases significant ($P<0.05$ level) (case of r=0.85 between Sl and Z; r=-0.68 between D and S), the only significant r coefficient between GBR and the terrain attributes was with D, the distance to gully head cut. The r of -0.11 was indicative of a decrease of GBR with increasing D or in other words that higher GBR were observed close to gully heads. The second higher r coefficient with GBR was -0.08 and was found with W, the width of gullies. The mean (±standard error) of GBR for value classes of the different terrain attributes revealed however same a certain degree of correlation between GBR and the selected terrain attributes exist. Excluding the lower class for attributes (e.g. the [0-10]×100 class for S), GBR decreased as As, S, CTI, Sl, SPI and $Curv_{pl}$ increased. Moreover, for W and D, the lower values exhibited the highest GBR range meaning that banks close to the gully head cut exhibit both high and low retreats.

Moreover, GBR did not significantly vary between the different parent materials and soil types. For soils, the higher GBR was found for Red Acrisols (mean=0.055 m y^{-1}) followed by Luvisols ((mean=0.040 m y^{-1}) and Gleiyc Luvisols with 0.024 m y^{-1}, but these differences were not significant at $P<0.005$. Similarly, the mean GBR of 0.055 m y^{-1} under dolerite was not significantly different than the 0.036 m y^{-1} value found under sandstones.

While the one to one relationships between GBR and the selected factors of the environment were low the multivariate analysis showed a general trend in the data. The two first axes of the principal component analysis (PCA) generated from the different terrain attributes explained 68% of the whole data variability (Fig. 25). The first axis of the PCA, accounting for 41% of the total variance, showed a trend associated with Z, SL and S. The second axis which explained 27% of the data variance correlated with SPI, As and the three curvatures. SL, S and Z showed a positive coordinate on axis 1 and could be interpreted as an axis of hillslope elevation and steepness. The second axis opposes the power of the stream with a negative coordinate to the level of convergence of the terrain's shape with a positive coordinate. The first PCA axis only little discriminated between GBR data thus showing that hillslope elevation and steepness had only a limited impact on GBR. The second axis discriminated between the higher GBR rates (mainly the slightly convex slopes with relatively low SPI) and the lower GBR rates with (either high convexity or concavity; or high and low SPI) (Fig.25). Larges distances from the gully heads and wide gullies with high As and SPI where characterized by low GBR values.

9. No-tillage as an alternative to reduce water, nutrient and soil organic carbon losses from landscapes

9.1. No tillage impact on runoff, soil losses and soil organic carbon erosion

A total of six 22.5 m² (2.25×10 m) runoff plots were installed on this experimental site. Three runoff plots were located on the till part of the site and the other three on the no-till portion of the site, as presented in Figure 26. The iron-sheet borders surrounding the micro-plots were inserted to a depth of 0.1 m, with minimum disturbances of tillage treatments that had been established in 2002. For each plot, a collector, a 10 times splitter and an 80 L non-removable collection tank were placed at the bottom end to collect surface runoff. For this study, the iron-sheet borders of runoff plots were re-inserted in October 2008 to the same depth as above. An 80 L removable collection tank was placed inside a 250 L collection tank, to allow easier accessibility and assessment of collected surface runoff and trans-located sediments.

On the 4th of January 2009, the no-till plots were treated with Glyphosate herbicide, at 4 L ha^{-1} to initially kill weeds before planting could be done. The till plots were conventionally tilled to a depth of 0.2 m, and planting was carried out on all experimental plots on January 08th 2009. For both treatments (till and no-till) the first fertilizer application of 40 kg N ha^{-1} was done on January 08th during planting, and a top-dressing, (also at 40 kg N ha^{-1}) was applied on March 10th. A cocktail of 24D, collisto, metagen and atrazine herbicides was applied twice during the growing season at a rate of 4 L ha^{-1} using backpack-mounted sprayers. The first of these herbicide applications was on January 09th and the second was on March 5th. The maize crop was harvested on June 5th 2009.

Soil samples, collected on the 3rd of March 2009, and sediments eroded from till and no-till runoff plots during the 2008/2009 rainy season were analysed for this study.

Figure 26. Location of the study site within the Tugela basin in South Africa. The position of the six runoff-plots, 22.5-m² (2.25×10 m) growing maize under till and no-till systems are also illustrated in this figure. The photograph was taken looking south-west.

The mean runoff coefficient (R) over the study period was 16.5%. No significant differences were observed between tilled plots (mean of 18.5%) and no-till plots (mean of 14.5%), as presented on Table 14. No runoff occurred for the three rainfall events (cumulative amount of 26.2 mm) that occurred between the 2nd and the 10th of January. Runoff started on the

10th of January after planting, with a cumulative rainfall of 39 mm and maximum rainfall intensity of 24 mm h^{-1}. Initially, more runoff was generated from no-till compared to tilled plots (Figure 4.5).

Thereafter, the cumulative runoff curve for both till and no-till exhibited a less steep increase up to February 15th, corresponding to event number 19 on Figure 4.5. Even for the largest event of the season, with a total rainfall of 80 mm and a maximum 6-min rainfall intensity of 3 mm h^{-1}, the increase in the cumulative runoff curve was constant. Later in the year, sharp increases of the cumulative runoff only occurred at rainfall events with high rainfall intensity, which were approximately 25 mm h^{-1}. Finally, R tended to be lower for tilled plots compared to no-till during the first half of the rainy season, and the reverse occurred during the second half of the season. A graphical presentation of this phenomenon is presented in Figure 27.

Mean sediment concentration (SC) in runoff was 1.43 g L^{-1}, and a maximum value of 8.2 g L^{-1} occurred on 10th of January on the tilled plots (Table 14). The distribution of SC data was skewed and more peaked than the normal distribution. Seventy five percent of data exhibited SC values lower than 1.9 g l^{-1}. Mean SC was 0.93 g L^{-1} for tilled treatments and 2.19 g L^{-1} for no-till, and these differences were statistically significant. The P values and level of significance for these means are presented on Table 15. Soil losses were 3.1 times greater under till plots (301.5 g m^{-2} y^{-1}) than under no-till (96.8 g m^{-2} y^{-1}). This difference was statistically significant at $P<0.001$, as presented in Table 15.

The average SOC content in sediments was 59.6 g C kg^{-1}. This was much higher than the average SOC content of the soil surface layer, which was observed to be 12.9 g C kg^{-1}. SOC content differences between the two treatments were not significant (Table 15 and Figure 28). Greater losses of DOC occurred from tilled plots. Losses averaged 7.9 mg C L^{-1} for tilled plots compared to 5.9 mg C L^{-1} from no-till plots. These values are presented on Table 14. The difference between the two treatments was highly significant, at $P<0.001$. Overall, DOC losses represent on average, 10.9% of total SOC losses by water erosion. The computed soil organic carbon losses were 16.2 g C m^{-2} y^{-1} for tilled systems and 7.7 g C m^{-2} y^{-1} for no-till systems. This result showed that tillage had a significant impact, $P<0.05$, on soil organic carbon losses (the P value is presented on table 15). These computed soil organic carbon losses corresponded to 6.0% of SOC stocks on tilled systems and 2.4% of stocks on no-till systems at the 0-0.02 m sampling depth.

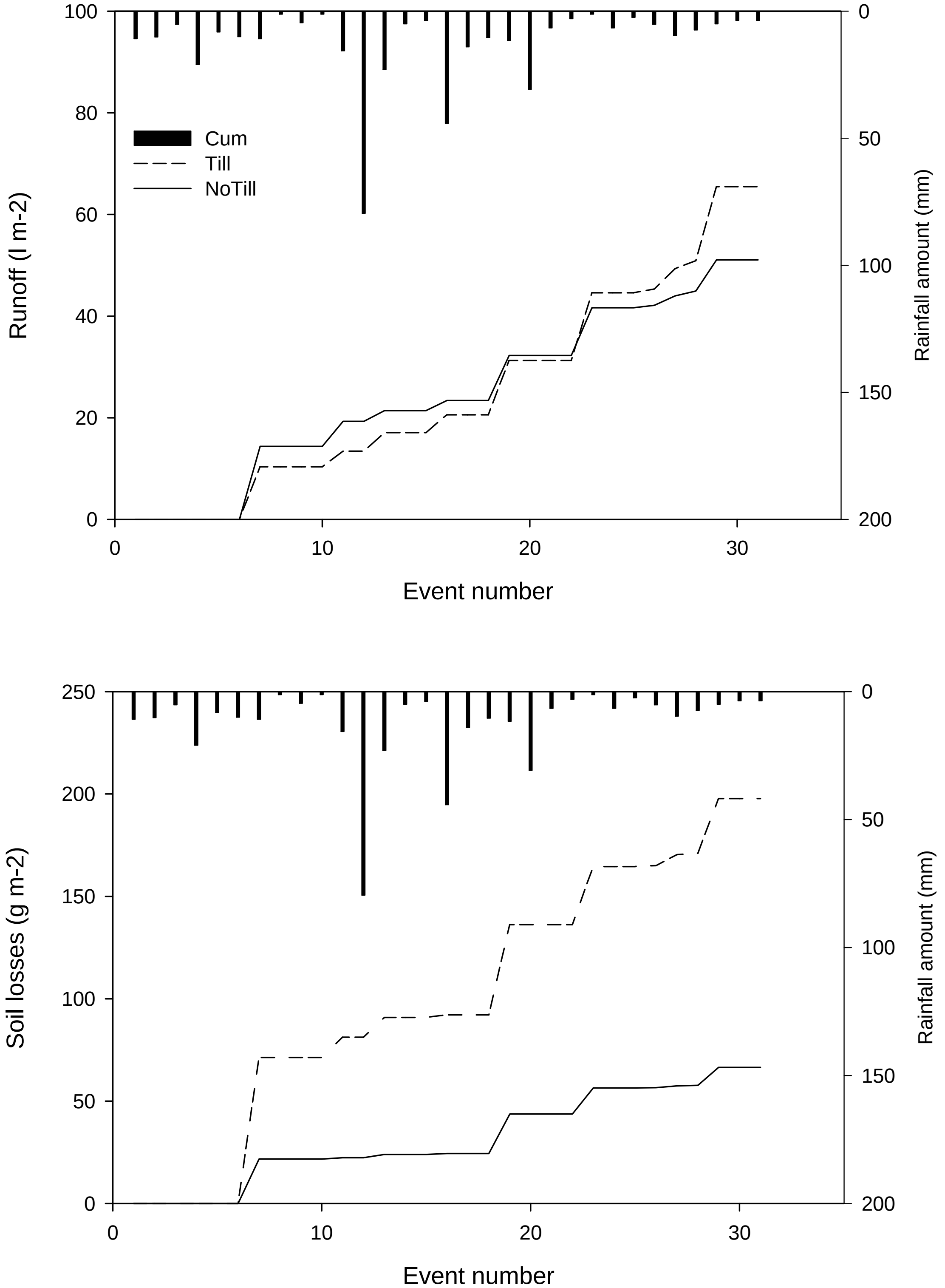

Figure 27. Mean cumulative runoff and soil losses over the 2008/2009 rainy season for till and no-till maize over 31 rainfall events. Data computed from 3 plot replicates per treatment.

Table 14. General statistics (minimum, maximum, average, median, variance, standard deviation, coefficient of variation, skewness, kurtosis, quartile 1 and quartile 3). Data computed from the 6 plot replicates of 22.5 m² and the 10 erosive events of the 2008/2009 rainy season

	R	SC	SL	DOC	SOC
	L	g L^{-1}	g m^{-2}	mg C L^{-1}	g C kg^{-1}
Min.	0.0	0.00	0.00	4.69	52
Max.	42.3	8.20	10.79	8.30	110
Av.	16.5	1.43	1.19	6.75	59.6
Median	8.0	0.90	0.23	6.64	52.2
Var.	128.7	2.44	3.59	1.55	50.1
StDev.	11.3	1.56	1.89	1.24	22.4
CV.	89	109	159	18	29
Skew.	0.84	2.15	3.12	-0.48	0.29
Kurt.	-0.35	6.38	13.02	-0.82	-1.55
Q1	3.4	0.25	0.07	6.47	48.0
Q3	21.1	1.90	1.78	7.66	96.0

Min. = minimum, Max. = maximum, Av. = average, Var. = variance, StDev. = standard deviation, CV. = coefficient of variation, Skew. = Skewness, Kurt. = kurtosis; Q1 = quartile 1, Q3 = quartile 3.

Table 15.Students' *t*-test statistics comparing till and no-till sample means for runoff, soil carbon, soil losses, soil organic carbon content, dissolved organic carbon and soil organic carbon losses from the runoff plots. Data computed from the 6 plot replicates of 22.5 m² and the 10 erosive events of the 2008/2009 rainy season

		Mean		t-value	df	p	Significance
		till	no-till				
R	%	18.50	14.50	0.19	18	0.85	NS
SC	g L^{-1}	0.93	2.19	3.02	48	0.00	***
SL	gm^{-2}	301.50	96.80	5.83	18	0.00	***
SOC	g C kg^{-1}	48.30	71.00	1.93	11	0.08	NS
DOC	Mg C L^{-1}	7.90	5.90	9.70	48	0.00	***
SOCL	g C m^{-2}	16.20	7.70	2.99	18	0.01	*

R = runoff, SC= soil carbon, SL = soil losses, SOC = soil organic carbon content, DOC = dissolved organic carbon and SOCL = soil organic carbon losses
Carbon

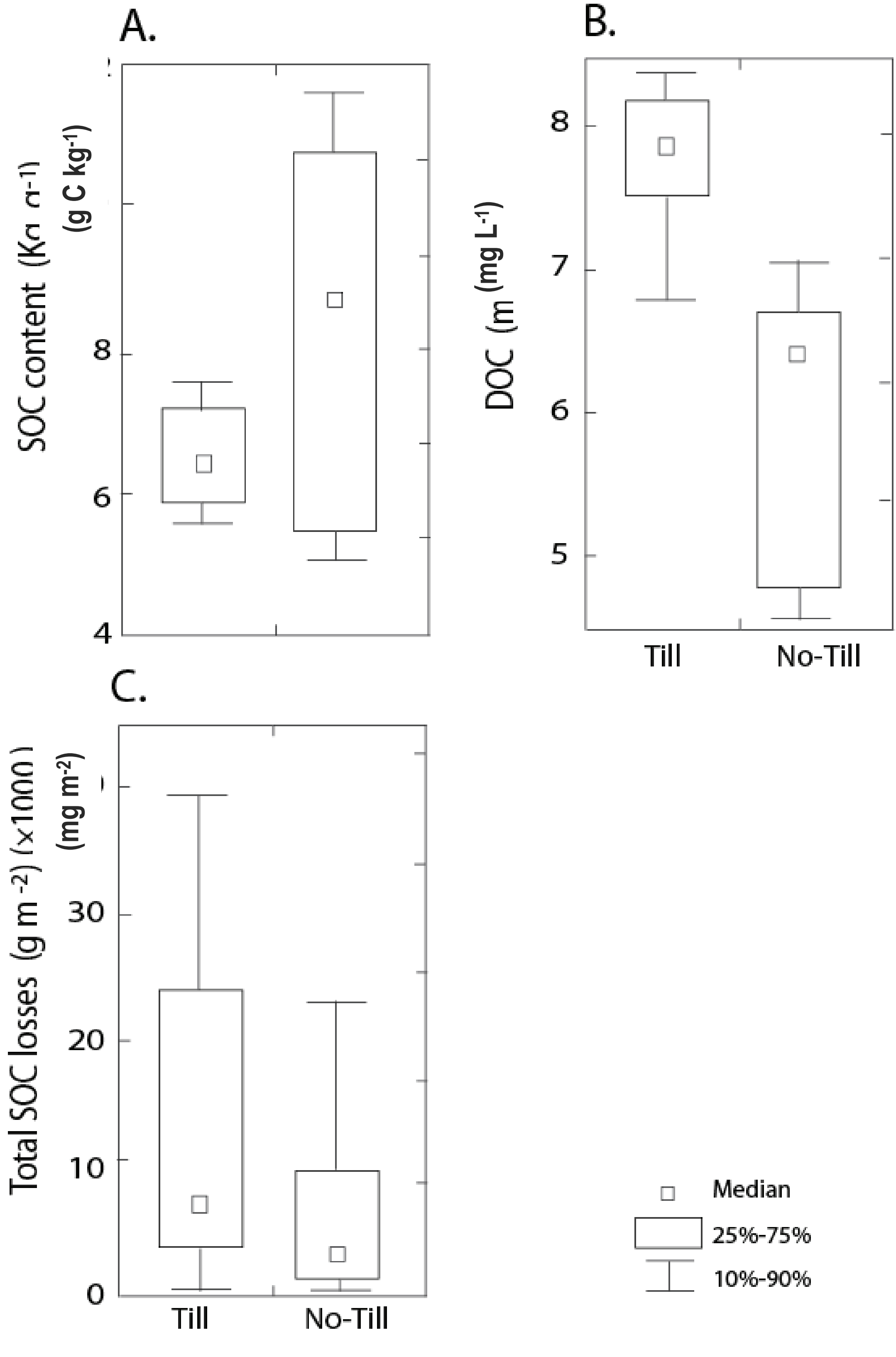

Figure 28. Box-plots for soil organic carbon content (SOC) in sediments, dissolved soil organic carbon (DOC) in runoff, and total SOC losses exported from the plots. Data computed from the 6 plot replicates and form 5 of the 10 erosive events.

9.2. No tillage impact on carbon dioxide emissions from soils and eroded sediments

Carbon dioxide emitted from soils and sediments collected from no-till and conventionally tilled plots were analysed and results are presented below.

9.2.1. The methods used

Three replicates of undisturbed soil samples were collected from the till and no-till plots at 0-0.02 m sampling depths using co-rings made from PVC. The samples were immediately wrapped in wet paper towels, placed in air-tight plastic-bags and placed in a cooler box on the field. In the laboratory, the samples were stored at –4°C to minimise microbial activity before analysis for biological activity.

Sediment samples were collected from each 80-L collection tank, after each rainfall event. The suspended sediments were filtered through a synthetic fine-filter and stored appropriately for biological activity analysis. The collection tank was then swirled to collect a sample of total (suspended plus settled) sediments with approximately 0.95 L of water in the collection tank. These samples were left to stand to enable sediments to resettle. The water was decanted and the sediments sampled. All samples were placed in air-tight plastic-bags and stored at –4°C in the laboratory for biological activity analysis.

Analyses of CO_2 emissions from soils and sediments were done at constant humidity and temperature of approximately 28°C. Soil and sediment samples were incubated in 0.6-L jars for 165 days. Carbon dioxide emissions were assessed on a daily basis using a Pp system EGM-1 carbon dioxide analyser (CO_2 analyser). To measure CO_2 emissions from soil or sediment samples, the jars were sealed with air-tight lids for 45 minutes to allow accumulation of the gas in the jar. The accumulated carbon dioxide was measured using the CO_2 analyser, as illustrated in Figure 29. The assessed CO_2 and incubation time were computed to obtain CO_2 emissions in a 24-hour incubation period. The cumulative CO_2 was expressed in kg C m^{-2}. The jars were then left open for the rest of the day to allow aeration.

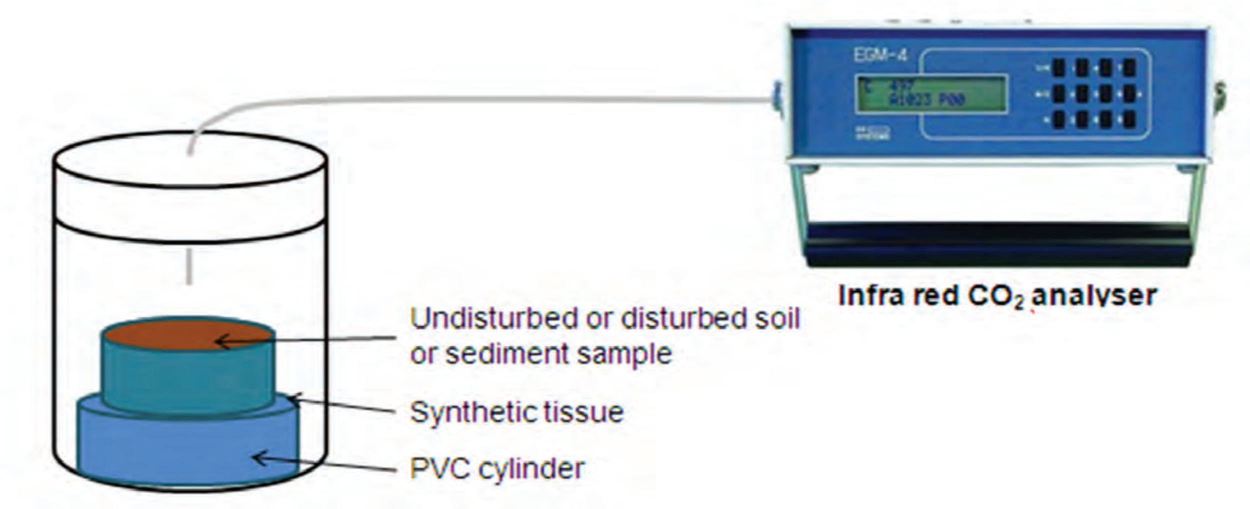

Figure 29. Incubation of undisturbed soils and settled and suspended sediments, and the analysis of accumulated CO_2 using the infrared CO_2 analyser.

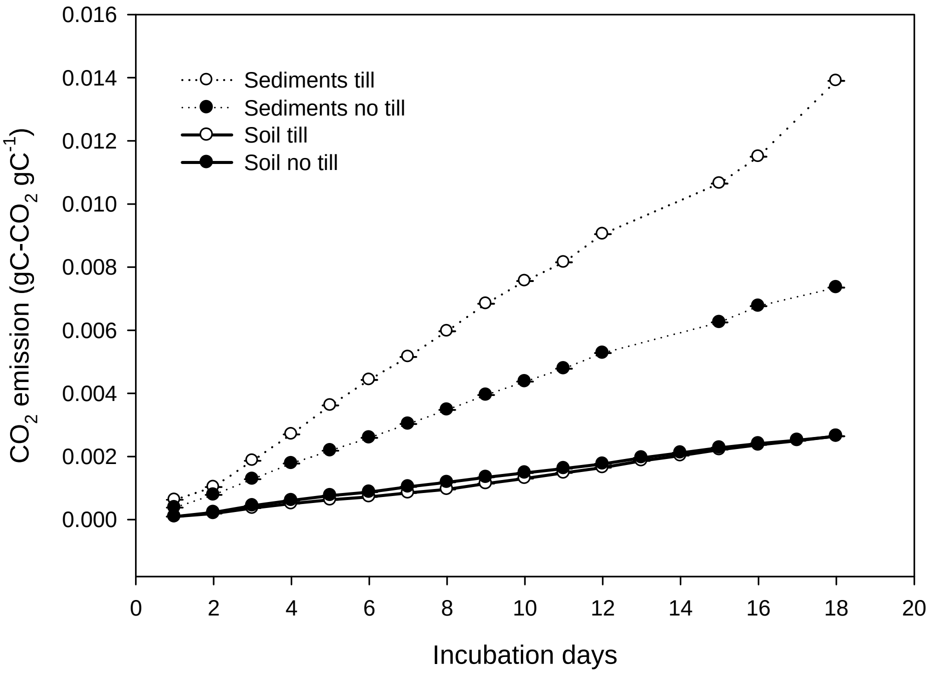

Figure 30. Mean of CO_2 emissions for soils (0-0.02 m) and sediments during the first 18 days of incubation and for the till and no till treatments. n=9.

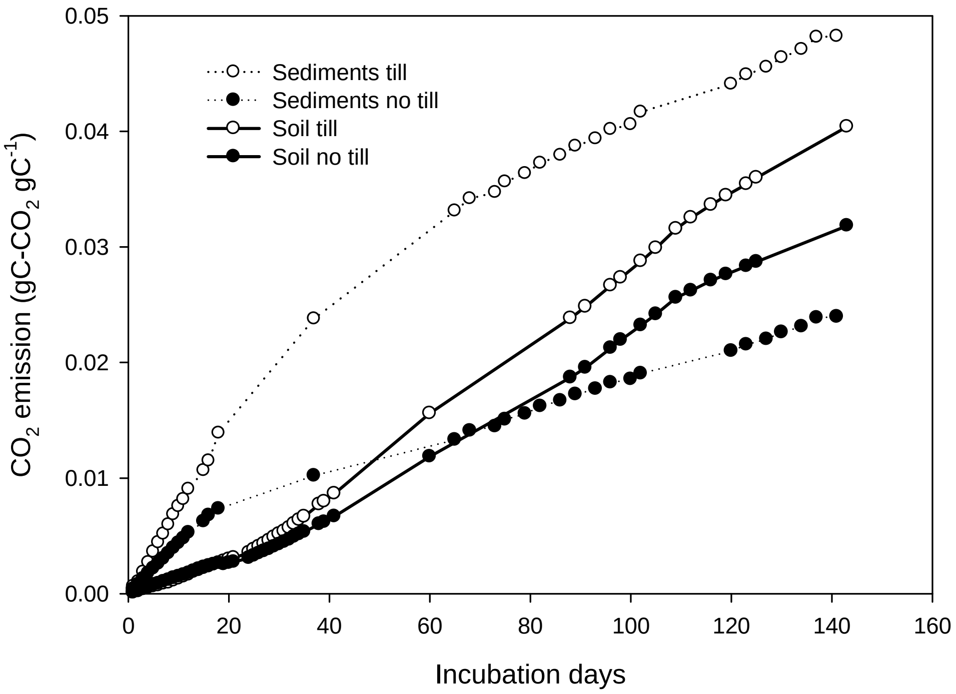

Figure 31. Mean of CO_2 emissions during the 145-day period for soils (0-0.02 m) and sediments from the till and no till treatments. n=9.

Measurements of soil microbial biomass C were done for all collected samples using the chloroform fumigation-extraction method. Soil microbial biomass carbon was analyzed using the method that was used by Voroney *et al*., 1993. However, certain modifications were done to the method. For this experiment, the soil suspension was centrifuged at 10 000 rpm for 2 minutes before filtration and analysis. Moreover, organic C was determined using the Total Carbon Analyzer (TOC) immediately after filtration. The standard solutions of 0, 10, 50 and 100 ppm C were made up using 0, 1, 5 and 10 ml of TOC stock solution (2.125 g of oven dry reagent grade potassium hydrogen phthalate ($C_8H_5KO_4$) per 1000 ml of deionised water).

9.2.2. Carbon dioxide emissions from soils and sediments

Figures 30 and 31 show the steady increase of CO_2 emissions from soils and sediments over the incubation period. Soil samples were collected at a sampling depth of 0-0.02 m from till and no-till plots, and sediments were collected from runoff plots located on the same till and no-till plots as above. Mean accumulative CO_2 emissions over 18 days of incubation was greater for sediments than soils for both tillage treatments. The highest accumulative emission was from sediments collected from tilled plots (till-sediments) with 0.014 g C-CO_2 g C^{-1} (Figure 30), followed by 0.007 g C-CO_2 g C^{-1} emitted from sediments collected from no-till runoff plots (no-till-sediments). Accumulative carbon dioxide emitted from soils collected from tilled plots (0.002 g C-CO_2 g C^{-1}) was not different to accumulative emissions from no-till plots (0.002 g C-CO_2 g C^{-1}) over the first 18 days of the incubation experiment.

However, at the end of the 145 day incubation period, accumulative g C-CO_2 g C^{-1} were greatest for till-sediments, 0.049 g C-CO_2 g C^{-1}, followed by 0.041 g C-CO_2 g C^{-1} from tilled soils, then 0.031 g C-CO_2 g C^{-1} from no-till soils, and the least being 0.024 g C-CO_2 g C^{-1} from no-till sediments (Figure 31). At the end of 145 days, accumulative CO_2 emissions had not reached a plateau.

Figure 31 illustrates that accumulative g C-CO_2 g C^{-1} from tilled soils was 18.33% higher than accumulative g C-CO_2 g C^{-1} from no-till soils after 145 days of incubation. This difference suggested that tillage had a significant impact on mean accumulative g C-CO_2 g C^{-1} emissions from soils at $P<0.05$. Moreover, accumulative CO_2 emissions from till-sediments were 44.52% higher than emissions from no-till-sediments. This difference also suggested that tillage had a highly significant impact on mean accumulative g C-CO_2 g C^{-1} emissions from sediments at $P<0.001$. The P values signifying a significant impact of tillage on CO_2 emissions from soils and sediments at the end of the 145 day incubation period are presented in Table 16. The P values in Table 16 and the curves on Figure 31 also suggest that CO_2 emissions were significantly higher from sediments originating from tilled plots compared to the tilled soils themselves. On the other hand, mean accumulative CO_2 emissions were higher for no-till soils at $P<0.05$ than for no-till sediments.

9.3. Carbon dioxide emissions from settled and suspended sediments

A steady increase in cumulative CO_2 emissions over 145 day incubation period from settled sediments collected from both till and no-till runoff plots are illustrated in Figure 32. Though these curves did not reach a plateau, the P values, computed from the mean accumulative CO_2 g C^{-1} and presented in Table 16, suggest that the difference between the means was not statistically significant. Thus, tillage did not have a significant impact on accumulative CO_2 emissions from settled sediments.

However, tillage had a highly significant impact on accumulative CO_2 emissions from suspended sediments. This was observed from the curves illustrated on Figure 33, where CO_2 emissions from suspended sediments eroded from tilled runoff plots quickly increased initially, and showed an exceptionally higher mean accumulative CO_2 emission at the end of the 145 incubation period, compared to no-till sediments. The P value suggesting the highly significance impact of tillage on accumulative CO_2 emissions from suspended sediments is presented in Table 16.

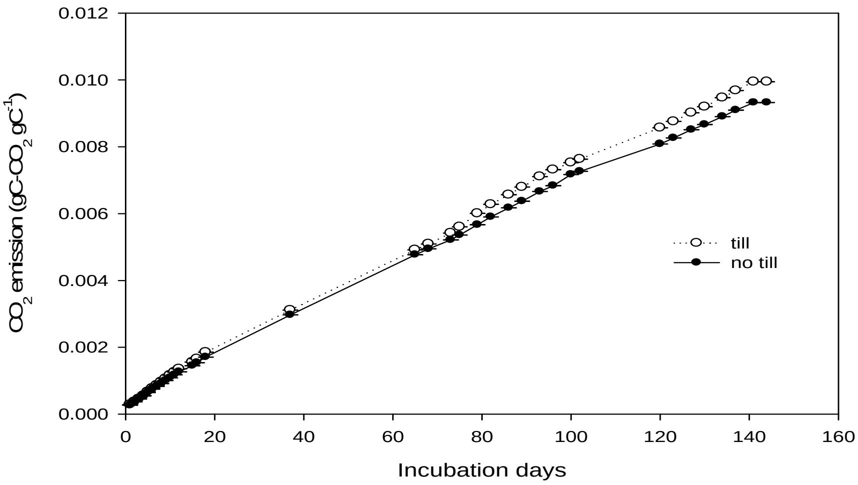

Figure 32. Mean of CO_2 emissions in settled sediments eroded from the till and no till plots. n=3.

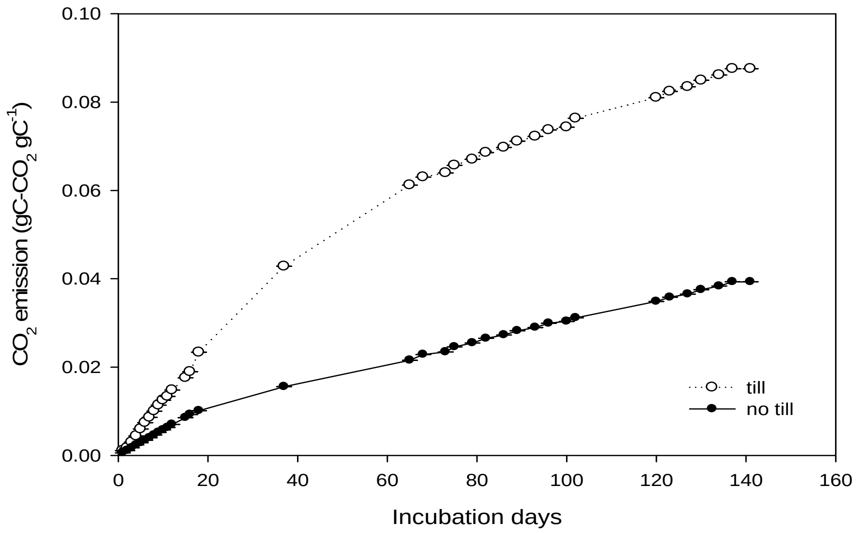

Figure 33. Mean of CO_2 emissions in suspended sediments eroded from the till and no till plots. n=3.

Table 16. T-test for CO_2 emissions for total sediments (Sed), soils, suspended sediments (Filter) and settled sediment (Gutter) for the till (T) and no-till (NT) treatments. n=9 for all samples.

	Mean(g C-CO_2 g C^{-1})	Mean(g C-CO_2 g C^{-1})	t-value	df	p	Significance
Sed T vs. Sed NT	0.05	0.02	16.97	30	0.00	***
Soil T vs. Soil NT	0.04	0.03	2.12	28	0.04	*
Filter T vs. Filter NT	0.08	0.04	19.82	28	0.00	***
Gutter T vs. Gutter NT	0.01	0.01	1.06	28	0.30	NS
Soil T vs. Sed T	0.04	0.05	-5.74	29	0.00	***
Soil NT vs. Sed NT	0.03	0.02	1.81	29	0.08	*

NS = Not significantly different; * = Significance at P<0.05; *** = Significance at P<0.001.

9.4. Analysis of microbial biomass carbon

Microbial biomass carbon at the 0-0.05 m sampling depth was higher in no-till soils compared to tilled soils, as illustrated by the bar graph below (Fig. 34). The impact of tillage on microbial biomass carbon was significant at P<0.05, where 16 mg C $kg^{-1}$was quantified from tilled soils and 37 mg C kg^{-1} was quantified from no-till soils.

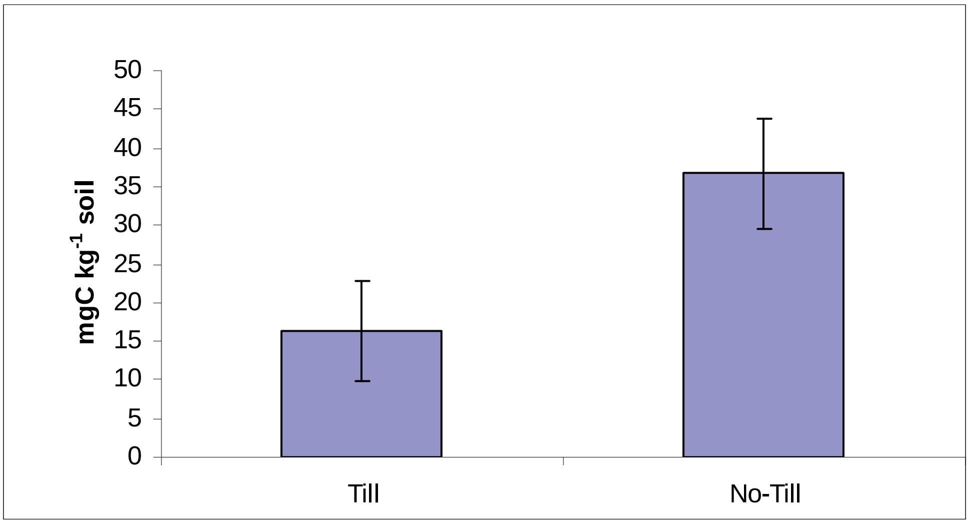

Figure 34. Microbial biomass carbon in till and no-till systems expressed in milligrams of microbial carbon per kilogram of soil. n =1.

10. DISCUSSION

10.1. Spatial and temporal variations of overland flow and controlling factors

As expected, it was found that the amount of OF generated varied within seasons in response to variations in rainfall characteristics (e.g. Bartley *et al*., 2006 and Bautista *et al*., 2007). For any given rainfall, OF response was found to be highly variable within the micro-catchment. Since OF is primarily controlled by the response of the soil surface to rainfall, any variations in rainfall characteristics will cause a large degree of variability in the overland flow that is produced by a rainfall event. The highest volume of OF was generated at the bottomland position followed by the midslope whilst the lowest was observed at the footslope. Following Dlamini *et al.* (2011) who investigated (in the same micro-catchment and using 2007/2008 data) the link between total OF and selected environmental factors of control, higher OF generated midslope can be explained by the higher occurrence of soil crusting. These results confirm as well previous observations by Chaplot *et al.* (2007), whereby soil crusting was found to mainly control OF in the sloping lands of south-east Asia. Similar results where the soil surface features controlled OF were found by Descheemaeker *et al.* (2006) in a study conducted in the Ethiopian Highlands. The present study confirms the major effect that soil surface conditions such as crusting has on OF volumes. What could be here considered as new is the fact that the impact of soil surface conditions may vary over time and especially as a function of the soil water status. Indeed, field observations of water fluxes at the different scales show that unless the soil cover was saturated by water, there was little connectivity between the different landscape compartments. Fluxes were found to be higher when the catchment was wet and whatever the soil surface conditions, soils were producing similar amounts of OF. There is indeed a need to further investigate at what levels of soil saturation by water (*i.e.* threshold value) that the role that crusting has on OF diminishes. Our belief is that when the soil is dry, crusting is likely to play a major role, while when soils wet up, the crusting impact on OF is likely to diminish.

10.1.1. Temporal variations of overland flow

In addition to the spatial variation across the landscape of total OF were variations of time to runoff initiation (TRI) with a 3 year average ranging from 0.2 to 6.4 minutes. TRI was found to be the lowest in the bottomlands and the highest at the footslope. This order of response was identical to that of total OF, meaning that the locations that produce the largest amount of OF also showed the fastest OF generation. TRI was highly spatially variable and this confirms several studies focussed on soil infiltration and OF generation. At a nearby site under soil and land use conditions but with a greater range of soil crusting, Podwojewski *et al.* (2011) using a rainfall simulator found large variations of OF response to rainfall. TRI estimated from the infiltration curves from a 30 $mm.h^{-1}$ rainfall event ranged from less than 2 minutes to about 5 minutes. This TRI range is in accordance with the results that were found in the present study. Similar results were found in the study by Devaurs and Gifford (1984) in the rangelands of Idaho, USA (0.6 <TRI<24 min.). The following part of the discussion investigates the reasons of such high variations in TRI.

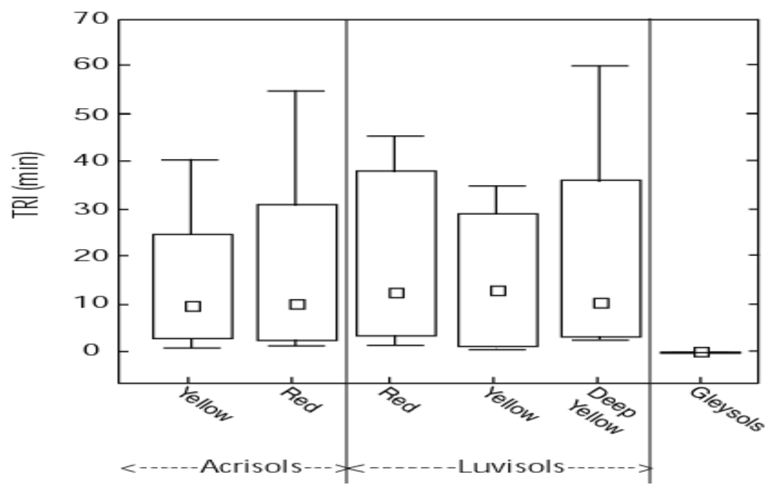

Figure 35. TRI as a function of soil types found in the study micro-catchment

Our results showed that within hillslopes, bottomlands exhibited a unique behaviour in respect of TRI. The bottomlands, with full surface coverage and no crusting, showed infiltration coefficients of either 100 or 0 percent, i.e. a TRI of 0 second or no response (infinity). The multivariate analysis performed from data coming from this slope position revealed that cumulative rainfall and soil water tension were the only controlling factors of TRI, with TRI being the longer early in the rainy season because of dry soil conditions (low cumulative rainfall and high soil water tensions). After a certain cumulative rainfall threshold necessary for the bottomland water table to reach the soil surface, TRI was found to be 0 sec., indicating instantaneous response to rainfall regardless of the characteristics of the event.

The rest of the hillslope exhibited a different behaviour. The multivariate analysis indicated that TRI was primarily controlled by soil and soil surface characteristics rather than the soil water status and rainfall conditions. Among the soil surface characteristics coverage and crusting have been shown to play an important role, with TRI decreasing as soil surface crusting increases. Ben-Hur *et al.* (1985) similarly found that soil crusting has a large influence on the infiltration process and hence overland flow. Podwojewski *et al.* (2011) explained that the differences in overland flow response can be a result of different soil surface coverage and crusting, where areas with low soil surface coverage and high crusting were found to have a faster response. Soil surface features impact overland flow through changes in soil porosity. The transport of water through soil takes place in the pore spaces between soil particles and soil aggregates. Soil crusts are surface layers of soils harder and less permeable than the underlying soil and forms by disaggregating compound soil particles (sand, silt, clay) reduces soil porosity of different size scales (e.g. Dexter and Richard, 2009), thus explaining the link between soil crusting and soil infiltration by water. Greater TRI at higher vegetation coverage can be explained according to Dexter (1988) by features such as plant roots and associated biopores. Miyata *et al.* (2010) suggested that the difference in infiltration along a slope can be explained by the rapid infiltration related to macropore flow. From these results, areas with a high degree of excess soil saturation or areas with a large degree of soil surface degradation will generate OF quickly and will therefore have a low TRI.

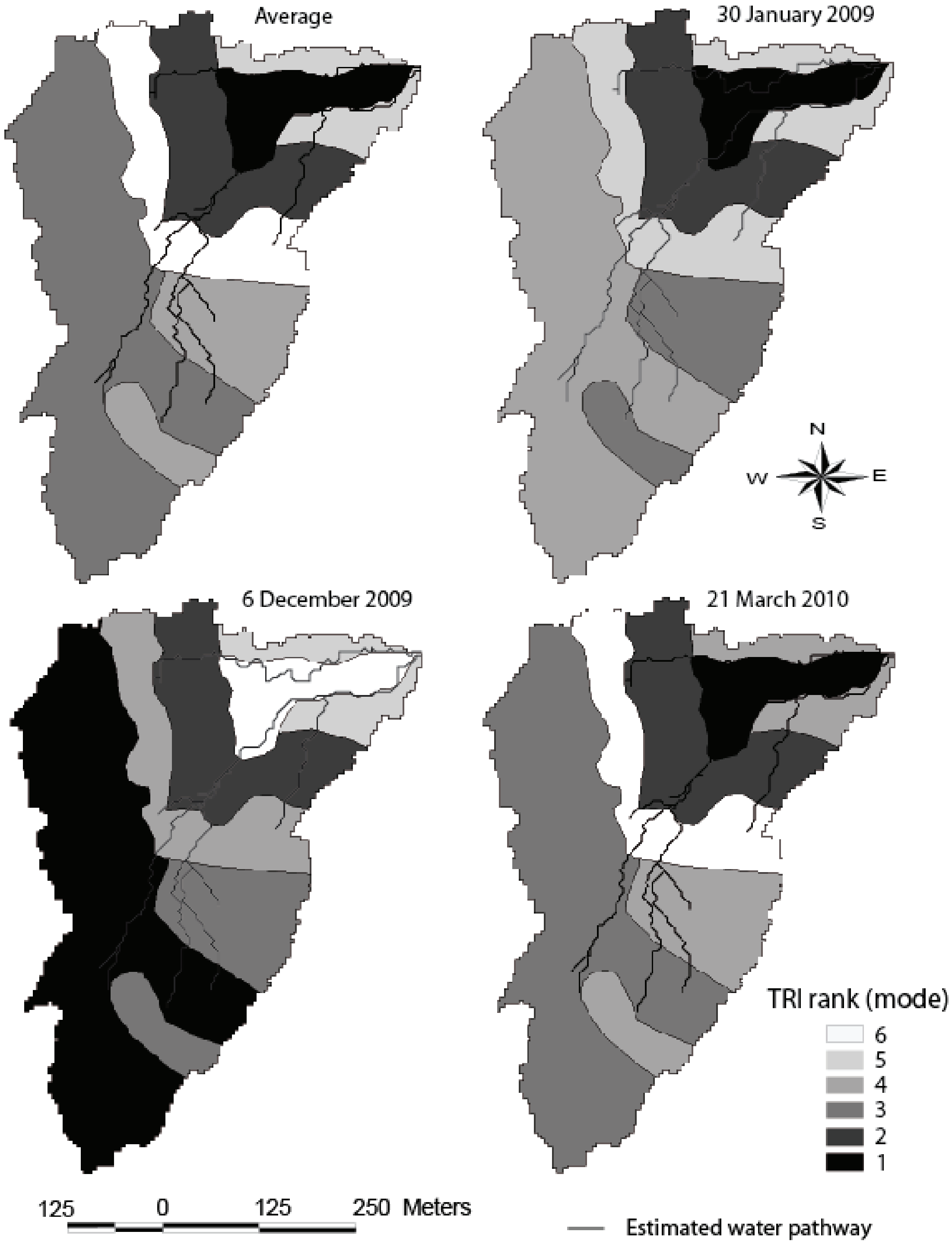

Figure 36. TRI ranking for three rainfall events of the 2007-2010 period

Soil characteristics were shown to be key in the control of TRI over the area. The different soil types found within the micro-catchment displayed different TRI characteristics, as shown in a box plot of TRI as a function of soil types found in the study micro-catchment (Figure 35).

The quickest response and lowest TRI was found to occur in the areas of the micro-catchment were Gleysols, followed by Acrisols with the greatest delay in OF generation occurring in Luvisols found within the micro-catchment. With the use of this finding, the ranking of each of the 6 soil types', found within the micro-catchment, response to 3 rainfall events has been ranked (Figure 36).

Such an approach allows for predictive modelling and assumptions to be made in different catchments in terms of OF response to rainfall. However, some considerations need to be made. As the highest and lowest TRI values were found in the soil types with the lowest soil clay content, soil clay content cannot be the sole explanatory variable for the differences in soil type response. Wakindiki and Ben-Hur (2002) suggested that clay mineralogy and aggregate stability can play an important role in the control of overland flow highlighting the need to further investigate the soil type effect on TRI. Moreover, TRI was shown to increase as soil clay content increased confirming the previous work conducted by Van Es *et al.* (1991) which contradicted to previous results from Williams *et al.* (1981). The positive correlation between clay content and TRI might be explained by the presence of stable aggregates, which as reported by Dlamini *et al.* (2011), decreases soil disaggregation therefore allowing for high infiltration rates and delayed overland flow generation.

This study added to the previous knowledge in the sense it allowed to rank the importance of the different factors of control of TRI with soil surface conditions playing a major role followed by soil characteristics. Soil water content becomes predominant when soils get waterlogged. This, not only occurs in the bottomlands during the wet season, but further up hillslopes, as the subsurface water table rises. Our results seem to indicate that OF within the area is of two types, i.e. saturation excess (in the bottomland) and Hortonian (on the rest of the hillslope). Again, it would be wise to investigate the ranking between such factors of control before and after the soils get wet.

A final aspect to be discussed is the generation of a predictive tool for TRI spatio-temporal variations. According to the linear regression models derived, crusting was able to explain over half of the variations for all events as illustrated by the strong linear relationships. Therefore, in areas with a high proportion of the soil surface covered by crusts, the models predict that the TRI will be low. A limitation to this approach is the exclusion within these models of the areas within the micro-catchment which are prone to waterlogging (*i.e.* Bottomlands) and thus potentially highly responsive to rainfall events. Since the results used to derive these simple models were obtained from only 6 microplot locations some caution needs to be taken. Extrapolating the result of relatively few 1 m^2 micro-plots to an entire catchment should be as well performed with caution.

10.2. Changes in water quantity and quality across the scales

Delivery ratios of the fluxes of runoff, selected nutrients and sediments (calculated from the end of the 2010/2011 rainy season yields) can be calculated using the obtained data. Subsequently, Figure 37 shows a summary of the Runoff, DOC, POC, Nitrates and sediment yields observed at the nested spatial scales ranging from 1 m^2 to 1000 ha for the 2010/2011 rainy season.

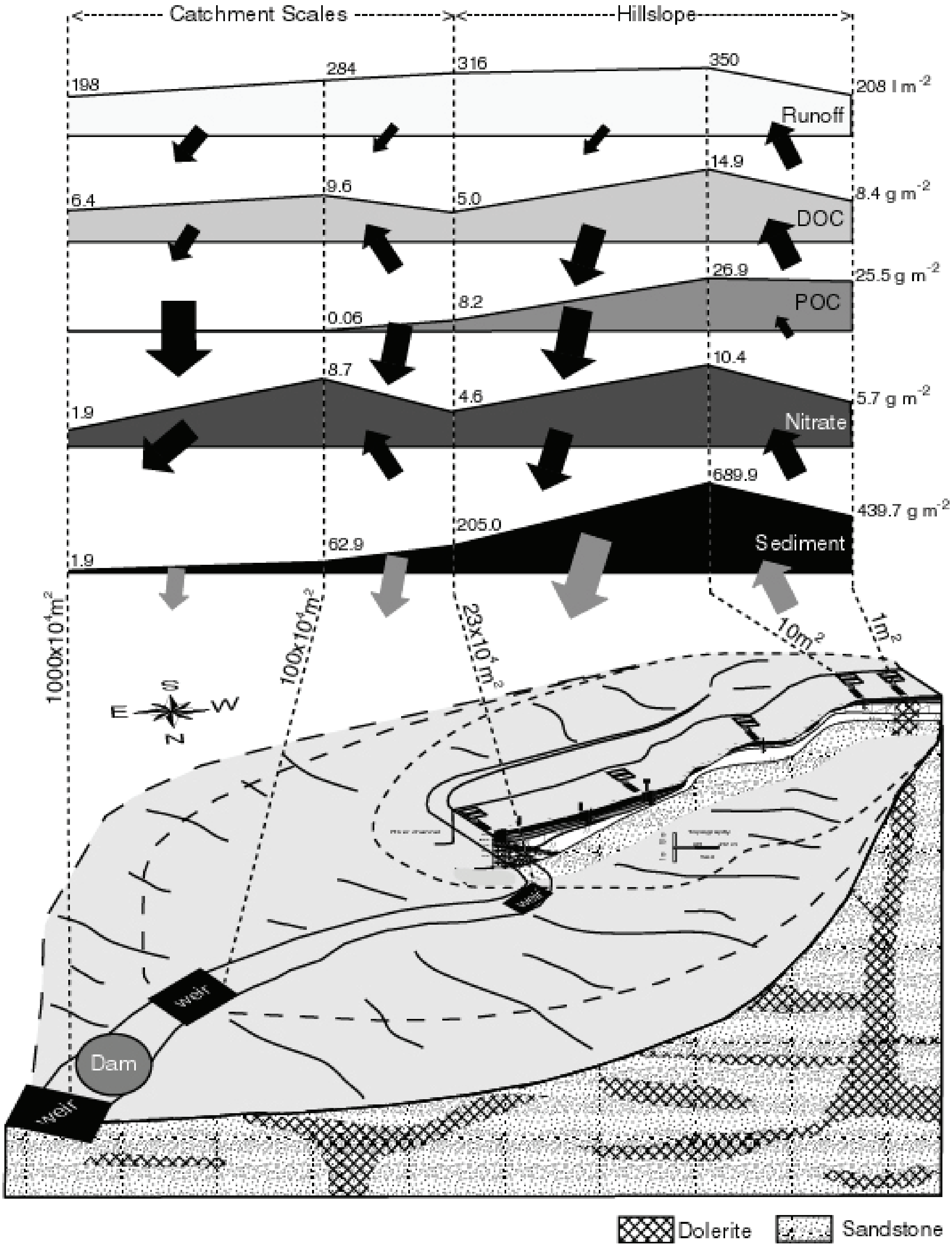

Figure 37. Runoff, DOC, POC, Nitrates and sediment yields observed at the nested spatial scales ranging from 1 m² to 1000 ha for the 2010/2011 rainy season

The scale ratio between the microplot and plot scales was 1.68. The scale ratio was 0.90 between plot and micro-catchment (*i.e.* the water flux at the micro-catchment level was 10% lower that at the plot level); 0.89 between micro-catchment and 100 ha catchment; and decreased sharply to 0.70 between 100 and 1000 ha catchments. The scale ratios for the period of 2010/2011 calculated show that there was a steady decrease in the delivery of water from the hillslope scale (*i.e.* overland flow measured at the plot scale) to the catchment scale. The scale ratio calculated from plot to hillslope was considerably higher than this obtained from other regions in the world. Among the few studies available, Chaplot and Poesen (2012) found the delivery ratio between plots and micro-catchment to be 0.04, meaning that the micro-catchment yearly flux of water was 4% only of this of plots. Conversely, the scale ratio calculated from hillslope to catchment of 0.9 was considerably lower than the 21.7 obtained in Laos by the same authors. Chaplot and Poesen (2012) state that the lower deliveries (of their study) at the micro-catchment outlet compared to the plot level is likely to come from the reinfiltration of water on the lower portions of slopes (which are later re-introduced within the catchment) as has been shown in other studies under different environmental conditions by, for instance, Cammeraat (2004) and Bracken and Croke (2007). The increase of runoff delivery from the hillslope to the catchment level by a factor 21.7 in Laos (Chaplot and Poesen, 2012) is likely to be due to the contribution of saturation overland flow at the foot of the hillslopes (seepage) as observed at the same site by Vigiak *et al*. (2008).

Our results (i.e. a 0.9 ratio between plot and micro-catchment) tend to show a continuity between overland flow from plot to micro-catchment. However, there might be either continuity of overland flow or overland flow infiltration in hillslopes, sub-surface downslope water movements and seepage into the river channel. Those two hypotheses can be valid but flux data alone can't be used to support one or the other. The tracer data and end member mixing analysis highlighted the fact that sub-surface water contributions increased as the soil moisture status increased at both the 23 ha micro-catchment and 100 ha catchment outlets. Field observations identified that infiltration followed by wetting up of the soil profile and further seepage into the river channel is a dominant process as shown by the many seepage faces observed along river banks (*e.g.* Figure 38).

Water fluxes subsequently decreased from the 23 ha micro-catchment to the 100 ha catchment by a ratio of 0.89. There might be different processes at play. From the ratio of 0.89 one can think of a relatively low loss of runoff flux either by evaporation or seepage. Other hypothesis such as high losses and gains during the downstream course of runoff can't however be discarded. Considering the presence of a dense vegetation within the stream channel from 23 to 100 ha, we believe that evaporation can explain the 10% loss of water. The differences in fluxes might, however, be the result of errors in the estimation of water fluxes such as these due to the use of weirs. This is a major concern for hydrologists and this issue is still under debate. Continuous calibration of weir fluxes using complementary methods such as on-site calibration have shown however that errors, at least for low flows, are of the order of few percents (data not presented here).

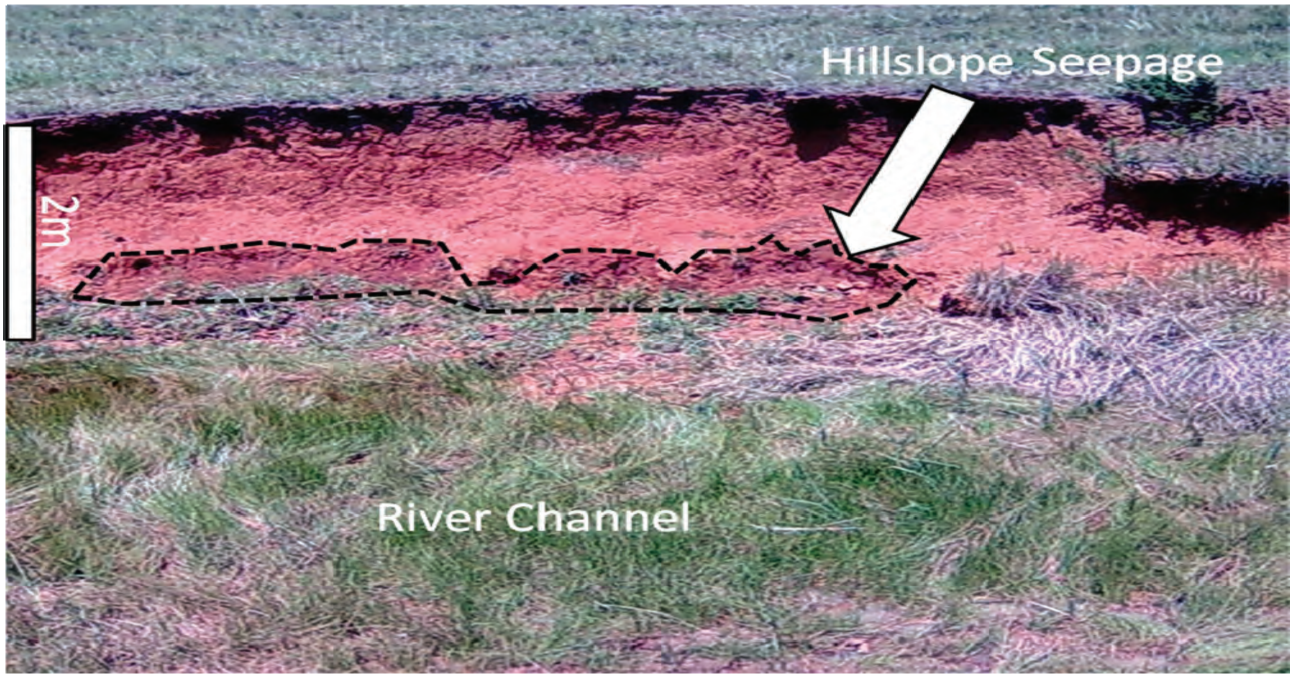

Figure 38. Example of hillslope seepage (presented as the darker shade red at the bottom of the channel bank) into the river channel 20 m upstream of the 23 hectare catchment outlet (photo taken on 10 February 2010)

There was a large decrease of water fluxes per surface unit from the 100 to the 1000 ha catchment. This could be explained by the presence of the 2 large dams, in-between these nested scales, used as storage for irrigation on a commercial farm. Besides water evaporating in the river channel, abstractions from the storage dams for application of irrigation water to crops as well as the evaporation of water from the dams will decrease the streamflow.

Note that in this evaluation, the cumulative flux data of the 10 m^2 plots were used rather the 1 m^2 microplots as the data representing the water generated on the hillslopes as a methodological error was identified after the research was conducted. The 1 m^2 microplots had a higher density of border perimeter bordering the plot which would cause preferential infiltration to occur and which, ultimately, decrease the amount of overland flow. However, an increase in the flux generated between the 1 m^2 microplots and the 10 m^2 plots could be a consequence of the greater connection between closed depressions or micropounds, thus leading to lower water pounding depths and associated decrease in soil infiltration (Hopp and McDonnell, 2009).

The delivery ratios for sediments was 1.57 between microplot and plot scales; 0.30 between the plot and 23 hectare catchment; 0.31 between the 23 hectare catchment and the 100 hectare catchment; and 0.03 between the 100 hectare catchment and the 1000 hectare catchment. The ratio between the plot scale and the 23 hectare catchment of 0.30 was significantly higher than the range of between 0.01 and 0.1 as reported in various studies (Trimble, 1983; Starr *et al.*, 2001; Beven *et al.*, 2005; Rommens *et al.*, 2005; de Vente *et al.*, 2007; Parsons *et al.*, 2006; Walling *et al.*, 2006). The present discussion will not attempt to explain the sources of the eroded sediment at the various nested scales as a study conducted by Oakes (2012) within the same Potshini research catchment addressed this issue. Oakes (2012) found that 73% of the sediments lost from the 23 hectares catchment are originated from deep soil horizons from gully banks. This points out that most of the exported sediments do not come from interrill erosion in hillslopes but from the collapse of river banks, a continuous process observed throughout the catchment (Chaplot *et al.*, 2010). From these results and those of Oakes (2012), it seems that most of the eroded sediments in the hillslope deposit (most likely at footslope positions) before reaching the river system, the recalculated delivery ratio (based on the results from Oakes, 2012) being closer to 0.08 than to 0.3; which corresponds to the upper range of available studies cited above. There were two other places in the landscape where sediments are deposited further downstream: (1) the river channel due to the decrease in the mean slope gradient from the 23 hectare to the 1000 hectare outlets one and (2) the presence of two dams upstream from the 1000 hectare catchment outlet.

The selected nutrients were Dissolved Organic Carbon (DOC), Particulate Organic Carbon (POC) and Nitrate (NO_3^-). The sediment delivery ratios between microplots and plots was 1.57. It was 0.30 between plots and the 23 hectare catchment and 0.31 between the 23 and 100 hectare catchments. The scale ratios of DOC between the overland flow generated on the hillslopes at plot scale (10 m^2) and the micro-catchment (23 hectare catchment) was 0.34, *i.e.* the DOC yields at the micro-catchment was 46 percent lower than that of the DOC yields from the plot scale; increased sharply 1.90 between the 23 hectare and 100 hectare catchments; and 0.67 between the 100 hectare and 1000 hectare catchments. The delivery ratio of POC between the microplots and plots was 1.05, which showed that there was more POC transported from the plots than the microplots. A reason for such behaviour can be explained by the different erosion and transport mechanisms occurring within the larger plot scale. Within longer plots there is a combination of both interrill and rill erosional processes which leads to an increase in the transport of soil particles and entire soil aggregates as shown by Oakes (2012) in the Potshini Catchment. The ratio decreased to 0.30 between the plot and 23 hectare catchment and to 0.01 between the 23 hectare and 100 hectare catchments. The scale ratio for POC between the 100 and 1000 hectare catchments was close to zero since the sediment fluxes at the 1000 hectare catchment were minimal.

The NO_3^- delivery ratio was 1.84 between the microplot and plot scales. It sharply decreased to 0.44 between the plot and 23 hectare catchment to subsequently increase to 1.90 between the 23 and 100 hectare catchment outlets and finally decreased to 0.22 to 1000 hectares.

For both the dissolved nutrients, DOC and NO_3^-, the delivery ratios had a similar trend occurring within the landscape. The trend was for the delivery ratio to decrease between the plot and 23 hectare catchment (which ranged between 0.34 for microplots and plots; and 0.44 between the plots and 23 hectare catchment); a steep increase between the 23 hectare catchment and the 100 hectare catchment (exactly 1.90); and a sudden decrease between the 100 hectare catchment and 1000 hectare catchment (range of 0.67 and 0.22). The decreases from plot scale to the 23 hectare catchment can be explained by the associated decrease in delivery ratios of runoff, which can result in differing nutrient yields. This document did not intend to find explanatory reasons on the variations of nutrient and carbon fluxes across scales. This being said, the increase in both DOC and NO_3^- between the 23 hectare catchment and the 100 hectare catchment is likely to come from the decomposition of organic matter which releases not only CO_2 to the atmosphere but as well NO_3^- to the water. In addition, the decay of the micro-organisms involved in OM decomposition increases DOC content in the water (Mchunu *et al.,* 2011). Aitkenhead *et al.* (1999) found that the increase in DOC concentration in streams correlated to the amount of wetlands occurring within a catchment. Indeed, the river channel from our 23 hectare micro-catchment to the 100 hectare outlet is braided into a myriad of connected wetlands. Furthermore, these additions can come from the small-scale agriculture in this area of the catchment. Fertilizers (both inorganic and organic) are used to supplement the natural soil fertility. Such practises are done to increase crop yields. The use of specific tracers such as Ur or Zn present in inorganic fertilisers could allow to conclude on this issue. The subsequent downstream decrease of nitrate levels may result either from an input of water to the river which has a lower nitrate concentration (dilution) or the consumption of nitrate itself within the river channel. Two compartments connected with the river may play a role: (1) the deep groundwater (sampled from boreholes), and (2) water sourced from the hillslopes of the catchment. The first two compartments are likely to have lower nitrate concentrations (Cirmo and McDonnell, 1997) and specifically nitrate concentrations (Grimaldi and Chaplot, 2000). In addition, chemical denitrification can take place in the presence of iron species in deep groundwater which are in contact with geological materials (Koelle *et al.*, 1985; Postma *et al.*, 1991). The decrease in nutrients between the 100 hectare and 1000 hectare catchments can be explained by the discontinuity in runoff resulting from the dams located the 2 monitored scales which are utilised on the commercial farm. Any dissolved nutrients in the catchment flow will be impounded by these dams.

The behaviour of the particulate Carbon delivery ratios between the microplot and plot scales showed there being an increase in the amount of particulate Carbon possibly due to more advanced erosion processes occurring at the plot scale (which is supported by the sediment delivery ratios between the different scales). The decrease in the delivery ratios between, both, the plot and 23 hectare catchment and between the 23 hectare catchment and 100 hectare catchment point to the depletion of particulate Carbon due to deposition along the hillslope and stream channel or the decomposition of the bonded Carbon by micro-organisms. Low carbon delivery ratios from plots to 1000 ha outlet pointed to the decomposition of DOC and possibly POC; POC could as well be deposited within the catchment. Specific studies on organic carbon fluxes at catchment level are to our knowledge very rare. These results are in concordance with those of Chaplot and Poesen (2012) on POC delivery ratios, which is one of the few papers on the scale issue for eroded organic carbon. Wang *et al.* (2010) in a study conducted in the Belgian Loess belt found that detached POC from the soil did not decompose but rather was re-deposited within the catchment boundary or further transported downstream in catchment runoff. Such a conclusion was based on the stability of the isotopic signatures and ratios of C^{13} and C^{12} across different spatial scales. Wang *et al.* (2010) based these conclusions on there being no decomposition occurring within the catchment and also does not take into consideration the changes of the ^{13}C isotope which may be compensated by the inputs due to the process of water erosion of organic matter which can be composed of high $^{13}C/^{12}C$ ratios. Such conclusions seem quite speculative and not applicable for this study. In the case of this study the decrease in the POC fluxes in conjunction with the increase in the fluxes of DOC and N, between the 23 hectare catchment and 100 hectare catchment, as well as the C^{13} ratios staying constant between the catchment outlets as found by Juarez (2010), tends to show that decomposition of POC is significant within the catchment.

There needs to be further research and investigation into the behaviour of nutrients such as DOC, POC and NO_3^--N beyond the fate of the microplot, plot and catchment boundaries. Such an approach requires a better understanding of the catchment's geochemistry and microbiology.

10.3. Depletion of soil stocks in organic carbon and nutrients due to water erosion

A study on soil stocks of carbon and nutrients was conducted at the same catchment by Dlamini (2010) with two main objectives as follows: (1) to evaluate soil organic carbon and nutrient stocks and their spatial variations under an overgrazed grassland ecosystem; and (2) to quantify the impact of some of the controlling factors on soil nutrient stocks, *i.e.* topography, parent material and soil properties in the upper portions of the Potshini Catchment (*i.e.* the 23 hectare catchment). Within the context of this study there is not a detailed assessment of the controlling factors of nutrient losses, transport and transformations from within the catchment as was the case for the soil nutrient stocks. Such an objective requires a complete understanding of the carbon and nitrogen cycles in relation to the hydrological processes and pathways in conjunction with the biological activity within the catchment at the various hydrologically important areas (hillslopes, channel and dams, *i.e.* where the samples were taken from in the catchment), which was beyond the scope of the research. In the study of Dlamini (2010), sampled the topsoil (0-0.05 m) of the 23 ha grassland micro-catchment at the nodes of a 20×20 m grid. The average stocks were found to be 12.2 t/ha for OC and 0.7 t/ha for soil organic nitrogen (ON) (Dlamini, 2010). Using these figures, the percentage loss of 0-0.05 m soil stocks by water erosion during the 2010/2011 rainy season would be as much as 2.8% for OC when microplot OC losses are considered, 3.4% for plots and 1.1% for the 23 hectare catchment. With reference to ON, the percentage of the soil Nitrogen stock lost during the 2010/2011 rainy season was 3.7% for 1 m^2; 4% for 10 m^2; 0.6% for the 23 hectare catchment; and 0.09% for the 100 hectare catchment.

The percentage of the soil organic nitrogen stocks lost at the different scales for this study are comparable to studies that have been conducted in other parts of the world. For example, Vanni *et al.* (2001) found that for a 50 hectare agricultural catchment in Ohio the total soil organic nitrogen stock lost in runoff had a yearly average of 1.1% (compared to 0.6% for our 23 hectare catchment) over a period of 5 years. However, the amount of soil organic nitrogen stocks lost from this study and the study of Vanni *et al.* (2001) are lower than those found by Ng Kee Kwong *et al.* (2002) in a study conducted in the sugarcane growing areas of tropical Mauritius. Ng Kee Kwong *et al.* (2002) found that the mean percentage of soil organic nitrogen stocks lost for a 70 hectare catchment was 12.3% over a 3 year period.

The amount of organic Carbon lost at the 1 m^2 (2.8%) and 10 m^2 (3.4%) microplot and plot scales is in the same range of soil organic carbon of sediments (2.4%<Sediment SOC<6%) found to have been lost from 22.1 m^2 runoff plots in the same Potshini Catchment but in the small-scale agricultural fields where maize is grown by Mchunu *et al.* (2011). The results of both this study and Mchunu *et al.* (2011) are in the same range (0-3.5%) of soil organic carbon losses as determined by Quinton *et al.* (2006) in a study conducted in the United Kingdom. However, the percentage of organic carbon lost at the different catchment scales are much lower (0.09%<OC<0.6%) and not within the range of OC losses reported by Mchunu *et al.* (2011). For both the results obtained in this study and the results of Mchunu *et al.* (2011), they are considerably lower than the losses of OC from runoff plots of 35 m^2 installed on different land management techniques found by Bertol *et al.* (2007) in a study conducted in the Santa Catarina Highlands of southern Brazil. Bertol *et al*. (2007) found that the OC in sediments lost from the soil had a range of between 100% and 117% depending on the land management technique. The soils of the study area used by Bertol *et al.* (2007) are of a similar soil type (Acrisols) to those of the ones found in the Potshini catchment. It is therefore apparent that the organic carbon losses occurring within the Potshini catchment are within the range of particulate carbon lost in different parts of the world.

The question of whether or not these losses are higher than the natural replenishment of the soil OC and ON remains needs to be addressed. Moreover, the fate of the eroded and transported soil organic carbon in between the different spatial scales of observation as well as in the sediments exported from the 1000 ha catchment needs to be further investigated. In a preliminary study conducted in the 23 hectare catchment of the Potshini catchment by Juarez *et al.* (2011) it was found that sediments with an OC enrichment factor of 1.8% were prone to high mineralization rates and CO_2 emissions to the atmosphere.

10.4. Landscape connectivity for runoff, organic carbon and nutrients

The end member mixing analysis was conducted as an initial attempt to evaluate the contribution of the different waters sources at the various spatial and temporal scales. There was a general increase in soil water contribution and a decrease in that of overland flow from the 23 ha micro-catchment to the 1000 ha catchment. Moreover, peak flows tend to be mainly composed of OF and SW, while low flows have a groundwater source. Such a finding is surprising as groundwater contributions are expected to continue to contribute some water to runoff during events. During periods of low flow, soil water which has moved deeper into the soil profile and reached the soil/bedrock interface is expected to continue contributing to runoff (Lorentz, 2012). The isotopic and tracer signals of groundwater sourced water may have been weak compared to that of the water sourced from overland flow and soil water. The results from the study were consistent with what has been reported elsewhere. For example, Brown *et al.* (1999) found for different events in a 24 ha catchment located in New York State that OF contributed between 21 and 53 percent and soil water between 10 and 31%, respectively. For their 109 ha catchment, overland flow contributed between 15 and 51% to catchment runoff whilst soil water contributions were between 18 and 46%, groundwater having a little contribution (Brown *et al*., 1999). Ribolzi *et al.* (2000) in a 91 ha Mediterranean catchment of Southern France found that the contribution of OF was more variable, since it ranged between 12 and 82%. Groundwater contribution to flows was in this study, high when compared to these international catchments but the fact that soil water and OF contributions were the highest during rainfall events was consistent with the previous studies. The fact that groundwater contributions increased with increasing catchment size is not uncommon since it has also been found by Hunt *et al.* (2005), Tetzlaff *et al.* (2007) and Tetzlaff and Soulsby (2008).

10.5. Impact of soil moisture and antecedent rainfall on landscape connectivity

Our results showed a sudden increase in the fluxes of water (Fig. 14) and nutrients (Fig. 15) during a specific period of the rainy season. In relation to this, the temporal variations of soil water tension at different depths and landscape positions is shown in Figure 39. When comparing Figures 14-15 and 39, some noticeable trends can be identified. The spatial variations of soil moisture as well the impact that soil moisture conditions can explain the temporal variations of the fluxes of water and nutrients within a catchment.

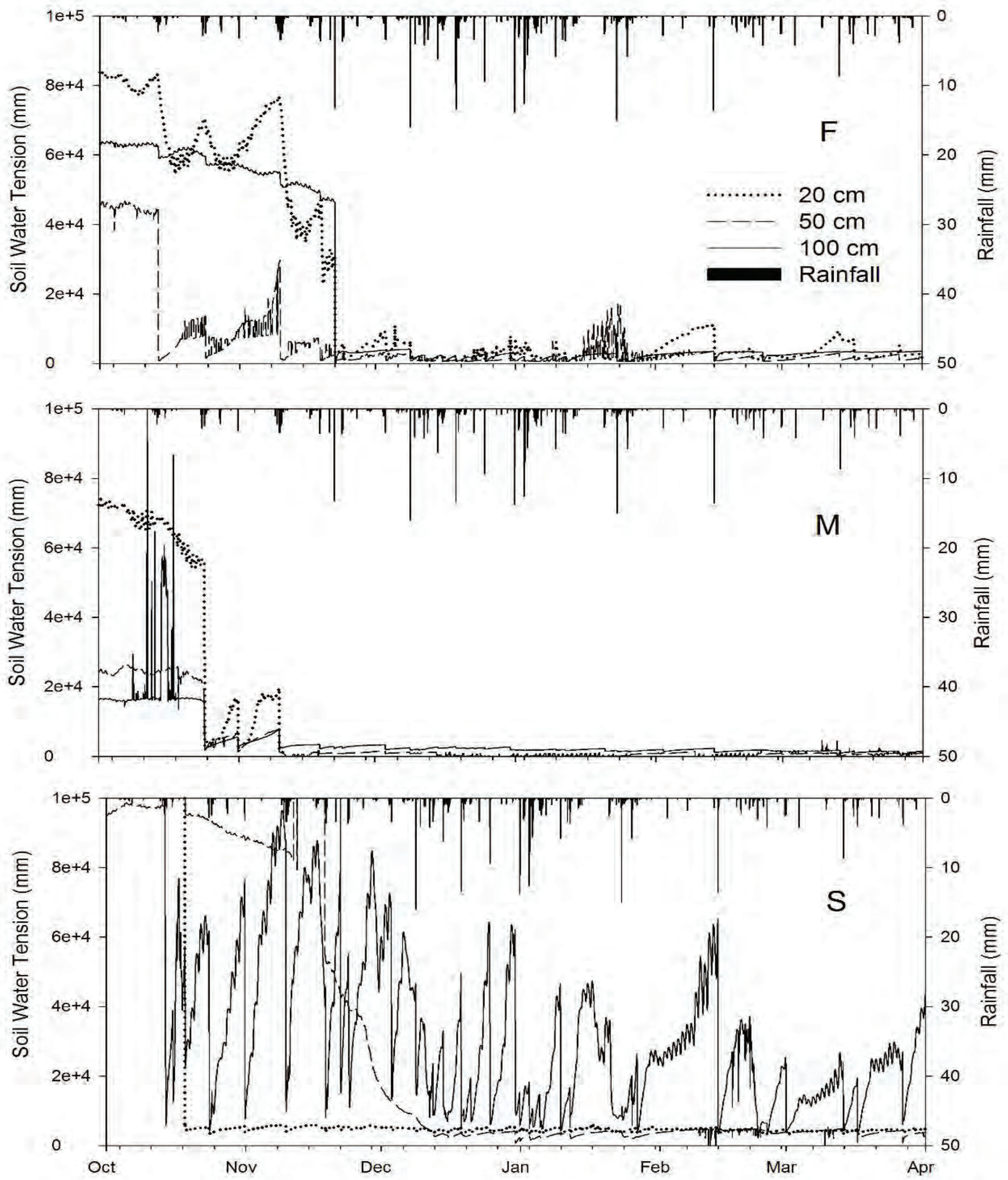

Figure 39. Temporal variations of soil water tension at different depths and landscape positions (2010/2011 rainy season). F for footslope, M for midslope and S for shoulder locations

The movement of water in the unsaturated zones of a catchment, *i.e.* the soils, needs to be monitored to better understand the conditions of the catchment when wet or dry. To achieve this, the investigation of soil water tensions. When comparing the soil water tensions of the Footslope and Midslope locations to the cumulative flux of the different scales (Figure 39), the impact of the degree of catchment saturation on the catchment response to rainfall can be viewed. The cumulative volume curves generated at the 1 m^2 microplots, 10 m^2, and 100 hectare catchment all showed a steep increase and change in the amount of water generated per unit area during the period of late November to December 2010 and late March 2011 which corresponded to the period in which the soil water tensions of all depths at the Footslope and Midslope and the soil at a depth of 20 cm and 50 cm at the Shoulder were low. This was indicative of the soil having increased saturation by water. The 23 and 1000 hectare catchment outlets showed cumulative volume curves indicative of consistent flow but during some periods of the rainy season there were sudden and steep increases in the cumulative flux curves which coincided with a period in which there was consistent rainfall and decreased/lower soil water tensions. The amount of water generated at all the different nested scales increased during specific periods when the soils within the catchment increased in wetness. Thus, connectivity between the different nested scales was found to have occurred. Such a result highlights the important role that the wetness of the soils within a catchment have on the spatial and temporal variations of runoff generation.

In addition, these periods also occurred when the soil water tensions of the Footslope and Midslope positions were low, which is associated increased soil water content (*e.g.* mid to late December 2010). Cumulative the sudden changes in the behaviour and decrease of the soil water tension (*i.e.* when the soil went from being dry to being wet) corresponded to a certain amount of rainfall. This rainfall corresponds to the period since the start of the rainy season until the date at which the change in the soil water tension occurs (a threshold amount of antecedent rainfall required to wet up the soil). The antecedent rainfall prior to the month of December 2010 was 226.2 mm. As the decrease in the soil water tensions corresponded to an increase in the water fluxes of the different scales, it is important to have an understanding of these thresholds to better understand and predict the behaviour of catchments with respect to floods. The use of a simple method such as a threshold amount of rainfall required to decrease the soil water tensions and increase the soil water content could prove to be valuable in predicting when there will be an increase in the flux of water within a catchment.

At the Footslope and Midslope positions a longer period of wetting up of the soil was observed. The Midslope position wetted up (and subsequently decreased soil water tensions) faster than that of the Footslope and Shoulder positions. This corresponded to the month of November. However, the Footslope location showed a delayed response (in comparison to the Midslope location), with the soil water tensions at 20 cm and 100 cm suddenly decreasing at the end of November. Thereafter, the soil water tensions for all depths for both these locations stayed low with there being some increases during periods of little to no rainfall. However, when rainfall occurred, all 3 depths at both locations responded instantaneously. At the Footslope and Midslope, the soil profile for both locations stayed relatively constant and low in terms of soil water tension for the duration of the rainy season. The Shoulder of the hillslope showed, initially, that the soil at a depth of 20 cm required less antecedent rainfall than the corresponding depths at the Midslope and Footslope positions to show characteristics of an increase in soil moisture. There was a great deal of variation in the soil water tension at the Shoulder location with the soil at a depth of 100 cm showing a trend of responding rapidly (decrease in the monitored soil water tension) to rainfall and then subsequently drying rapidly (increase in the monitored soil water tension) when there was no rainfall.

10.6. Tillage impact on runoff generation, soil surface conditions, soil organic carbon erosion and microbial biomass carbon

The experiment done to evaluate SOC erosion by water on no-till and conventionally tilled plots yielded results that show the ability of no-till to highly decrease SOC losses. Results from this experiment are discussed in detail below.

10.6.1 Runoff generation and soil surface conditions in till versus no-till plots

Under the conditions of the study, no-till systems did not decrease runoff ($P<0.05$). This result was also surprising considering that soil infiltration pathways are more likely to be preserved by the absence of tillage. In Minnesota, Lindstrom *et al.* (1998) studied the response of runoff to tillage regimes using rainfall simulation (70 mm hr^{-1}) on till and no-till plots. These studies revealed that no-till decreased runoff from 24-66% to approximately 3%, which corresponded to a runoff decrease as high as 93%. This was a maximum runoff decrease value to be obtained in such studies. Zheng *et al*. (2004) undertook a review of different experiments performed in the United States of America, the review revealed that the median decrease was 10-40% with only one experiment out of 12 with a runoff decrease of more than 90%.

In the present study, differences in terms of soil crusting between till and no-till plots (for example, the predominance of sedimentary and depositional crusts on tilled plots and of structural crusts on no-till plots), were expected to have induced differences in term of runoff. Indeed, soil surface conditions, which include factors such as soil crusting, have been shown to play an important role on soil infiltration and runoff production (Casenave and Valentin, 1992). In their evaluation of 87 runoff plots from 10 sites in Niger, Burkina Faso, Ivory Coast, Togo and Cameroon, Casenave and Valentin (1992) found the infiltration rate of structural crusts with a limited number of microlayers to range between 0 and 20 mm h^{-1}, and between 0 and 7 mm h^{-1} for sedimentary and depositional crusts. In the present study, the reason for the lack of significant differences in terms of runoff between tillage treatments might be due to similar infiltration characteristics of the two crust types at the study site and/or the presence, at both treatments, of preferential infiltrations linked to faunal activity.

Moreover, our results showed that despite having no overall difference between tilled and no-tilled plots, higher runoff under no-till (compared to tilled plots) was observed at the beginning of the rainy season and the vice versa towards the end of the season. Such a trend has not been yet reported in other studies. This result needs to be further investigated and the significance of the observed trend further tested. Among the possible explanations of a greater infiltration under tilled plots after sowing is the presence of greater soil porosity while the further decrease of infiltration on the same plot is likely to come from a collapse of the man made soil structure. Proposed investigations may answer questions such as ‘Is the observed trend seasonal or consistent over the year; will it remain long-term; how long does it take for the porosity resulting from tillage to clog up; and, what are the controlling factors of this porosity?

10.6.2. Soil organic carbon erosion and microbial biomass carbon

No-till technique has long been recognised to be an efficient way to reduce soil erosion (Wend *et al*., 1985; Choudhary *et al*., 1997; Zheng *et al*., 2004). Choudhary *et al.* (1997) showed that soil erosion was markedly affected by tillage practices. They observed that no-till reduced soil erosion by a factor of 1.60 to 1.85. In their review, Zheng *et al*. (2004) showed a reduction in soil erosion rates of between 30 and 99%. Two third of the studies in their review reported a reduction of over 60%. For instance, Lindstrom *et al.* (1998) reported that the adoption of no-till decreased soil erosion from 6.7-18.2 t $ha^{-1}y^{-1}$ to 0.2 t $ha^{-1}y^{-1}$. In small 0.6 ha-catchments in Laos, Valentin *et al*. (2008) showed that sediment yield decreased from 5.7 t $ha^{-1}y^{-1}$ to 0.7 t $ha^{-1}y^{-1}$. In the present study, no-till reduced soil losses from 3.0 to 0.96 t $ha^{-1}y^{-1}$. This represents a decrease of 68% which falls in the upper range of rates reviewed above.

While the review of literature indicates that the overall reduction of soil erosion under no-till is commonly attributed to the presence of crop residues on the soil surface that limit the impact of raindrops and favour infiltration (Bradford and Huang, 1994; Choudhary *et al.,* 1997; Rao *et al.,* 1998), our study suggest a different “scenario”. Indeed, the fact that runoff did not differ between treatments and that surface mulch was absent on both treatments tend to show that differences cannot be attributed to differences in soil infiltration by water. The assessment of soil surface characteristics revealed that the greater resistance of soils under no-till might come from the development of biological crusts (Malam Issa *et al.,* 1999; Malam Issa *et al.,* 2001). A study done by Chaplot *et al.* (2007) in the sloping lands of Laos and under clayey soil conditions, showed that water erosion decreased with increasing proportion of structural crusts (from 24.33 to 6.21 t $ha^{-1}y^{-1}$ for soil and from 1.46 to 0.31 t $ha^{-1}y^{-1}$for SOC). This occurred not only due to the higher hardness of these, but also because of the greater occurrence of algae and microbial activity on surface soils. The presence of these microorganisms promotes physical protection through binding and holding together soil aggregates by the filaments and secondary metabolites (Malam Issa *et al.,* 2001).

However, no significant surface colonization by algae was found in our study, but a greater occurrence of structural crust characterized the no-till treatment. Algae have not been observed on those crusts but a greater microbial biomass carbon was observed under no-till plots (Mchunu *et al.*, 2010) compared to conventionally tilled plots. These results were similar to those observed by Feng *et al.* (2003), who concluded that a higher microbial biomass on-site may induce a greater release of metabolites that hold aggregates together, improving the physical structure of the soil (Feng *et al.,* 2003; De-Polli, 2009) and its resistance to erosion. Moreover, the higher microbial biomass carbon on no-till plots (despite the absence of crop residue on the surface of soils) did not only reduce SOC erosion, but also reduced greenhouse gas emissions, CO_2 in the case of this study.

Our results showed that most of the SOC transported with sediments was in a particulate form (about 90% against 10% for dissolved organic carbon). The dissolved fraction, which is easily mineralizable (Gregorich *et al.,* 2003; Cookson *et al.,* 2005), was much lower than the

29-70% range observed by Jacinthe *et al.* (2002) and no significant differences existed between till and no-till treatments. Overall, both till and no-till soils proved to be very sensitive to preferential SOC erosion. The SOC enrichment ratio (ER, the ratio of the concentration of SOC in the eroded materials to that in the contributing soils) was on average 4.5 (4.3 for conventional tillage and 4.8 for no-till, but these differences were not significant). A number of investigators have reported ER values of greater than one, where the eroded material is enriched when compared to the bulk soil (Stoltenberg and White, 1953; Sharpley, 1980; Avnimelech *et al.,* 1984; Zobeck and Fryrear, 1986; Sutherland *et al.,* 1998; Songwei *et al.,* 2007; Chaplot *et al.,* 2007; Schiettecatte *et al*., 2008). Enrichment of sediments in SOC is possible since poorly decomposed soil organic materials that are light and non-cohesive are the most physically mobile fractions of soils (Ghadiri and Rose, 1991). In the present study, the average ER was as high as 4.5 which corresponded to the highest levels reviewed by Avnimelech and McHenry, (1984) for soils poor in SOC. This shows that these soils are very sensitive to preferential SOC erosion. The enrichment ratio was slightly lower for tilled plots when compared to no-till, probably because ER tends to decrease as the intensity of soil erosion increases since SOC is mainly concentrated close to the soil surface (Ritchie and McHenry, 1977).

10.7. Differences in carbon dioxide emissions between the plots

Carbon dioxide emitted from soils and sediments collected from no-till and tilled plots was evaluated and results showed that tillage increased CO_2 emissions from both soils and sediments. Obtained results are discussed below.

10.7.1. Carbon dioxide emissions from soils and sediments

Soil CO_2 emissions increased steadily with time. However, there were no differences in CO_2 emissions between till and no-till treatments for the first 18 days of the incubation experiment. The absence of the effect of tillage on CO_2 emissions might be due to soil sampling time, since sensitivity and response of mineralizable C to treatment may depend on time of sampling (Soon *et al*., 2007). For this study, tillage was done in January 2009 and samples were collected two months later. Thus, the immediate flush of CO_2 from tilled soils due to aggregate breakage (Franzluebbers *et al*., 2005; Reicosky and Archer, 2007 and Franchini *et al*., 2007) was not observed. But this needs to be confirmed. However, after 145 days of the incubation experiment, CO_2 emissions from no-till soils were 18.33% less than emissions from tilled soils (0.031 g C-CO_2 g C^{-1} from no-till and 0.041 g C-CO_2 g C^{-1} from tilled soils) and this corresponded to a significant difference. These results are comparable to those obtained in several similar studies, such as those observed by Franchini (2005), Chatskikh and Olesen (2007) and Ussiri and Lal (2009). Greater CO_2 emissions for the tillage treatment might be due to the slight increase in diversity of soil micro-fauna in tilled soils, due to increased aeration, incorporation of root biomass and availability of organic matter for microbial turn over (Buyanovsky and Wagner, 1983; Doran *et al*., 1989; Fang and Moncrieff, 2001 and Vinher and Dahlmann-Hansen, 2005).

Reduced soil disturbances in no-till plots aided the protection of organic matter from microbial decomposition, thus yielding lower CO_2 emissions when compared to soils from tilled plots (Müller *et al*., 2009). The results obtained from SOC stocks, content analysis and CO_2 emissions then indicate that a greater proportion of C in tilled soils is emitted to the atmosphere as CO_2 whereas only a smaller proportion of C in no-till is converted to atmospheric C, but most of it is protected in the soil. Thus, the lower CO_2 emissions from no-till soils containing greater C content and stocks may indicate that the stored C is likely to remain in the soil rather than be emitted to the atmosphere.

The effect of tillage and erosion on cultivated soils can be detrimental. Tillage breaks up the soil surface and renders it susceptible to subsequent erosion (Reicosky *et al*., 2005). The eroded topsoil, richest in labile C due to fresh plant residue and root biomass, may then be redistributed within the landscape or deposited in aquatic environments such as rivers and dams (Gregorich *et al*., 1998; Jacinthe *et al*., 2004). In this study, the highest cumulative CO_2 emissions were observed from sediments as opposed to the soil samples from tilled plots (Figure 4.8). This result is similar to that obtained by Mora *et al.,* in 2007, where eroded sediments emitted higher levels of CO_2 when compared to surface soils (1419 vs. 386 mg C-CO_2 kg^{-1}). The reason for this observation in this study may be the fact that with tillage, soils were susceptible to subsequent erosion processes. These erosion processes break up the coarser aggregates, usually enriched in labile SOC, and enrich the eroded sediments with readily mineralizable C. In addition, adapted biodegrades may also be relocated to deposition sites with sediments (Vanveen and Kuikman, 1990; Jacinthe *et al*., 2002; Rodríguez Rodríguez *et al*., 2002). The lowest accumulative emissions were from no-till sediments. This result was most likely due to the biochemical nature and physicochemical stability of SOC eroded from tilled plots – recalcitrant C forms are less susceptible to mineralization (Izaurralde *et al.,* 2001).

10.7.2. Carbon dioxide emissions from settled and suspended sediments

Tillage did not have a significant impact on accumulative CO_2 from settled sediments. However, suspended sediments eroded from tilled soils emitted significantly higher accumulative CO_2 emissions compared to those eroded from no-till soils. Studies on rainfall and soil erosion on this site have shown that the rainfall intensity for the 2008/2009 rainy season were generally of low-intensity (class 1) storm (Chaplot *et al*., 2010). The energy levels for such storms usually favour the deposition of coarser and denser sediments near detachment points (Jacinthe, 2004). Thus the similar amount of CO_2 mineralized from these sediments (though they were from different tillage treatments) suggests that SOC in these sediments may have been physically protected from microbial turnover by the nature of eroded sediments, coarse and unbroken.

The lower CO_2 emissions observed from suspended sediments eroded from no-till soils may be due to the recalcitrant nature of the eroded SOC. This may suggest a lower microbial activity and lower CO_2 emissions due to the lower content of labile organic matter. The lower CO_2 emissions might also be observed because suspended sediments contain mainly of already decomposed organic matter, which decomposes cannot further breakdown and release CO_2. Though studies on SOC eroded from these sites show a higher quantity of SOC eroded from no-till plots, the nature of this SOC favours the sequestration of C, allowing erosion to act as a sink of atmospheric CO_2 (Van Oost *et al.,* 2007). The higher CO_2 emissions observed from suspended sediments eroded from tilled plots may be due to the loose aggregates being broken up by raindrops, releasing less dense aggregates with accessible labile SOC that is readily available for degradation (Polyakov and Lal, 2008).

11. CONCLUSIONS AND RECOMMENDATIONS

The following section is divided into two parts. In a first part we summarize the key findings on the landscape functioning in respect of water, sediment, nutrient and soil organic carbon fluxes. Based on the results published in international publications (e.g. 9 published papers in international journals; 2 in press and 5 submitted, see Appendix B), a 3D diagram of the area showing the different water compartments, their contributions to water, sediment, nutrient and SOC fluxes at the different scales (1 m²; 10 m²; 23 ha, 100 ha, 1000 ha) is proposed. The second part consists of key recommendations. Land degradation, either by sheet of linear erosion, being a key mechanism of control of the different fluxes in the landscape, mitigating land degradation and the associated loss of soil surface coverage by vegetation is seen as an operative way to reduce the water, nutrient and SOC losses. Key recommendations are also given in respect of the management of agricultural soils, on how the practice of zero tillage might constitute an effective mean to mitigate water scarcity, water pollution, dam siltation and climate change. Finally, owing to the large number of post-graduate students involved in this project (13 graduated from this project, 100% completion rate), the numerous interactions promoted between farmers, secondary schools, academics and support staffs, some recommendations are made for an improved capacity building and dissemination of results.

11.1. Key findings on the landscape functioning in respect of water, sediment, nutrient and soil organic carbon fluxes.

The main results on runoff, organic carbon and nutrient fluxes at different scales are summarized in Figure 40, a schematic representation of the fluxes interpreted from field observations and tracers interpretations. The study landscape appears to be constituted of three distinct compartments, each with a specific behaviour:

1. Hillslope;
2. First order stream;
3. Dam-impacted stream.

The hillslope experienced high water, SOC and nutrient fluxes, with most of the water being groundwater sourced. Sediments and SOC fluxes were the highest at the plot scale. Fluxes increased from the microplot to the plot level increased as interrill erosion mechanisms become more efficient and sharply decreased to the first order stream as OF infiltration and sedimentation at footslopes occurred. Most of the water and nutrients exported from the hillslope have a shallow water table origin.

The first order stream experienced a steady decrease in runoff and a sharp decrease for sediments and particulate nutrient fluxes. However, there was an increase in the fluxes of both DOC and PON that could be explained by an increased decomposition of the deposited organic matter. Such a process ultimately leads to the release and increase of N and DOC to the stream as well as increased emissions of CO_2 to the atmosphere. Temporally, water, sediment and nutrient fluxes at both the 23 hectare micro-catchment and 100 hectare catchment outlets increased as the soils of the catchment increased in saturation by water. There appeared to be an interaction, between both scales, with deep groundwater with some soil water and overland flow contributions at both scales to catchment runoff, especially during events.

The Dam-impacted stream experienced a sharp decrease of runoff, nutrients and sediment fluxes in the dam-impacted stream and the resulting exports from the 1000 hectare catchment outlet were found to be considerably low for sediments, particulate nutrients and nitrate. This was accompanied by a slight decrease in dissolved organic carbon which probably reflects biochemical reactions within the dams, which need to be further investigated. The decrease in water fluxes in this compartment lies on dam extraction through direct evaporation and irrigation as evidenced by the isotopic signature of the water. In comparison, the catchment water outflows have a groundwater signature.

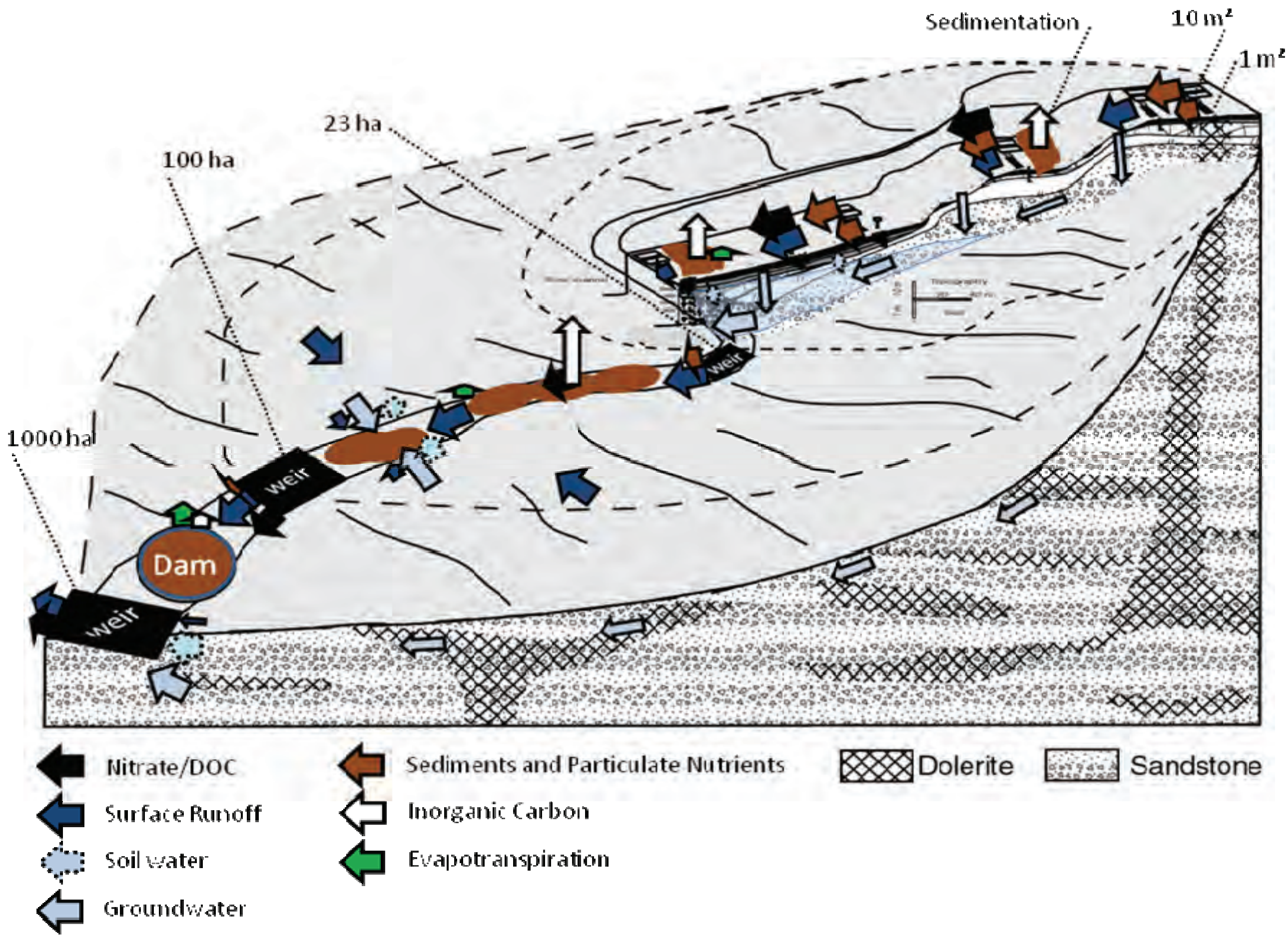

Figure 40. Schematic representation of water, sediment, organic/inorganic carbon and nutrient fluxes at the catchment level and interpreted from fluxes and tracers evaluation

11.2. Main recommendations

The following graphics have been produced to illustrate the key messages of this research to the farmers.

Recommendations to mitigate land degradation by "*Sheet erosion*"

(WRC project K5-1904)

Problem statement:

Sheet erosion induces :

> **Loss of nutrient-rich soil material and soil organic carbon;**
> **Indirect consequences on main soil functions** (food production, water holding capacity, …), air (increased CO_2 emissions) and **water** quality (pollution and siltation).

Figure. Example of sheet erosion in the Drakensberg foothills. Note the link between abandoned contour banks and land degradation.

Main results:

> **Less vegetation cover induces more soil nutrient losses** (up to 2.6 times more soil C and N: *Mchunu and Chaplot, 2012*);
> **Soil water content, crusting, clay content and crop and livestock management** are **other key factors** controlling sheet erosion (*Dlamini et al; 2010; Orchard et al., 2012*);
> **Rain-impacted flow is the main mechanism** driving sheet erosion (*Oakes et al; ESPL, 2012*).

Recommendations to mitigate sheet erosion

> **Increase soil surface cover:**
- **Mulching;**
- Intercropping and intracropping;
- **Avoid undergrazing and formation of cattle and human pathways by promoting pasture rotation**; increased cow density for short periods of time.

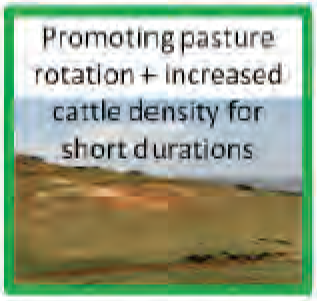

DlaminiP., C. Orchard, G. Jewitt, S. Lorentz, L. Titshall, V. Chaplot 2011. Quantifying interrill erosion in a sloping-land-agricultural catchment of KwaZulu Natal, South Africa. **Agriculture Water Management** 98, 1711-1718.
Oakes E.G.M., Hughes, J.C., Jewitt, G.P.W., Lorentz, S.A., Chaplot, V.A.M. 2012. Controls on a scale explicit analysis of sheet erosion. . Earth Surface Processes and Landforms. In press.
Orchard C., Lorentz, S., Jewitt, G., V. Chaplot 2012. Spatial and temporal variations of overland flow at the microcatchment level. **Hydrological Processes.** In press.
Mchunu, C., Chaplot V. 2012. Soil organic carbon erosion and soil CO2 emissions from degraded pastures. **Geoderma.** 179, 72-79.

Recommendations to mitigate land degradation by "*Linear erosion*"

(WRC project K5-1904)

Problem statement:

Linear erosion induces:

> **Loss of land** and associated main soil functions (food production, water holding capacity, …);
> **Major contributor of stream sediments, dam siltation;**
> **Land inaccessibility**.

Figure. Example of linear erosion on in the Drakensberg foothills. Note the link between paths and gullies.

Main results:

> **Piping** rather than overland flow is the **main process of gully formation** (*Chaplot and Beckedahl, submitted*);
> **Paths** created due to land mismanagement **are key in the initiation of pipes** and gullying (*Figure; Chaplot and Beckedahl, submitted; Chaplot et al. 2011*).
> **Gully extension is due to bank collapse** rather than by high velocity overland flow or overgrazing (*Chaplot et al., 2011*)

Recommendations to mitigate gullying

> **Set up land management practices that do not allow paths to form;**
> **Improve soil structure** through a control of soil pH and clay saturation in certain cations; find preferential soil water paths;
> **Reshape gully banks to the angle of repose** and revegetate banks rather than use gabions.

Chaplot Vincent; Jacqueline Brown; Phesheya Dlamini; Tarryn Eustice; Jean-Louis Janeau; Graham Jewitt; Simon Lorentz; Lauren Martin; Chermaine Nontokozo-Mchunu; Ernest Oakes; …. 2011. Rainfall simulation to identify gully bank retreat. Agriculture Water Management. 98, 1704-1710.
Chaplot V., Jewitt, G. Lorentz, S, 2011. Predicting plot-scale water infiltration using the correlation between soil apparent electrical resistivity and various soil properties. 2011. Physics and Chemistry of the Earth. 36, 1033-1042.
Chaplot and Beckedahl. Impact of terrain attributes, parent material and soil types on gully banks retreat. Submitted to Geomorphology.

Tillage or No Tillage?

Recommendations from WRC project K5-1904

Problem statement:

Tillage induces:

> **Loss of topsoil through increased water erosion** with associated decline of soil functions and decreased agricultural sustainability;

> **Water quality** problems, loss of **biodiversity,** decreased **carbon sequestration and climate change mitigation.**

Figure. *Example of subsidence tillage practice in the Drakensberg foothills.*

Main results:

No-tillage:

> **Decreases soil, soil carbon and nitrogen** by up to 3.8 times;

> **Decreases CO_2 emissions** from soils up to 20% and from sediments by 45%;

> **Increases overall soil infiltration;**

> **Yields equal to higher crop production;** *(Chaplot et al. submitted)*

> **Does not change soil carbon stocks.** *(Mchunu and Chaplot, 2012)*

Recommendations

> **No-tillage** with low residue density practiced in small-scale farming, **yields high economic and environmental benefits.** Thus recommendations are as follows:

- **Promote no-tillage;**
- Allow **cows to utilise crop residues;**
- **Promote intercropping and winter cover crops to promote soil C sequestration** and soil protection while increasing 'cattle-feed';
- **Communicate on** the environmental benefits together with **low equipment cost, labor inputs and technicity.**
- **Lobby for carbon credits** not due to increased soil C stocks but decreased C erosion and CO_2 emissions.

Mchunu, C., Manson, A., Jewitt, G. Lorentz, S., Chaplot, V. No-Till impact on soil and Soil organic carbon erosion under crop residues scarcity in South Africa. Soil Science Society America Journal. 75 (4) 1503-1512.

Mchunu, C., Chaplot V., Manson, A., Jewitt, G. Lorentz, S. 2011. Water erosion-induced CO2 emissions from tilled and no-tilled maize plots in Africa. Agriculture Environment and Ecosystems. Under correction.

Recommendations for improved capacity building (WRC project K5-1904)

Problem statement:

> **Low dissemination and adoption rate of successful land management practices by farmers;**

> **Postgrade students often do not complete their degree;** more often **taking much longer** to complete their degree **than international counterparts;**

> **Low publication rate** in international journals.

Figure. *Example of community-based capacity building. Case of land use change and its impact on soil erosion.*

Main results:

> **No-tillage is being adopted by the small-scale farmers** in the Potshini area;

> **Farmers and children recognize the link between their agricultural practices and the quality of their environment;**

> **Completion rate is 100%** for the 13 post-graduate students

> **16 articles** in international publications **come from the main scientific results obtained by the students** (9 published; 2 in press; 5 submitted)

> 18 communications at workshops (10 with publications); 4 posters; 2 workshops for scientists; 4 restitution meetings in the field; 15 meetings with the community leaders; 2 in-field days for local schools; 2 schools for UKZN and SADEC MSc/PhD students (co-funding IRD, WATERNET, UKZN);

Recommendations for improved capacity building

> **Constant communication with the community** (during meetings at schools) from project onset to result restitution: **participation of a *"farmer support Group"*;**

> **Build a team constituted by all partners with common and achievable objectives;**

> **Foster researchers-students interactions** (both in the field and in the laboratory) **as a way to master the different steps of the *Research Process*** (from identification of a research question to scientific writing).

12. FUTURE OUTLOOK

This project allowed for an improved understanding of the processes of land degradation (either by sheet and linear erosion), their impact on vegetation coverage, land management and their consequences on the fluxes of water, nutrient and organic carbon from the microplot to the landscape level. This constitutes one of the most important evaluation prerequisites for successful improvement of the ecosystem functioning. As suggested by the results on gully formation and evolution, adequate mitigation of linear erosion can only be achieved by means lessening soil piping and bank collapse. No-tillage not only decreases soil erosion, but when the mulch is exported (as forage for small-scale farms or as a potential source of energy/biofuel in large scale farming), can also reduce soil CO_2 emissions and thus mitigate climate change. Land degradation has heretofore been attributed in the region to overgrazing, which our results tend to contradict. A simple shift in the way cows are managed, where pasture rotation could replace free grazing, could help to rehabilitate the land and increase cow density in the future. These recommendations constitute a range of research and outreach perspectives that need to be carefully tested. 4 PhD students and 2 MSc started their research studies on ways to improve the functioning of landscapes through adapted land management practices (e.g. case of grassland rehabilitation impact, see below) and their impacts, larger scale, on water, nutrient and carbon fluxes.

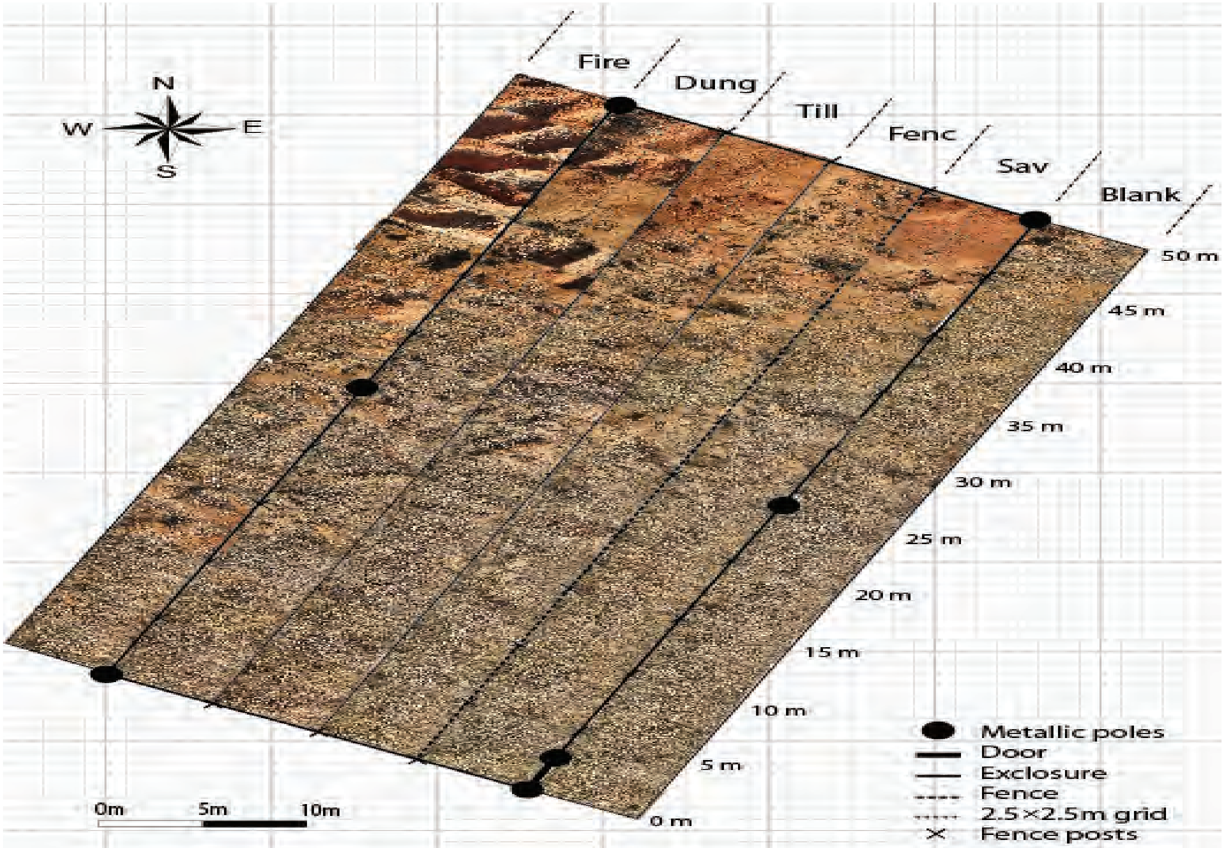

Figure 41. Grassland rehabilitation trial with different treatments from Blank, Sav (high cow density for short periods of time names "Sav" from Alan Savory); Fenc: cow exclosure; Till: cow exclosure + soil tillage; …..). Land rehabilitation and soil stocks of nutrients study by Phesheya Dlamini in the framework of his PhD.

REFERENCES

Aitkenhead, J.A., Hope, D., and Billett, M.F. 1999. The relationship between dissolved organic carbon in stream water and soil organic carbon pools at different spatial scales. *Hydrological Processes* 13, 1289-1302.

Auzet, A.V., Poesen, J., and Valentin, C. 2004. Soil surface characteristics: dynamics and impacts on soil erosion. Editorial. *Earth Surface Processes and Landforms* 29, 1063-1064.

Bartley, R., Roth, C.H., Ludwig, J., McJannet, D., Liedloff, A., Corfield, J. Hawdon, A., and Abbot, B. 2006. Runoff and erosion from Australia's tropical semi-arid rangelands: influence of ground cover for differing space and time scales. *Hydrological Processes* 20, 3317-3333.

Bautista, S., Mayor, A.G., Bourakhouadar, J., and Bellot, J. 2007. Plant Spatial Pattern Predicts Hillslope Runoff and Erosion in a Semiarid Mediterranean Landscape. *Ecosystems* 10, 987-998.

Ben-Hur, M., Shainberg, I., Keren, R., and Gal, M. 1985. Effect of water quality and drying on soil crust properties. *Soil Science Society of America Journal* 49, 191-196.

Bergkamp, G. 1998. A hierarchical view of the interactions of runoff and infiltration with vegetation and microtopography in semiarid shrublands. *CATENA* 33(3-4), 201-220.

Bertol, I., Engel, F.L., Mafra, A.L., Bertol, O.J., and Ritter, S.R. 2007. Phosphorus, potassium and organic carbon concentrations in runoff water and sediments under different soil tillage systems during soybean growth. *Soil and Tillage Research* 94, 142-150.

Beven, K., Heathwaite, L., Heathwaite, L., Haygarth, P., Wailing, D., Braizer, R., Withers, P., 2005. On the concept of delivery of sediment and nutrients to stream channels. *Hydrological Processes* 19, 551-556.

Bloschl, G. and Sivapalan, M., 1995. Scale issues in hydrological modeling: A review. *Hydrological Processes*, 9: 251-290.

Bracken, L.J., and Croke, J. 2007.The concept of hydrological connectivity and its contribution to understanding runoff-dominated geomorphic systems. *Hydrological Processes*, 21: 1749-1763.

Brown, V.A., McDonnell, J.J., Burns, D.A., and Kendall, C. 1999. The role of event water, a rapid shallow flow component, and catchment size in summer stormflow. *Journal of Hydrology*, 217: 171-190.

Cammeraat, E.L.H. 2004. Scale dependent thresholds in hydrological and erosion response of a semi-arid catchment in southeast Spain. *Agriculture, Ecosystems & Environment*, 104: 317-332.

Casenave, A. and Valentin, C. 1992. A runoff capability classification system based on surface features criteria in semi-arid areas of West Africa. *Journal of Hydrology*, 130(1992): 231-249.

Cerdan, O, Le Bissonnais, Y, Govers, G, Lecomte, V, van Oost, K, Couturier, A, King, A and Dubreuil N. 2004. Scale effect on runoff from experimental plots to catchments in agricultural areas in Normandy*. Journal of Hydrology* 299: 4-14.

Chaplot, V., and Walter, C. 2003. Subsurface topography to enhance the prediction of the spatial distribution of soil wetness. *Hydrological Processes* 17: 2567-2580.

Chaplot, V., Khampaseuth, X., Valentin, C., and Le Bisonnais, Y. 2007. Sheet erosion in the sloping lands of northern Laos submitted to shifting cultivation. *Earth Surface Processes and Landforms* 32: 415-428.

Chaplot, V., Brown, J., Dlamini, P., Eustice, T., Janeau, J-L., Jewitt, G., Lorentz S., Martin, L., Mchunu C., Oakes, E., Podwojewski, P., Revil, S., Rumpel C., and Zondi, N. 2010. Rainfall simulation to identify the storm-scale mechanisms of gully bank retreat. *Agriculture Water Management* 98: 1704-1710.

Chaplot, V., and Poesen, J. 2012. Sediment, soil organic carbon and runoff delivery at various spatial scales. *Catena* 88 (2012): 46-56.

Cirmo, C.P. and McDonnell, J.J. 1997. Linking the hydrologic and biogeochemical controls of nitrogen transport in near-stream zones of temperate-forested catchments: a review. *Journal of Hydrology* 199, 88-120.

Descheemaeker, K., Nyssen, J., Poesen, J., Raes, D., Haile, M., Muys, B., and Deckers, S. 2006. Runoff on slopes with restoring vegetation: A case study from the Tigray highlands, Ethiopia. *Journal of Hydrology* 331, 219-241.

Detty, J.M., and McGuire, K.J., 2010. Topographic controls on shallow groundwater dynamics: implications of hydrologic connectivity between hillslopes and riparian zones in a till mantled catchment. *Hydrological Processes* 24: 2222-2236.

Devaurs, M., and Gifford, G.F. 1984. Variability of Infiltration within Large Runoff Plots on Rangelands. *Journal of Range Management* 37:6, 523-528.

De Vente, J., Poesen, J., Arabkhedri, M., Verstraeten, G., 2007. The sediment delivery problem revisited. *Progress in Physical Geography*, 31: 155-178.

Dexter, A.R., 1988. Advances in characterization of soil structure. *Soil Tillage Research* 11, 199-238.

Dexter, A.R., and Richard, G. 2009. The saturated hydraulic conductivity of soils with n-modal pore size distributions. *Geoderma* 154, 76-85.

Dlamini, P.E. 2010. An assessment of soil organic carbon and nutrient stocks in the Potshini catchment, KwaZulu-Natal, South Africa. Unpublished MSc Dissertation, School of Bioresources Engineering and Environmental Hydrology, University of KwaZulu-Natal, Pietermaritzburg, RSA.

Dlamini, P., Orchard, C., Jewitt, G., Lorentz, S., Titshall, L., and Chaplot, V. 2011. Controlling factors of sheet erosion under degraded grasslands in the sloping lands of KwaZulu-Natal, South Africa. *Agricultural Water Management* 98(11), 1711-1718.

ESRI, 2004. Understanding GIS. The ArcView GIS 3.2’. ESRI, 380 New York Street, Redlands, CA, USA, p. 92273.

Fujimoto, M., Ohte, N., and Tani, M. 2011. Effects of hillslope topography on runoff response in a small catchment in the Fudoji Experimental Watershed, central Japan. *Hydrological Processes* (2011), 1-13.

Grimaldi, C., and Chaplot, V. 2000. Nitrate depletion during within-stream transport: Effects of exchange processes between the streamwater, the hyporheic and riparian zones. *Water, Air, and Soil Pollution* 124: 95-112.

Heathwaite, A.L. and Johnes, P.J., 1996. Contribution of Nitrogen Species and Phosphorus Fractions to Stream Water Quality in Agricultural Catchments. *Hydrological Processes*, 10: 971-983.

Hernandez, T. *et al.,* 2003. Modelling runoff from variable source areas in humid, shallow water table environments. *Journal of American Water Resources Association* 39: 75-85.

Hewlett J.D., Hibbert A.R. 1967. Factors affecting the response of small catchment to precipitation in humid areas. In *Forest Hydrology*, Supper WE (ed). Pergamon: New York; 275-290.

Hopp, L., and McDonnell, J.J. 2009. Connectivity at the hillslope scale: Identifying interactions between storm size, bedrock permeability, slope angle and soil depth. *Journal of Hydrology* 376 (2009). 378-391.

Horton RE. 1933. The role of infiltration in the hydrologic cycle. *Transactions of American Geophysical Union* 14: 446-460.

Hunt, R.J., Coplen T.B., Haas, N.L., Saad, D.A., and Borchardt, M.A. 2005. Investigating surface water-well interaction using stable isotope ratios of water. *Journal of Hydrology* 302, 154-172

Huth, A.K., Leydecker, A., Sickman, J.O., and Bales, R.C. 2004. A two-component hydrograph separation for three high-elevation catchments in the Sierra Nevada, California. *Hydrological Processes* 18, 1721-1733.

ISSS Working Group RB, 1998. World Reference Base for Soil Resources. In: Deckers, J.A. Nachtergaele, F.O., Spargaren, O.C. (Eds.) Introduction 1st edition. ISSS.ISRC. FAO. Acco Leuven, Belgium.

Iwagami, S., Tsujimura, M., Onda, Y., Shimada, J., and Tanaka, T. 2010. Role of bedrock groundwater in the rainfall-runoff process in a small headwater catchment underlain by volcanic rock. *Hydrological Processes*, 24 (2010). 2771-2783.

James, A.L., and Roulet, N.T. 2009. Antecedent moisture conditions and catchment morphology as controls on spatial patterns of runoff generation in small forest catchments. *Journal of Hydrology*, 377(2009). 351-366.

Jencso, K.G., McGlynn, B.L., Gooseff, M.N., Wondzell, S.M., Bencala, K.E., and Marshall, L.A. 2009. Hydrologic connectivity between landscapes and streams: Transferring reach- and plot-scale understanding to the catchment scale. *Water Resources Research*, 45. pp 16.

Jordán, A., Martínez-Zavala, L. and Bellinfante, N., 2008. Heterogeneity in soil hydrological response from different land cover types in southern Spain. *CATENA*, 74: 137-143.

Joel, A., Messing, I., Seguel, O., and Casanova, M. 2002. Measurement of surface water runoff from plots of two different sizes. *Hydrological Processes* 16, 1467-1478.

Juarez, S. 2010. Carbon mineralization and lignin content of eroded sediments within a small-scale agricultural watershed of South-Africa. Unpublished MSc Dissertation, Department of Agronomy, AgroParisTech, Cedex, France.

Juarez, S., Rumpel, C., Mchunu, C., and Chaplot, V. 2011. Carbon mineralization and lignin content of eroded sediments from a grazed watershed of South-Africa. *Geoderma* 167-168, 247-253.

Koelle, W., Strebel, O. and Boettcher, J.1985. Formation of sulfate by microbial denitrification in a reducing aquifer. *Water Supply* 3, 35.

King, G.M., 2002. An explanation of the 1:500 000 general hydrogeological map, Dept. of Water Affairs and Forestry, Pretoria, Republic of South Africa.

Latron, J., and Gallart, F. 2008. Runoff generation processes in a small Mediterranean research catchment (Vallcebre, Eastern Pyrenees). *Journal of Hydrology*, 358 (2008). 206-220.

Li, X.J., Li, X.R., Song, W.M., Gao, Y.P., Zheng, J.G., and Jia, R.L. 2008. Effects of crust and shrub patches on runoff, sedimentation, and related nutrient (C, N) redistribution in the desertified steppe zone of the Tengger Desert, Northern China. *Geomorphology*, 96 (2008). 221-232.

Lorentz, S.A. 2012. Personal Communication, School of Bioresources Engineering and Environmental Hydrology, Pietermaritzburg, South Africa, 27 February 2012.

Los Gatos Research. 2007. DLT-100 Liquid-Water Isotope Analyzer Automated Injection: Manual Rev 07-C.

McBratney, A.B., Webster, R., 1983. How many observations are needed for regional estimation of soil properties? *Soil Science* 135, 177-183.

McGlynn. B.L., McDonnell, J.J., and Brammer, D.D. 2002. A review of the evolving perceptual model of hillslope flowpaths at the Maimai catchments, New Zealand. *Journal of Hydrology,* 257 (2002). 1-26.

McGlynn, B.L., McDonnell, J.J., Seibert, J., and Kendall, C. 2003. Scale effects on headwater catchment runoff timing, flow sources and groundwater-streamflow relations. *Water Resources Research, 40.* 40 pp.

McGlynn, B.L., and McDonnell, J.J. 2003a. Role of discrete landscape units in controlling catchment dissolved organic carbon dynamics. *Water Resources Research,* 39(4). 18 pp.

McGlynn, B.L., and McDonnell, J.J. 2003b. Quantifying the relative contributions of riparian and hillslope zones to catchment runoff. *Water Resources Research* 39(11), 20 pp.

McGuire, K.J., and McDonnell, J.J. 2010. Hydrological connectivity of hillslopes and streams: Characteristic time scales and nonlinearities. *Water Resources Research* 46, 17 pp.

Mchunu, C., Lorentz, S., Jewitt, G., Manson, A., and Chaplot, V. 2011. No-Till Impact on Soil and Soil Organic Carbon Erosion under Crop Residue Scarcity in Africa. *Soil Science Society of America Journal* 75(4), 1502-1511.

McNamara, J.P., Chandler, D., Seyfried, M., and Achet, S. 2005. Soil moisture states, lateral flow, and streamflow generation in a semi-arid, snowmelt-driven catchment. *Hydrological Processes,* 19 (2005). 4023-4038.

Mekki, I., Albergel, J., Ben Mechlia, N., and Voltz, M. 2006. Assessment of overland flow variation and blue water production in a farmed semi-arid water harvesting catchment. *Physics and Chemistry of the Earth* 31 (2006) 1048-1061

Meyles, E., Williams, A., Ternan, L., and Dowd, J. 2003. Runoff generation in relation to soil moisture patterns in a small Dartmoor catchment, Southwest England. *Hydrological Processes* 17: 251-264.

Meyles, E.W., Williams, A.G., Ternan, J.L., Anderson, J.M., and Dowd, J.F. 2006. The influence of grazing on vegetation, soil properties and stream discharge in a small Dartmoor catchment, Southwest England, UK. *Earth Surface Processes and Landforms* 31: 622-631.

Miyata, S., Kosugi, K., Nishi, Y., Gomi, T., Sidle, R.C., and Mizuyama, T. 2010. Spatial pattern of infiltration rate and its effect on hydrological processes in a small headwater catchment. *Hydrological Processes* 24, 535-549

Murphy, S.R., Lodge, G.M., Harden, S. 2004. Surface soil water dynamics in pastures in northern New South Wales. 2. Surface runoff. *Australian Journal of Experimental Agriculture* 44, 283-298

Ng Kee Kwong, K.F., Bholah, A., Volcy. L., and Pynee, K. 2002. Nitrogen and phosphorus transport by surface runoff from a silty clay loam soil under sugarcane in the humid tropical environment of Mauritius. *Agriculture, Ecosystems and Environment* 91, 147-157.

Oakes, E.G.M. 2012. Erosion Dynamics at the Catchment Level: Spatial and Temporal Variations of Sediment Mobilization, Storage and Delivery. Unpublished MSc Dissertation, School of Bioresources Engineering and Environmental Hydrology, University of KwaZulu-Natal, Pietermaritzburg, RSA.

Ocampo, C.J., Sivapalan, M. and Oldham, C., 2006. Hydrological connectivity of upland-riparian zones in agricultural catchments: Implications for runoff generation and nitrate transport. *Journal of Hydrology*, 331: 643-658.

Parsons, A.J.,Wainwright, J., Brazier, R.E., Powell,D.M., 2006. Is sediment delivery a fallacy? *Earth Surface Processes and Landforms*, 31: 1325-1328.

Podwojewski, P., Janeau, J-L., Grellier, S., Valentin, C., Lorentz, S., and Chaplot, V. 2011. Influence of grass soil cover on water runoff and soil detachment under rainfall simulation in a sub-humid South African degraded rangeland. *Earth Surface Processes and Landforms*, 36: 911-922.

Postma, D., Boesen, C., Kristiansen, H. and Larsen, F. 1991. Nitrate reduction in an unconfined sandy aquifer: water chemistry, reduction processes, and geochemical modeling. *Water Resources Research,* 27(8), 2027.

Quinton, J.N., Catt, J.A., Wood, G.A., Steer, J. 2006. Soil carbon losses by water erosion: Experimentation and modeling at field and national scales in the UK. *Agriculture, Ecosystems and Environment*, 112: 87-102.

Ribolzi, O., Andrieux, P., Valles, V., Bouzigues, R., Bariac, T., and Voltz, M. 2000. Contribution of groundwater and overland flows to storm flow generation in a cultivated Mediterranean catchment. Quantification by natural chemical tracing. *Journal of Hydrology* 233, 241-257.

Rommens, T., Verstraeten, G., Poesen, J., Govers, G., Van Rompaey, A., Peeters, I., 2005.Soil erosion and sediment deposition in the Belgian loess belt during the Holocene: establishing a sediment budget for a small agricultural catchment. *The Holocene*, 15: 1032-1043.

Sanjari, G., Yu, B., Ghadiri, H., Cielsiolka, C.A.A., Rose, C.W. 2009. Effects of time controlled grazing on runoff and sediment loss. *Australian Journal of Soil Research*, 47: 796-808.

Sen, S., Srivastava, P., Dane, J.H., Yoo, K.H., Shaw, J.N. 2010. Spatial-temporal variability and hydrologic connectivity of runoff generation areas in a North Alabama pasture—implications for phosphorus transport. *Hydrological Processes* 24, 342-356 (2010)

Schulze, R.E., 1997. South African Atlas of Agrohydrology and Climatology. TT82/96. Water Research Commission, Pretoria, RSA

Shock, C, Barnum, JM, Seddigh, M. 1998. Calibration of Watermark soil moisture sensors for irrigation management, pp.139-146, Proceedings of the International Irrigation Show, San Diego, CA. Irrigation Association.

Sidle, R.C., Tsuboyama, Y., Noguchi, S., Hosoda, I., Fujieda, M., and Shimizu, T. 1995. Seasonal hydrologic response at various spatial scales in a small forested catchment, Hitachi Ohta, Japan. *Journal of Hydrology,* 168 (1995). 227-250.

Soil Classification Working Group, 1991. Soil Classification. A Taxonomic System for South Africa. Department of Agricultural Development, Pretoria, South Africa.

Starr, G.C., Lal, R., Kimble, J.M., and Owens, L. 2001. Assessing the impact of erosion on soil organic carbon pools and fluxes. In: Lal, R., et al. (Ed.), Assessment Methods for Soil Carbon. CRC Press, Boca Raton, pp. 417-426. Fla.

Tetzlaff, D., Waldron. S., Brewer, M.J., and Soulsby, C. 2007. Assessing nested hydrological and hydrochemical behaviour of a mesoscale catchment using continuous tracer data. *Journal of Hydrology* 336, 430-443.

Tetzlaff, D., and Soulsby, C. Sources of baseflow in larger catchments – Using tracers to develop a holistic understanding of runoff generation. *Journal of Hydrology* 359, 287-302.

Trimble, S.W. 1983. A sediment budget for Coon Creek basin in the Driftless Area. *American Journal of Science* 283, 1853-1977.

Uhlenbrook, S., and Hoeg, S. 2003. Quantifying uncertainties in tracer-based hydrograph parations: a case study for two-, three- and five-component hydrograph separations in a mountainous catchment. *Hydrological Processes* 17, 431-453.

Vanni, M.J., Renwich, W.H., Headworth, J.L., Auch, J.D., Schaus, and M.H. 2001. Dissolved and particulate nutrient flux from three adjacent agricultural watersheds: A five-year study. *Biogeochemistry* 54, 85-114.

Wakindiki, I.I.C., and Ben-Hur, M. 2002. Soil Mineralogy and Texture Effects on Crust Micromorphology, Infiltration, and Erosion. *Soil Society of America Journal* 66, 897-905.

Walling, D.E., Collins, A.L., Jones, P.A., Leeks, G.J.L., 2006. Establishing fine-grained sediment budgets for the Pang and Lambourn. *Journal of Hydrology*, 330: 126-141.

Wang, Z., Govers, G., Steegen, A., Clymans, W., Van den Putte, A., Langhans, C., Merckx, R., and Van Oost, K. 2010. Catchment-scale carbon redistribution and delivery by water erosion in an intensively cultivated area. *Geomorphology* 124, 65-74.

Wenninger, J., Uhlenbrook, S., Lorentz, S., and Leibundgut, C. 2008. Identification of runoff generation processes using combined hydrometric, tracer and geophysical methods in a headwater catchment in South Africa. *Hydrological Sciences Journal* 53 (1), 16 pp.

Williams, J.R., Allmaras, R.R., Renard, K.G., Lyles, L., Moldenhauer, W.C., Langdale, G.W.,

Meyer, L.D., Rawls, W.J., Darby, G., Daniels, R., and Magleby, R. 1981. Soil erosion effects on productivity: A research perspective. *Soil Water Conservation* 36, 82-90.

Williams, J. and Bonell, M. 1988. The influence of scale of measurement on the spatial and temporal variability of the Philip infiltration parameters – an experimental study in an Australian savannah woodland. *Journal of Hydrology* 104, 33-51.

Van Es, H.M., Cassel, D.K., and Daniels, R.B. 1991. Infiltration Variability and Correlations with Surface Soil Properties for an Eroded Hapludult. *Soil Society of America Journal* 55.

Van de Giesen, N., *et al*., 2010.Scale effects in Hortonian surface runoff on agricultural slopes in West Africa: Theory, models, and field data. *Agriculture, Ecosystems and Environment*. 2010.

Zehe, E. and Bloschl, G., 2004. Predictability of hydrologic response at the plot and catchment scales: Role of initial conditions. *Water Resources Research* 40(W10202): 1-21.

APPENDIX A

CAPACITY BUILDING

Post graduate degrees (13 competed; 4 registered)

Table 17. List of post graduate students, name, origin and subject.

KSA	PROJECT N	STUDENT NAME	CITIZENSHIP	INSTITUTION	SPECIALISATION	YEAR READY FOR EMPLOYMENT	Supervisison	Co-sup.	THESIS TITLE
K5	1904	Phesheya Dlamini	Swaziland	UKZN	Soil Scien	Honors in 2008	P. Podwojewski		Suil distribution in the landscape
K5	1904	Craig Orchard	SA	UKZN	Hydrology	Honors in 2008	V. Chaplot		On runoff generation
K5	1904	Craig Orchard	SA	UKZN	Hydrology	Master in :	V. Chaplot	S. Lorentz	Spatial and temporal variations of surface runoff at the catchment level
K5	1904	Charmaine Mchunu	SA	ARC*	Hydrology/	Master 20	V. Chaplot	S. Lorentz	Impact of soil erosion on soil organic carbon decomposition
K5	1904	Phesheya Dlamini	Swaziland	UKZN	Soil Scien	Master in :	V. Chaplot	L. Titshall	Soil carbon an nutrient stocks at the catchùent level:
K5	1904	Ernest Oakes	SA	UKZN	Hydrology	Master in :	V. Chaplot	J. Hughes	Dynamic of soil erosion at the catchment level
K5	1904	Machila Pasi	Swaziland	UKZN	Hydrology	Honors in :	V. Chaplot		Scale issue between 1 and 10 m² plots for soil erosion
K5	1904	Gareth Tuffney	SA	UKZN	Soil Scien	Honors in :	J. Hughes	V. Chaplot	Use of pedotransfer functions to estimate soil organic carbon stocks
K5	1904	Lian Barbieri	Brasil	ESALQ*	Soil Scien	Master in :	V. Chaplot		Mapping macrobial biomass at the catchment level
K5	1904	Lucas Comte	Brasil	ESALQ*	Soil Scien	Master in :	V. Chaplot		Mapping soil agregate stability at the catchment level
K5	1904	Sabrina Juarez	France	AgroPAris	Soil Scien	Master in :	V. Chaplot	C. Rumpel	Soil carbon erosion and OM quality
K5	1904	Sonia Rudowski	France	AgroPAris	Soil Scien	Master in :	V. Chaplot	C. Rumpel	water chemistry and dissolved organic carbon
K5	1904	Auke Terlouw	Netherland	Univ. Twen	Soil Scien	Master in :	V. Chaplot	G. Jewitt	Soil erosion and controlling factors
K5	1904	Noman Mhazo	Zimbabwe	Univ Swaz	Soil Scien	PhD expec	V. Chaplot	S. Lorentz	No-tillage and soil erosion
K5	1904	Phesheya Dlamini	Swaziland	UKZN	Soil Scien	PhD expec	V. Chaplot	J. Hughes	Land rehabilitation
K5	1904	Charmaine Mchunu	SA	ARC*	Hydrology/	PhD* expe	V. Chaplot	A; Manson	Impact of no-tillage on the quality of soil organic carbon erosion
K5	1904	Daniel Muller-Nedebo	SA	ARC*	Hydrology/	Master ex	V. Chaplot	S. Lorentz	soil organic carbon erosion at different spatial scales

Papers submitted to international journals:

Published papers (9)

1. Chaplot V. Simon Lorentz; Pascal Podwojewski, Graham Jewitt. 2010. Digital mapping of A-horizon thickness using the correlation between various soil properties and soil apparent electrical resistivity. **Geoderma.** 157, 154-164.
2. Podwojewski P., Janeau J-L, Grellier S., Valentin C., Lorentz S., Chaplot V. 2011. Influence of grass soil cover on water runoff and soil detachment under rainfall simulation in a sub-humid South African degraded rangeland. **Earth Surface Processes and Landforms**. 36, 911-922.
3. Dlamini P., C. Orchard, G. Jewitt, S. Lorentz, L. Titshall, V. Chaplot.. 2011. Quantifying interrill erosion in a sloping-land-agricultural catchment of KwaZulu-Natal, South Africa. **Agriculture Water Management**. 98, 1711-1718.
4. Chaplot Vincent; Jacqueline Brown; Phesheya Dlamini; Tarryn Eustice; Jean-Louis Janeau; Graham Jewitt; Simon Lorentz; Lauren Martin; Chermaine Nontokozo-Mchunu; Ernest Oakes; Pascal Podwojewski; Sylvain Revil; Cornelia Rumpel; Nhlakanipho Zondi. 2011. Rainfall simulation to identify the storm-scale mechanisms of gully bank retreat. **Agriculture Water Management**. 98, 1704-1710.
5. Mchunu, C., Manson, A., Jewitt, G. Lorentz, S., Chaplot, V. No-Till impact on soil and Soil organic carbon erosion under crop residues scarcity in South Africa. **Soil Science Society America Journal**. 75 (4) 1503-1512.
6. Chaplot V., Jewitt, G. Lorentz, S, 2011Predicting plot-scale water infiltration using the correlation between soil apparent electrical resistivity and various soil properties. 2011. **Physics and Chemistry of the Earth**. 36, 1033-1042.
7. Juarez, S., Rumpel, C., MChunu, C., Chaplot, V. 2011. Carbon mineralization and lignin content of eroded sediments from a grazed watershed of South-Africa. **Geoderma** 167-168, 247-253.
8. Chaplot V. and Poesen J. 2012. Sediment, soil organic carbon and runoff delivery at various spatial scales. **Catena.** 88, 46-56

9. Mchunu, C., Chaplot V.., 2012. Soil organic carbon erosion and soil CO_2 emissions from degraded pastures. **Geoderma.** 179, 72-79.

In press (2)

10. Oakes E.G.M., Hughes, J.C., Jewitt, G.P.W., Lorentz, S.A., Chaplot, V.A.M. 2011. Controls on a scale explicit analysis of sheet erosion. . **Earth Surface Processes and Landforms.** In press.
11. Orchard C., Lorentz, S., Jewitt, G., V. Chaplot. 2011. Spatial and temporal variations of overland flow at the microcatchment level. **Hydological Processes.** In press.

Submitted (5)

12. Chaplot V., Mchunu, C., Manson, A., Jewitt, G. Lorentz, S. 2011.Water erosion-induced CO_2 emissions from tilled and no-tilled soils. **Agriculture Ecosystems and Environment.** Accepted with moderate corrections.1.
13. Dlamini submitted Geoderma
14. Dlamini submitted Physics and Chemistry of the Earth
15. Oakes submitted Physics and Chemistry of the Earth
16. Chaplot, V., Beckedahl. H. Impact of terrain attributes, parent material and soil types on gully banks retreat. Submitted to **Geomorphology**.

Communications at workshops with publications (10)

1. Chaplot, V., Pascal Podwojewski, Jean-Louis Janeau, Victor Kongo, Job Rotich, and Graham Jewitt. 2007. Understanding basin outputs through the spatial assessment of runoff and water erosion. SSI: Smallholder Water System Innovations in Integrated Watershed Management, Same (Tanzania), 20 of January 2008.
2. Podwojewski, P., Chaplot V., and Jean-Louis Janeau. 2008. Some results of land degradation and erosion processes: recommendations. SSI: Smallholder Water System Innovations in Integrated Watershed Management, Same (Tanzania), 20 of January 2008.
3. Dlamini, P., Podwojewski, P. Janeau, J-L Lorentz, S. Jewitt, G., V. Chaplot. 2008. Controlling factors of Interrill erosion of sloping-land-agricultural-soils in KwaZulu-Natal (South Africa). 9th waternet/WARFSA/GWP-SA Symposium, Pretoria (South Africa), October 29-31, 2008. 10p.
4. Chaplot., V., S. Lorentz, P. Podwojewski, J-L Janeau, C. Valentin, G. Jewitt. 2008. Degradation of sloping-land-agricultural-soils in South Africa: Potential consequences on water and carbon cycles. 9th Waternet/WARFSA/GWP-SA Symposium, Pretoria (South Africa), October 29-31, 2008. 11p.
5. Lorentz, S., Berry, S., Chaplot, V., Miller, J., Lechler, P and Lord, M. 2009. Connectivity of Non-Point Source Pollution Migration in a Commercial Agricultural Catchment in KwaZulu-Natal. *14th SANCIAHS SYMPOSIUM: Pietermaritzburg, 21-23 September 2009*
6. Orchard, C.M. J.L. Janeau, J.J. Pretorius, S.A. Lorentz, G.P.W. Jewitt, V.A.M. Chaplot. 2010. Spatial and temporal variations of runoff at the microcatchment level. 11th WaterNet/WARFSA/GWP-SA, 27-29 October 2010. Victoria Falls, Zimbabwe. 8p.
7. Oakes, E.G.M., M.J. Pasi, Janeau, J.J, P. Podwojewski, S.A. Lorentz, G.P.W. Jewitt, V.A.M. Chaplot. 2010. Soil erosion dynamic within a catchment. 11th WaterNet/WARFSA/GWP-SA, 27-29 October 2010. Victoria Falls, Zimbabwe. 10p.
8. Chaplot, V.A.M. Jewitt, G.P.W. J.L., P. Podwojewski, Janeau, J.J. Pretorius, S. Lorentz. 2010. Water erosion impact on the pedosphere, hydrosphere and atmosphere:

Learned lessons from research/capacity building activities at Potshini. 11th WaterNet/WARFSA/GWP-SA, 27-29 October 2010. Victoria Falls, Zimbabwe. 8p.

9. Oakes E.G.M., Chaplot, V.A.M. J.C., Jewitt, G.P.W., Lorentz, S.A., 2011. Soil and sediment colour, texture, C and N content coupled with sediment flux estimation at embedded spatial scales to understand landscape soil erosion dynamics. 12th WaterNet/WARFSA/GWP-SA, 26-28 October 2011. Maputo Mozambique. 14p.
10. Dlamini P., Lorentz S., Pascal Podwojewski P., Janeau J-L; Jewitt, G.P.W. Chaplot, V. 2011. Performance of interpolation techniques for estimating secondary variables: volumetric water content. 12th WaterNet/WARFSA/GWP-SA, 26-28 October 2011. Maputo Mozambique. 15p.
11. Chaplot, V. Beckedahl H., Lorentz S., Podwojewski P., Jewitt, G.P.W. 2011. Impact of terrain attributes, parent material and soil types on gully banks retreat. 12th WaterNet/WARFSA/GWP-SA, 26-28 October 2011. Maputo Mozambique. 16p.

Communications at workshops without publications (8)

1. Chaplot V., Pascal Podwojewski, Jean-Louis Janeau, Séraphine Grellier. 2007. Le chantier « Afrique du Sud » de l'UR176 : un positionnement stratégique dans le schéma général des sites à situations pédo-climatique et processus de dégradation des terres différents. Journées Big-Bang, 27-28 mai 2008.

2. Chaplot V., P. Podwojewski, J-L Janeau, S. Grellier, S. Lorentz, G. Jewitt. 2008. Restitution meeting of results obtained on soil degradation at the Potshini catchment to the Potshini community of South Africa. Potential consequences on water and carbon cycles. 6 about 2008. Presentation oral.

3. Podwojewski P.; J-L Janeau; S. Lorentz; V. Chaplot; G. Jewitt. 2009. Storm-scale mechanisms of gully bank retreat. 14th SANCHIAS Symposium, 21-23 September, University of KwaZulu-Natal, Pietermaritzburg, South Africa. Oral.

4. Chaplot V.; G. Jewitt; P. Podwojewski; J-L Janeau; S. Lorentz. 2009. Erosion impact on the soil and the water resources: Learned lessons from research activities at Potshini and perspectives. 14th SANCHIAS Symposium, 21-23 September, University of KwaZulu-Natal, Pietermaritzburg, South Africa. Oral.

5. Mchunu, CN *A. Manson*, S.Juarez, P. Podwojewski, J-L Janeau, G. Jewitt, S.Lorentz, V. Chaplot. 2009. The hydrologic impact on the global carbon cycle: Case study from erosion plots in KZN. 14th SANCHIAS Symposium, 21-23 September, University of KwaZulu-Natal, Pietermaritzburg, South Africa. Oral.

6. Dlamini, P., J-L Janeau, C. Orchard, S. Lorentz, L. Titshall, G. Jewitt, P. Podwojewski, V. Chaplot. 2009. Interrill erosion under steep slope pastures at Potshini (KZN). 14th SANCHIAS Symposium, 21-23 September, University of KwaZulu-Natal, Pietermaritzburg, South Africa. Oral.

7. Chaplot, V., S. Lorentz, G. Jewitt. 2009. New water quality challenges associated with agriculture. Lessons learned from a small-scale Catchment in KwaZulu-Natal. 14th SANCHIAS Symposium, 21-23 September, University of KwaZulu-Natal, Pietermaritzburg, South Africa. Oral.

8. Orchard, C.; P. Podwojewski; J-L Janeau; G. Jewitt; S. Lorentz. V. Chaplot. 2009. Uncertainty in estimating spatial and temporal variations of infiltration and surface runoff: case of a small agricultural catchment in KZN. 14th SANCHIAS Symposium, 21-23 September, University of KwaZulu-Natal, Pietermaritzburg, South Africa. Oral.

Posters (4)

1. Orchard, C., P. Dlamini, J-L Janeau, P. Podwojewski, S. Lorentz, G. Jewitt, V. Chaplot. 2008. Mapping Runoff and Interrill erosion in a sloping-land-agricultural catchment (KwaZulu-Natal, South Africa). 9th Waternet/WARFSA/GWP-SA Symposium, Pretoria (South Africa), October 29-31, 2008. Poster.
2. Chaplot V., S. Lorentz, P. Podwojewski, J-L Janeau, C. Valentin, G. Jewitt. 2008. Degradation of sloping-land-agricultural-soils in South Africa. Potential consequences on water and carbon cycles. Journées Big-Bang, 27-28 mai 2008.
3. Tuffney, G.M.V., L. Titshall, J. Hughes, P. Dlamini, G.P.W. Jewitt, S. Lorentz, V.A.M. Chaplot. 2010. Use of pedotranfer functions for the spatial estimation of volumetric soil water content at catchment level. 11th WaterNet/WARFSA/GWP-SA, 27-29 October 2010. Victoria Falls, Zimbabwe.
4. Chaplot, V.A.M., E.G.M. Oakes, P. Dlamini, G.P.W. Jewitt, J.L., P. Podwojewski, Janeau, J.J. Pretorius, S. Lorentz. 2010. On land degradation. 11th WaterNet/WARFSA/GWP-SA, 27-29 October 2010. Victoria Falls, Zimbabwe.

Other papers (2)

1. Le sol met sa carapace. 2011. Sciences au Sud (IRD journal), 59. p 4.
2. No tillage to limit soil carbon losses. UKZN newsletter November 2011.